ELECTROMECHANICAL RESONATORS AS MEASURING TRANSDUCERS

by

ANWAR HASSAN

Submitted for the Degree of

Doctor of Philosophy

at

The University of Aston in Birmingham

November 1980

ELECTROMECHANICAL RESONATORS AS MEASURING TRANSDUCERS

by

ANWAR HASSAN

A thesis submitted to the
University of Aston in Birmingham
for the degree of
Doctor of Philosophy 1980

Summary

With the increasing use of digital computers for data acquisition and digital process control, frequency domain transducers have become very attractive due to their virtual digital output. Essentially they are electrically maintained oscillators where the sensor is the controlling resonator. They are designed to make the frequency a function of the physical parameter being measured. Because of their high quality factor, mechanical resonators give very good frequency stability and are widely used as sensors.

For this work symmetrical mechanical resonators such as the tuning fork were considered to be the most promising. These are dynamically clamped and can be designed to have extensive regions where no vibrations occur. This enables the resonators to be robustly mounted in a way convenient for various applications. Designs for the measurement of fluid density and tension have been produced.

The principle of the design of the resonator for fluid density measurement is a thin gap (trapping a lamina of fluid) between its two members which vibrate in antiphase. An analysis of the interaction between this resonator and the fluid lamina has been carried out. In gases narrow gaps are needed for a good sensitivity and the use of the material fused quartz, because of its low density and very low temperature coefficient, is ideally suitable. In liquids an adequate sensitivity is achieved even with a wide lamina gap. Practical designs of such transducers have been evolved. The accuracy for liquid measurements is better than 1%. For gases it was found that, in air, a change of atmospheric pressure of 0.3% could be detected. This corresponds to a density sensitivity of about 4×10^{-3} kg m^{-3}.

In constructing a tension transducer using such a mechanical sensor as a wire or a beam, major difficulties are encountered in making an efficient clamping arrangement for the sensor. The use of dynamically clamped beams has been found to overcome the problem and this is the basis of the transducer investigated.

Keywords

DENSITY TENSION TRANSDUCER GAS LIQUID

ACKNOWLEDGEMENTS

The author wishes to express his debt to:

Dr. J.F.W. Bell for his guidance, advice and encouragement throughout this study.

Professor J.E. Flood, Head of the Department of Electrical and Electronic Engineering, for laboratory facilities.

The Association of Commonwealth Universities, London, for a scholarship.

Miss N.P. Freeman for the typing.

A brief account of the fluid density transducers was presented at the Wembley Transducer Conference in July 1980.

CONTENTS

LIST OF FIGURES AND TABLES

TABLES

CHAPTER 1

ELECTROMECHANICAL RESONATORS AS MEASURING TRANSDUCERS - A REVIEW

1.1 INTRODUCTION

The Instrument Society of America has defined a transducer as a device that converts physical phenomena and chemical composition into electric, pneumatic or hydraulic output signals. However the electric form is mostly desirable in measurement and control systems, whether in laboratory, production plant or aviation. This is because of the convenience of subsequent operations on the data.

Thus a measuring transducer may be looked upon as a device to convert non-electrical measurands into electrical quantities. Transducers may be genuine energy converters, called active transducers, or they may require an auxiliary energy source and are therefore energy controllers, called passive transducers. Distinction can also be made between a sensor and a complete transducer in that a sensing element or sensor can be said to be that part of a transducer that responds directly to the measurand. A diaphragm, for example, can respond directly to changes in pressure by mechanical displacement. No electrical output is produced. However a resistance strain gauge attached to the diaphragm can modify a

supplied voltage in proportion to the strain in the disk. The combination of the two elements forms an electro-mechanical transducer.

Figure 1.1 shows the place of such a tranducer in a general functional diagram of a measuring system. As output quality of the system can be no better than the quality of the input, the vital role played by the measuring transducer is quite evident. Gardiner[1] has described it as "an unfortunate fact of life that in any measurement and control system, the system accuracy is largely dependent on the accuracy and repeatability of the transducers or prime measuring elements". So there is a continuous effort for the development of new improved transducers. Most of the earlier developed transducers provide outputs in analog form. Table 1.1 gives a list of some physical effects employed in these transducers.

The recent increasing use of digital computers for data acquisition and digital process control has stimulated development for transducers with digital output. Schuler[2] has defined four types of digital transducers:

(1) analog-to-digital (A-D) transducers
(2) direct digital transducers
(3) indirect digital transducers
(4) quasi-digital transducers.

When computers were first used for control purposes digital instruments were not generally available so A-D converters were developed to provide digital data formats which the

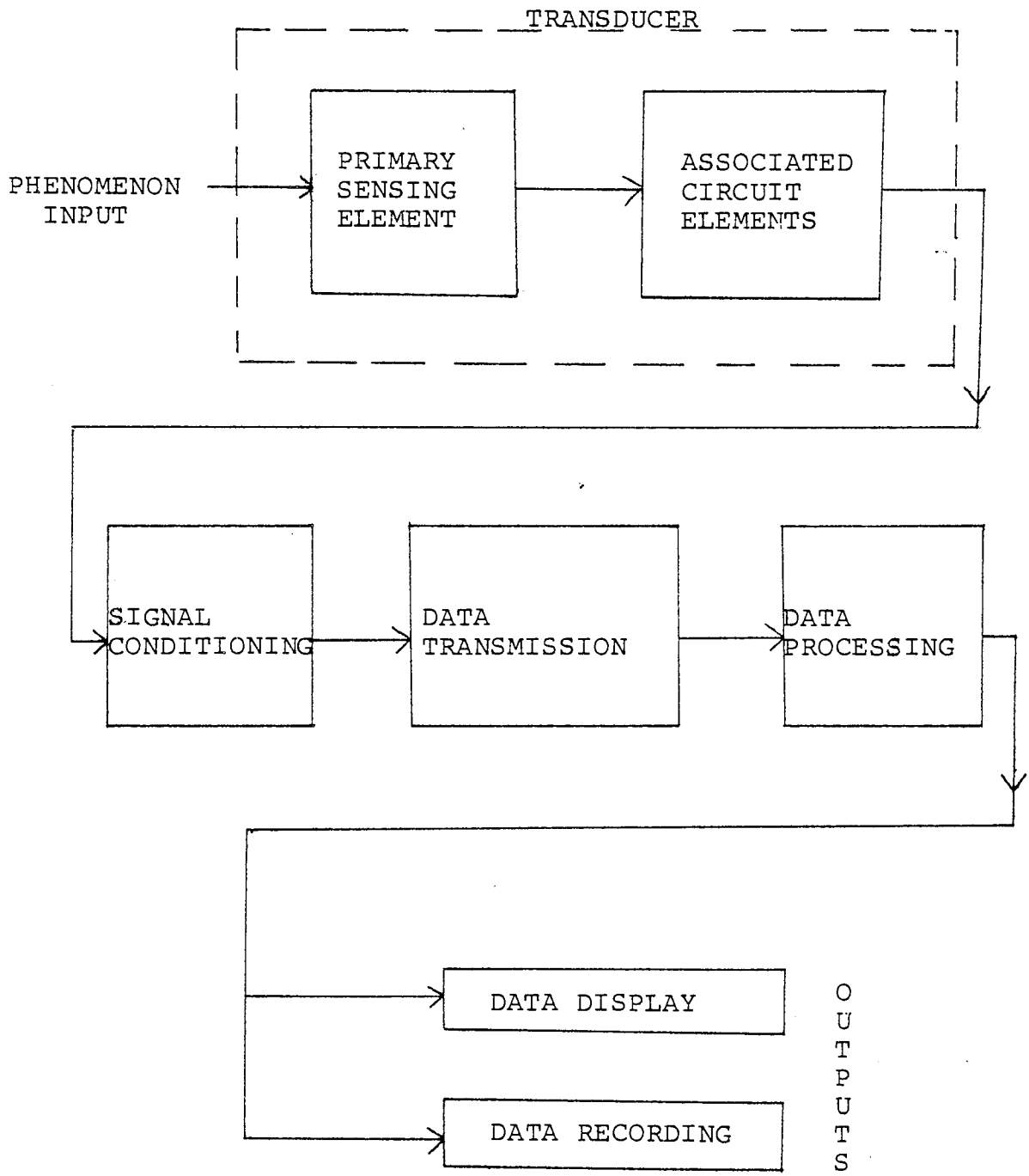

FIGURE 1.1 A general functional diagram of a measuring system.

PHYSICAL EFFECTS USED IN 'ACTIVE' (ENERGY-CONVERTING) TRANSDUCERS	PHYSICAL EFFECTS USED IN 'PASSIVE' (ENERGY-CONTROLLING) TRANSDUCERS
Electromagnetic	Resistance)
Piezoelectric	Inductance) Controlled by geometry
Magnetorstrictive (as a generator)	Capacitance)
Thermo-electric	Mechano-resistance (strain)
Photo-electric	Magneto-resistance
Photo-voltaic	Thermo-resistance
Electro-kinetic	Photo-resistance Piezo-resistance
Pyro-electric	Magnetostrictive (as a variable inductance)
	Hall effect
	Radioactive ionization
	Radioactive screening
	Ionization (humidity in solids

TABLE 1.1 LIST OF SOME PHYSICAL EFFECTS USED IN MEASURING TRANSDUCERS

computer could interpret. The direct digital transducer uses no analogue phenomenon or counting technique to obtain a digital output. There have been attempts to develop a transducer of this type but as yet none have been successfully developed[2,4]. Indirect digital transducers use an analogue phenomenon, such as displacement, for sensing and conversion to a digital output. However developments of this type are very few and until now the shaft angle encoder seems to be the only practical one of this type[3,4]. Quasi-digital transducers are those which have frequency or pulse rate or pulse duration outputs. Of these perhaps the most versatile is the first one. Sometimes this type is called frequency domain or variable frequency transducer. Actually they are electrically maintained oscillators where the sensor is the phase sensitive controlling element. Thus the oscillator frequency is a function of the parameter being measured such as temperature, fluid density, fluid pressure, etc. The advantages of an electrical frequency output from a transducer, in contrast to voltage or current, have a radical effect on the data handling methods employed to process the outputs[5,6,7,8]. A main one arises from the virtual digital nature of the output which hence can be processed, transmitted and stored by high reliable low cost digital techniques. Practical advantages also arise as immunity to plant vibration, the ease with which safety techniques such as zener safety barriers and transformer coupling may be applied to the output signal without loss

of accuracy.

Variable capacitance or variable inductance transducers can be incorporated in the tuned resonant circuit or so called tank circuit of an L-C oscillator as to control the frequency of oscillation and thus producing frequency domain transducers. There are few practical transucers of this type. Even changes of resistance can be used in f.d. technique. One interesting development of this type is the digital force transducer by Dorrity and Gilliland[4]. It is based on the variation of a strain gauge resistance with force; the resistance being connected to control the run time of a monostable multivibrator. However perhaps widely used sensors in frequency domain technique are mechanical resonators. This is because of the high quality factor, versatility and other practical advantages such as good repeatability, low hysteresis, excellent stability, etc. of a mechanical resonator. Derrick[9] has called it "measurement tool of the Seventies". The natural frequency of resonance of a mechanical system depends upon physical quantities such as density, stress, elasticity, dimensions, temperature, etc. When this variation in natural resonant frequency can be arranged to respond to changes in only one of these physical quantities with high immunity to changes of the others, then the resonant frequency may be effectively employed as a measure of the former physical variable.

1.2 FUNDAMENTALS OF FREQUENCY DOMAIN TECHNIQUES WITH MECHANICAL RESONATORS

This may be best understood by consideration of an idealized mechanical vibrator with one degree of freedom. Such a system, as shown in Figure 1.2, consisting of mass M, spring of stiffness K and viscous damping R_m has the

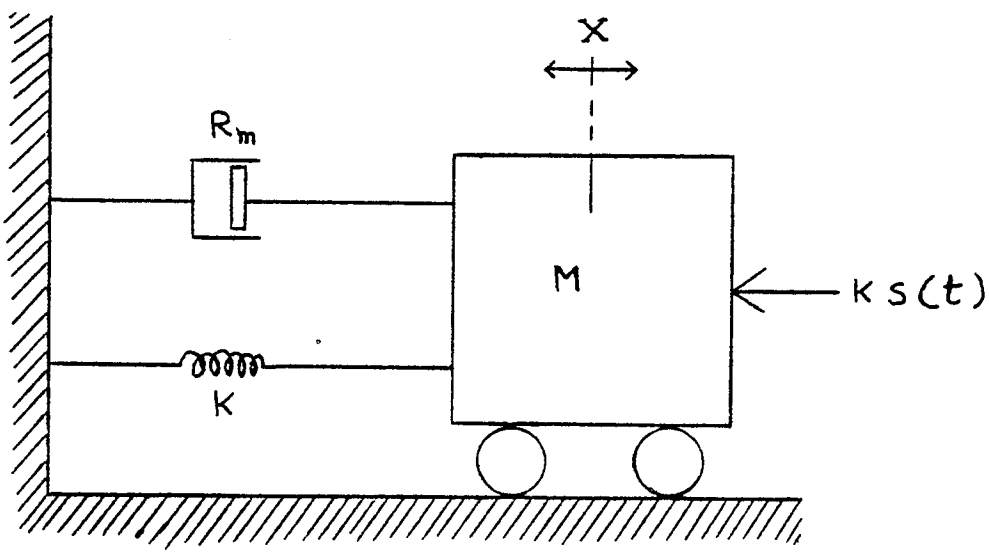

Figure 1.2 AN IDEALIZED MECHANICAL SYSTEM WITH MASS, SPRING AND DAMPING

equation of motion

$$M\ddot{X} + R_m\dot{X} + KX = KS(t) \qquad (1.1)$$

where KS(t) is the driving force and

S(t) is a function of time

$$\text{or} \qquad T_o^2 \ddot{X} + T_1 \dot{X} + X = S(t) \tag{1.2}$$

where $T_1 = \frac{R_m}{K}$ and $T_o = \sqrt{\frac{M}{K}}$

For sinusoidal excitation of $S(t) \equiv Ae^{j\omega t}$, the output $X(t)$ is given by

$$X(t) = F(j\omega)Ae^{j\omega t}$$

$$= \frac{Ae^{j\omega t}}{1+j\omega T_1 - \omega^2 T_o^2} \tag{1.3}$$

where $F(j\omega)$ is the complex frequency response of the system.

$$\text{or} \qquad F(j\omega) = \frac{1}{1+j\omega T_1 - \omega^2 T_o^2} \tag{1.4}$$

Therefore relative amplitude response

$$|F(j\omega)| = \frac{1}{\sqrt{\{(1-\omega^2 T_o^2)^2 + \omega^2 T_1^2\}}} \tag{1.5}$$

and phase angle ϕ between the input and output signals is

$$\phi = \tan^{-1}\{\omega T_1/(1-\omega^2 T_o^2)\} \tag{1.6}$$

Rearranging equations (1.5) and (1.6) and introducing

$$\omega_o = 1/T_o = \sqrt{K/M} \qquad \left|\begin{array}{l}\text{undamped natural frequency} \\ \text{(circular)}\end{array}\right.$$

and $R = T_1/2T_o = R_m/2\sqrt{MK}$

we have,

$$|F(j\omega)| = \frac{1}{\sqrt{\{|1-(\omega/\omega_o)^2|^2+4R^2(\omega/\omega_o)^2\}}} \qquad (1.7)$$

and

$$\phi = \tan^{-1}\frac{2R(\omega/\omega_o)}{1-(\omega/\omega_o)^2} \qquad (1.8)$$

Equations (1.7) and (1.8) have been plotted in Fig. 1.3 for various values of ω/ω_o, the damping ratio R being a parameter. It can be seen from the curves that oscillations of the system can be maintained at a precise stable state at its natural frequency of resonance ω_o, by electrical circuits with proper phase and gain; provided damping parameter R is of low value, say below 0.4. ω_o is $|K/M|^{\frac{1}{2}}$, so that any factor contributing to a variation in K or M will result in a change in the frequency of the maintained oscillation and this frequency may be employed as a measure of such variations.

1.3 PHYSICAL QUANTITIES MEASURABLE

As stated above any physical variable which contributes to changes in the mass or stiffness of the vibrating resonator will cause a change in the maintained oscillation frequency. Changes in mass may be made by density changes of surrounding fluid or by direct change of solid mass. In this way the

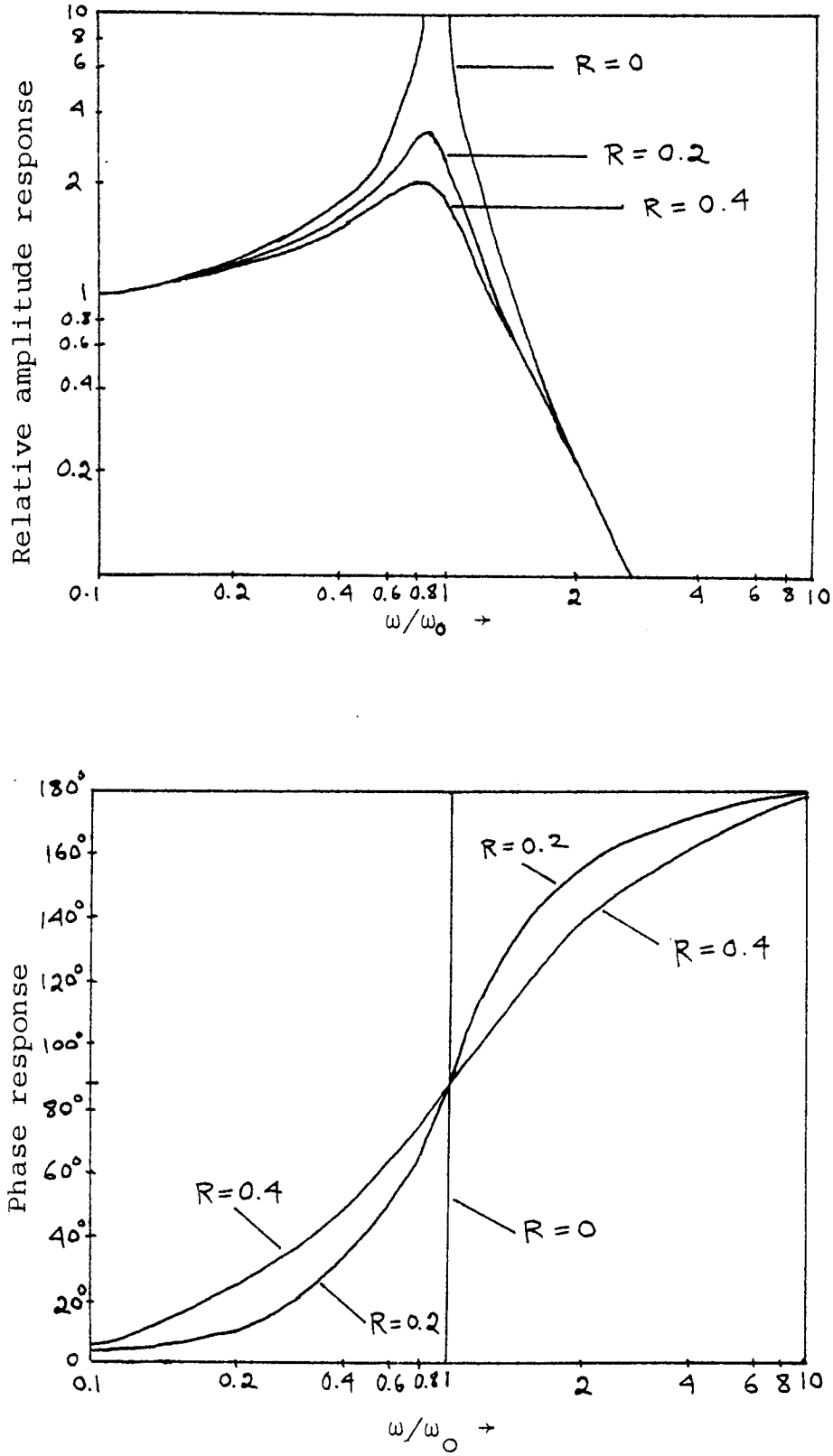

FIGURE 1.3 Response curves of an idealized mechanical system with mass, spring and damping (see Figure 1.2).

frequency domain technique may be used to design fluid density transducers or as detectors of solid deposition. An example of the latter case is the common use of vibrating quartz crystals in vacuum chambers to monitor the thickness of evaporated or sputtered films. As a film builds up on workpieces and crystal monitor, the extra vibrating mass causes a reduction in resonant frequency. Very fine control of film thickness is achievable with this method. Changes in the stiffness of the system may be arranged to be a direct effect of changes in compressive or tensile stress on such physical elements as vibrating wires or prismatic beams. This may be used to design load cells, pressure transducers, etc. Again the dependence of resonant frequency on temperature because of the large temp. coefficient of elasticity of some materials and to a smaller extent the expansion coefficients of the materials, may be utilized to design a thermometer. This catalogue is by no means exhaustive, and many other variables may be measured either directly or by implication. A brief discussion of operating principles and main features of some of the important transducers based on mechanical resonators is given in the following sections.

1.4 A REVIEW OF SOME MEASURING TRANSDUCERS BASED ON MECHANICAL RESONATORS, USING FREQUENCY DOMAIN TECHNIQUES

1.4.1 Fluid Density Transducers[6,10]

(a) Solartron liquid density meter:[6] The transducer consists of a pair of nickel-iron alloy tubes welded

to a common support at each end so that they lie

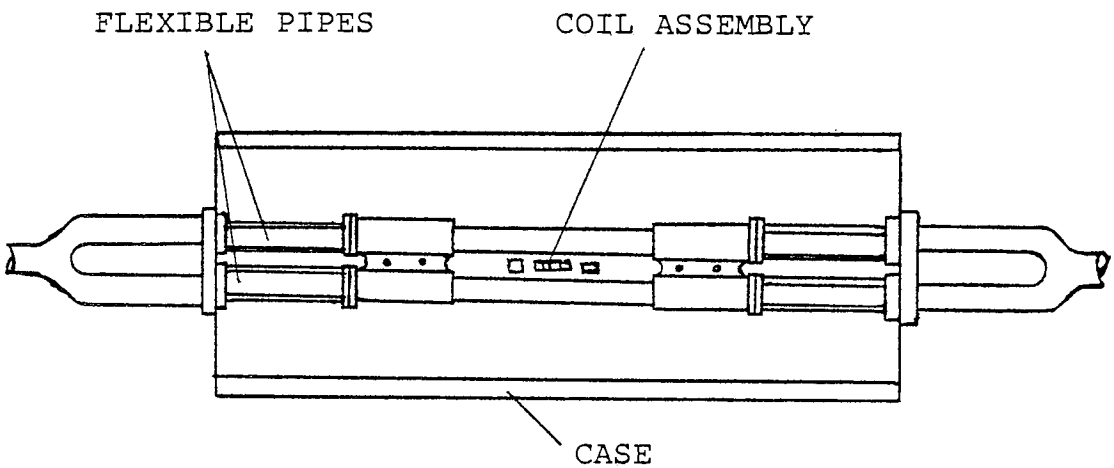

Figure 1.4 SOLARTRON LIQUID DENSITY METER

parallel to each other (Figure 1.4). Suspended from the end supports and lying between the two tubes is an electromagnetic drive and pick-up coil assembly. With the use of a maintaining amplifier, the coils drive the tubes in the fundamental lateral mode at their mean natural frequency. The tubes and coils are held to the transducer case with anti-vibration mounts and the liquid whose density is to be measured flows through both tubes. This is arranged by 'Y' coupling tubes and flexible connecting pipes as shown in the illustrations. Since the natural frequency of oscillation of the tubes is a function of their mass per unit length, it is also a function of the density of the liquid contained in the tubes. By measuring this frequency, it is therefore

possible to compute the liquid density. The tubes vibrate at a frequency of about 1.3 kHz when filled with air. When water filled the frequency is reduced to about 1 kHz giving a 20% reduction in frequency (or 25% increase in periodic time) for a density span of 1000 Kg/m^3. The use of nickel-iron alloy makes it possible to have a very low instrument temperature coefficient of less than 0.02 Kg/m^3/deg. C. The density/frequency relationship is given by

$$\rho_\ell = \rho_o \left| (f_o^2/f_\ell^2) - 1 \right| \qquad (1.9)$$

where ρ_ℓ = liquid density

f_ℓ = frequency output at density ρ_ℓ

f_o = frequency output at zero density

ρ_o = sensitivity constant.

In practice f_o and ρ_o are the calibration constants. This transducer is expensive but provides high orders of accuracy[9].

(b) Solartron gas density transducer[6]: The sensing element of this transducer is a thin walled cylinder resonated in 'hoop' or radial mode. Figure 1.5 shows a diagrammatic representation of the cylinder and its hoop vibration mode. The maximum vibration amplitude occurs at the middle of the cylinder length with nodes at the ends. The cylinder is therefore clamped at one end with a free node-forming ring at the other end. The gas, whose density is to be measured, is passed over both the inside and outside of the cylinder. Gas is thus brought into

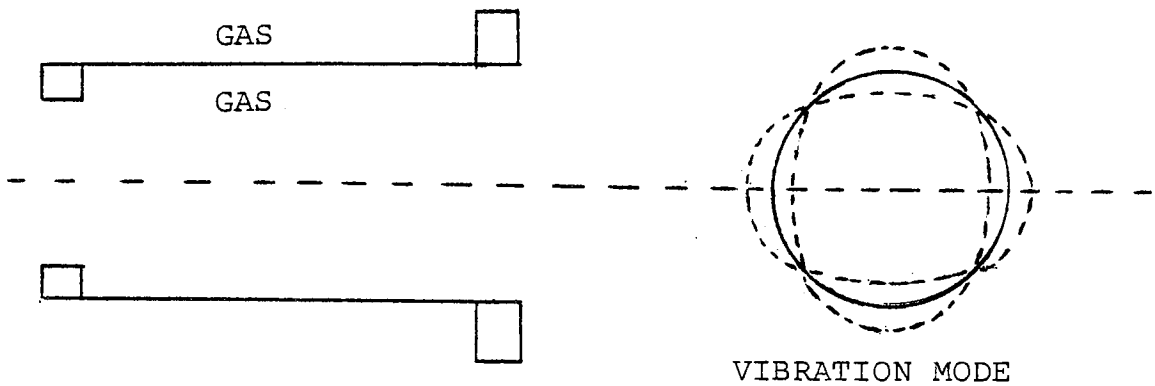

Figure 1.5

oscillation by the vibrating walls and contributes to the mass of the walls by an amount which depends on the density of the gas. An increase in density will increase the effective mass of the vibrating system and thus lower the natural resonant frequency. Oscillation is again maintained electromagnetically by positioning drive and pick-up coils inside the cylinder and coupling them to a maintaining amplifier ciruit. A low instrument temperature coefficient is achieved by machining the cylinder sensing element from the same nickel-iron alloy used for the liquid density transducer giving a near zero thermoelastic coefficient. The cylinder wall thickness varies between 5×10^{-5}m to 30×10^{-5}m, depending on the density range to be measured. A 20% frequency reduction is chosen to correspond to full scale density range with ranges such as 4.9 kHz to 3.9 KHz for 0 to

60 Kg/m^3 and 7 kHz to 5.6 kHz for 0 to 120 Kg/m^3. A strong housing is used to withstand pipeline pressures and filters are provided to help ensure that the sensing element is kept clean. The density/frequency relationship is given by

$$\rho_g = \frac{C_1}{f^2_g} + \frac{C_2}{f_g} + C_3 \qquad (1.10)$$

where ρ_g = gas density

f_g = transducer frequency output at ρ_g

C_1, C_2, C_3 = caliberation constants

(c) Agar vibrating spool density meter[10]: The principle of operation is shown in Figure 1.6. The sensing

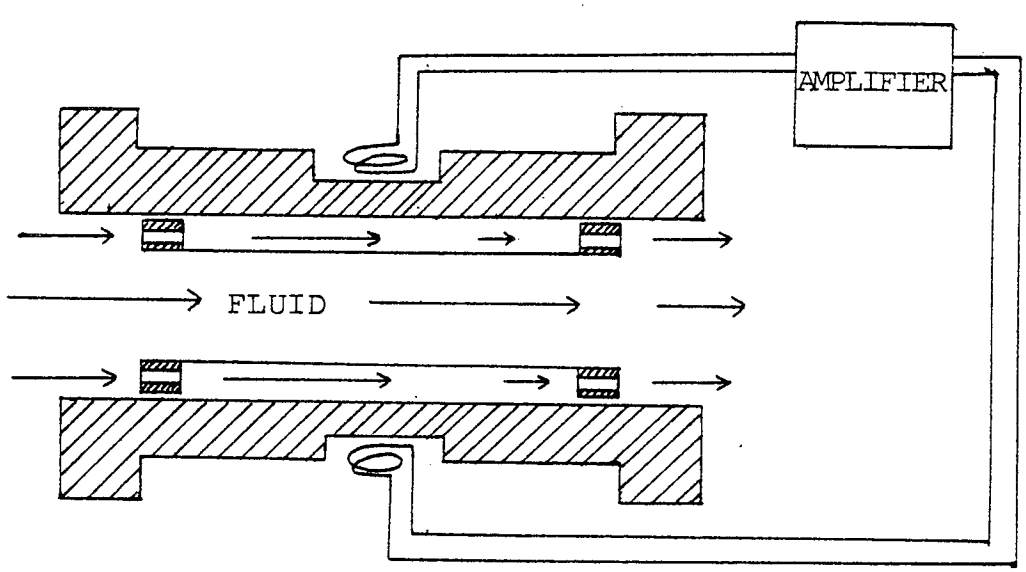

Figure 1.6

element is a tube thickened at the two ends (spool), which is set in the circumferential mode of oscillation. The

spool is maintained in oscillation by a feedback amplifier. The fluid to be measured is allowed to surround the spool and thus is set in oscillation as well. The frequency of oscillation is a function of the mass of the surrounding fluid. An increase in the density of the fluid lowers the frequency of oscillation. The output of the amplifier is monitored by a frequency meter whose display is calibrated in the desired units of density. The periodic time/density relationship is given by the empirical formula

$$\rho_f = \rho_o \left| (T_f/T_o)^2 - 1 \right| \qquad (1.11)$$

where ρ_f = measured fluid density

ρ_o = scale factor

T_f = measured periodic time of oscillation at ρ_f

T_o = periodic time at vacuum.

A typical sensitivity is a change of periodic time from 300×10^{-6}s to 330×10^{-6}s for a density span of 100 Kg/m^3. Sufficient information is not available about the driving technique and other important criteria such as geometrical dimensions, materials, etc. of this transducer.

1.4.2 Gas Pressure Transducers[11-15]

A typical example of these transducers is one developed by Meyer[11]. The sensing element consists of an assembly of two concentric closed-end cylinders - a

vibrating inner one and a protective outer one. These cylinders are fastened to a common base at one end and are free at the other. A schematic representation of this configuration is shown in Figure 1.7. An additional central structure is built from the base, and this is called the spool body. The spool body serves as a support

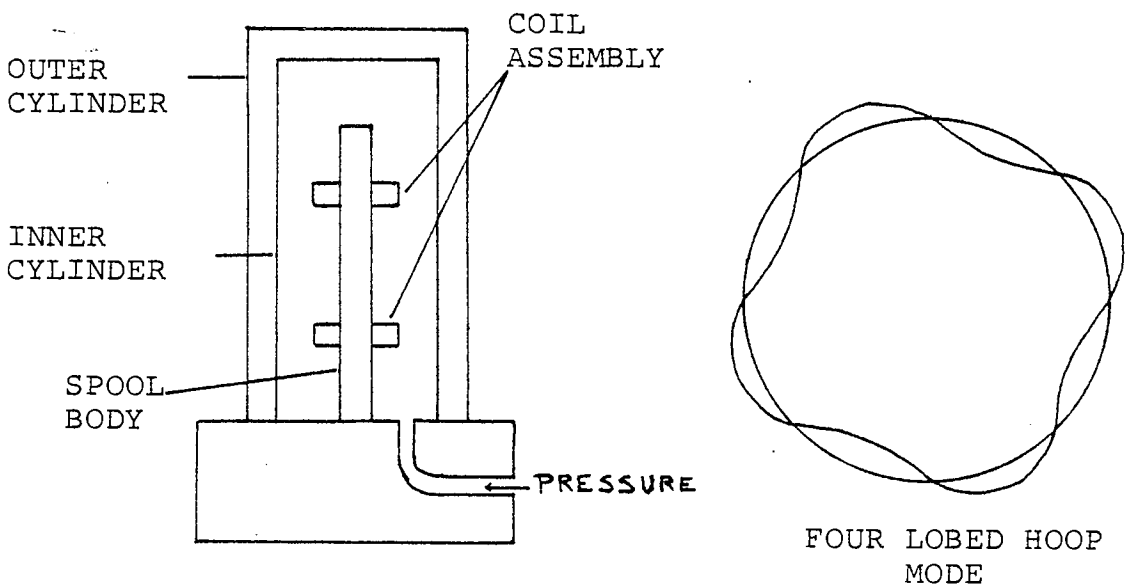

Figure 1.7

for electromagnets used in (1) exciting the vibrating inner cylinder and (2) detecting its motion and frequency. The space between the vibrating inner cylinder and the protective outer cylinder is evacuated to serve as the absolute pressure reference. The cavity volume between the vibrating inner cylinder and the spool body receives the input pressure, generally through porting passages in the transducer base. The wall elements of the cylinder are tensioned by the pressure acting over the

cylinder internal area. This tension causes the cylinder natural frequency to increase as a function of the increased pressure. The mode of vibration of the cylinder is chosen to operate in the four lobed symmetrical hoop mode as shown in Figure 1.7. The expression for pressure as a function of vibratory cylinder frequency is

$$P = B_1(f_p - f_o) + B_2(f_p - f_o)^2 + B_3(f_p - f_o)^3 \qquad (1.12)$$

where constants B_1, B_2, B_3 are derived from calibration and f_p and f_o are the transducers frequencies at pressure P and at zero pressure respectively. The effect of density of gas is removed during the calibration process for a given gas. The vibrating cylinder is typically 45×10^{-3}m long; 19×10^{-3}m diameter and a wall thickness of 75×10^{-5}m. Typically a 20% frequency change is chosen over full working range with a nominal frequency of 5 kHz to about 16 KHz, depending on the pressure range. Full-scale ranges available are 1 to about 7×10^7 pascal.

1.4.3 Temperature Transducers[16-20]

Changes in the elasticity, due to thermal effect, of a vibrating body, will cause variations in resonant frequency. In most cases this is an undesirable effect and materials are chosen to give a very low thermo-elastic coefficient (as mentioned in previous sections). Obviously the above effect may be turned to advantage in the design of a thermometer with a frequency output. In this case,

materials are chosen to give the greatest possible effect of temperature changes on elasticity and physical dimensions resulting in the maximum sensitivity of frequency to temperature. Thermometers are available employing this technique using a quartz crystal sensing element[16]. In this case the reverse design criteria apply to those used to produce high stability frequency standards. This is achieved by employing an angle of cut to give the largest possible temperature coefficient. In the commercially available Hewlett-Packard thermometer the crystal is approximately 6.5×10^{-3}m diameter and sealed in an inert atmosphere in a small container. The frequency temperature relation is given by

$$f_T = f_{oo}(1 + aT) \qquad (1.13)$$

where f_{oo} = fundamental frequency at $T = 0^{\circ}C$

f_T = frequency at temperature $T^{\circ}C$

a = calibration constant.

A convenient slope is 1000 Hz per $^{\circ}C$ at a fundamental frequency of approximately 28 MHz. The operating temperature range is $-40^{\circ}C$ to $+ 230^{\circ}C$ which limits the application. However, the very high 'Q' factor gives a correspondingly high frequency stability, and although the temperature coefficient is relatively small the result is a high sensitivity instrument.

1.4.4 Force Transducers[21-26]

This type of transducer is based on the change of resonant frequencies of wires or beams, due to force applied on them in the form of compression or tension. A number of transducers have been built on this principle. A typical one described by Wyman[21] consists of a vibrating titanium wire ($.63 \times 10^{-4}$m diameter and 32×10^{-3}m long) located between the poles of a permanent magnet as shown in Figure 1.8.

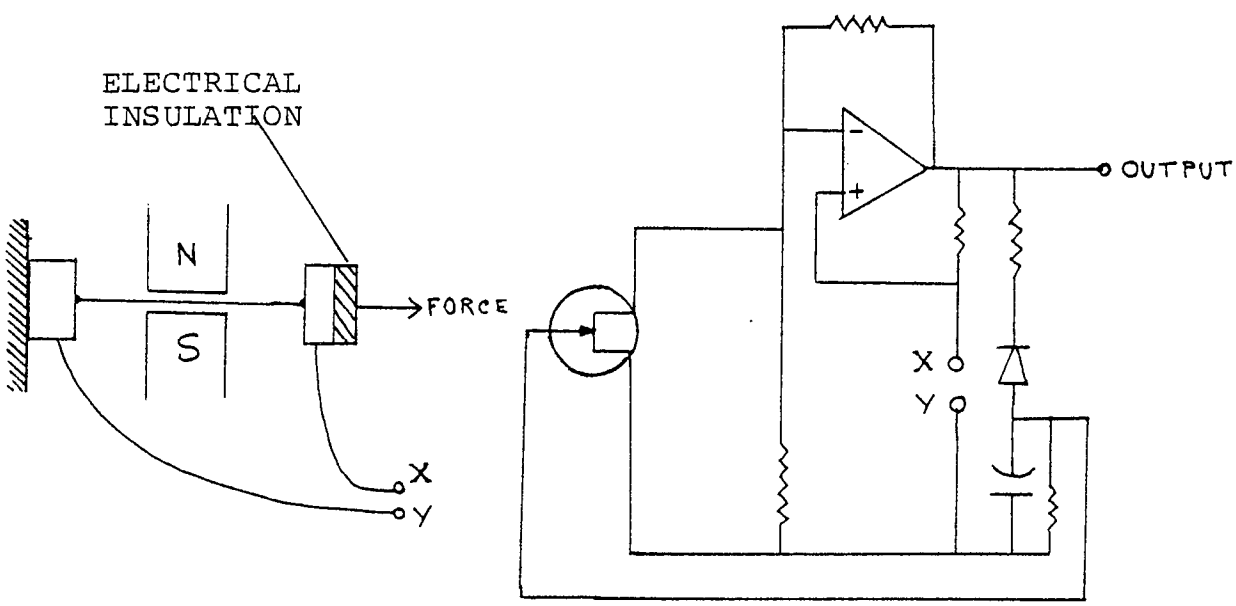

Figure 1.8

Tensile force is applied to the wire through insulated anchorages. The wire forms part of the electrical detecting network which maintains the wire vibrating at the frequency of its transverse resonance. The electrical impedance of such a wire vibrating in a

magnetic field peaks sharply when vibrating at this frequency. The oscillator circuit consists of an amplifier with broad-band negative feedback and narrow-band positive feedback. The centre frequency of the narrow band is set at the mean frequency of vibration over the operating range required. The output amplitude is regulated by overall control of the loop gain by the field effect transistor. This circuit will maintain the output at a frequency equal to the natural frequency f of the tensioned wire. This frequency is given by

$$f = \frac{1}{2L_w}\sqrt{\frac{T}{m}} \text{ hertz} \qquad (1.14)$$

where L_w = length of wire

T = tension force

m = mass per unit length.

The transducer has a centre frequency of about 3700 Hz for a tension load of 0.81N. Maximum force measurable is around 100N. It is particularly important to terminate the wire efficiently, so that no relative movement exists between the wire and any part of the clamping arrangements.

1.5 OTHER TECHNIQUES OF MEASURING TRANSDUCERS WITH MECHANICAL RESONATORS [27-36]

Though frequency domain technique seems to be very attractive for designing transducers with mechanical resonators, there are a good number of developments

using other techniques. Mason[27] used impedance method to measure fluid properties. This method employs the fact that electrical impedance of a driving unit used to set forced vibration in a mechanical system, immersed in a medium, varies with the properties of the medium.

Another important technique, which has been widely used mainly for measuring fluid viscosity[28-34], is the resonance decay method. It consists of measuring the amplitude time decay of free vibrations of a resonator. A brief discussion of two transducers of this type is given below to have an understanding of the working principles and other related features of this method.

(a) Ultra-viscoson: This instrument developed by Roth and Ritch[28] utilises the interaction of ultrasonic elastic waves with the fluid whose viscosity is to be measured. A thin metal strip, as shown in Figure 1.9, is excited magnetostrictively in its fundamental longitudinal mode by an impulsive signal. If the strip is in a vacuum so that the movement of its surface is unimpeded, once an eastic disturbance is established, it will propagate along the strip with a velocity of propagation equal to the so-called "long bar" velocity. If internal losses are negligible, the disturbance will propagate along the strip without suffering any attenuation. If this same strip is now immersed in a viscous liquid, its surfaces are no longer unimpeded

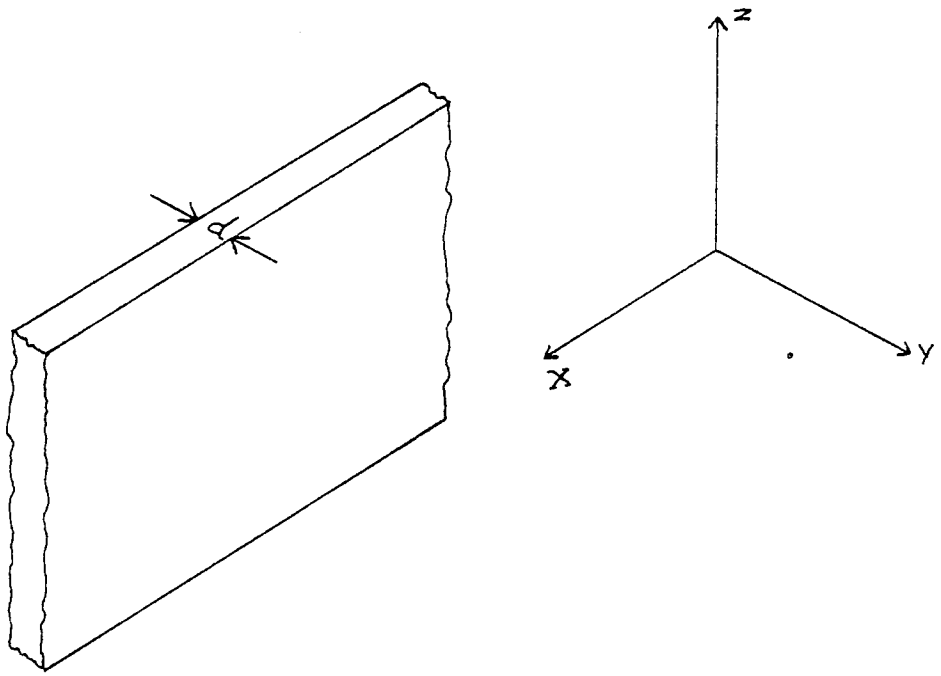

Figure 1.9

- the velocity will be reduced, and the elastic disturbances will be attenuated as it propagates along the strip. The viscometer operates by measuring this attenuation as a function of time. The strip is held at its centre and only one half of its length L is immersed in the material to be measured. The particle displacement $\xi(x,t)$ at any point along the strip under the above condition, is given by

$$\xi(x,t) = \xi_o e^{-(a-jb)t} \sin\frac{n\pi x}{L}, \quad n=1,3.... \qquad (1.15)$$

where $$a = \frac{R_o}{2\rho_m d} - \left|\frac{1}{2}(\{C^2 + D^2\}^{\frac{1}{2}} - C)\right|^{\frac{1}{2}}$$

$$b = -\frac{X_o}{2\rho_m d} + \left|\frac{1}{2}(\{C^2 + D^2\}^{\frac{1}{2}} + D)\right|^{\frac{1}{2}}$$

Z_o = driving point impedance of the medium

$= R_o + jX_o$

$$C = \left(\frac{n\pi C_m}{L}\right)^2 + \left(\frac{X_o}{2\rho_m d}\right)^2 - \left(\frac{R_o}{2\rho_m d}\right)^2$$

$$D = \frac{R_o X_o}{2\rho_m{}^2 d^2}$$

ρ_m = density of strip material

$C_m{}^2 = E/\rho_m$

E = Young's modules

The amplitude is seen to comprise a sinusoidal oscillation of frequency which decays exponentially with time. For a viscous material Z_o is given by

$$Z_o = \left|\frac{\omega\rho_f\eta}{2}\right| \quad (1+j) \qquad (1.16)$$

where ρ_f = density of the fluid

η = viscosity of the fluid

ω = circular frequency of oscillation

and a then becomes

$$a = \left(\frac{n\pi C_m \rho_f \eta}{8L\rho_m{}^2 d^2}\right)^{\frac{1}{2}}, \quad n = 1, 3 \ldots \qquad (1.17)$$

An electronic computer is used to generate the impulse that sets the probe into vibration and then produces an electrical output proportional to a. From equation 1.17,

$a = K_1 \rho_f \eta$ where K_1 is system constant. The instrument thus reads (viscosity x density) of the fluid.

(b) Viscometer designed for biological fluids[29]:
The basic principle of design involves the electronic measurement of the damping constant of a tuning fork which is damped by the fluid immersion of needle-like leg projection, as shown in Figure 1.10. The elctro-magnetic driver and receiver are connected as part of an amplifier and phase locked loop circuit. In operation,

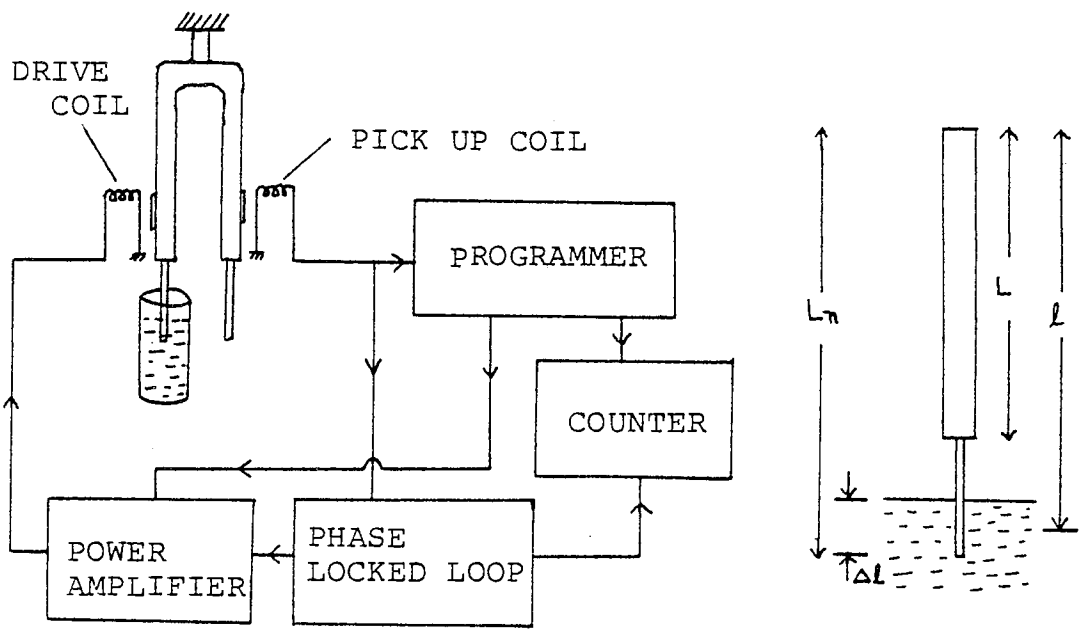

Figure 1.10

the tuning fork is part of an oscillatory system and quickly builds up to a pre-established maximum amplitude. The driver amplifier is then shut off by a programmer system and the oscillations naturally decay in amplitude exponentially. An electronic counter counts the number of oscillations, and provides a digital readout of these counts, until the amplitude of oscillation decays

1/e of the initial maximum amplitude. The electronic programmer then turns on the driver again, and the fork is driven to the maximum amplitude again to start the cycle over again. The digital readout of the number of cycles in the decrement, or natural decay is the parameter for the desired measurement. The number of cylces f_e, until the oscillation decays to 1/e of its initial amplitude is given by

$$f_e \simeq \frac{\sqrt{\delta\{\frac{1}{3}\rho_c|A_cL^3+A_n(L_n^3-L^3)|+\frac{1}{3}K_aM_a'L^2+K_\ell M_\ell'\ell^2}}{\pi\left|\frac{1}{3}K_a'M_a'\omega L^2+K_\ell'M_\ell'\omega\ell^2+K''\right|} \qquad (1.18)$$

where δ is the stiffness coefficient, ρ is material density, A the cross sectional area, L is the length of the tuning fork prong, $\Delta\ell$ is the length of the immersed part of the needle, ℓ is the distance from the pivot to the mid-point of $\Delta\ell$, L_n is the total length of the cylinder plus needle (Figure 1.10). The subscript c stands for tuning fork cylinder, n for the needle, a for air, and ℓ for test liquid. Thus M_a' and M_ℓ' represent, respectively, the mass of air displaced by the tuning fork and the mass of test liquid displaced by the immersed part of the needle, and K_a, K_a' and K_ℓ, K_ℓ' the Stokes coefficients for the air and liquid respectively. For fixed physical and geometric configurations, everything in equation 1.18 is known except K_ℓ and K_ℓ'. K_ℓ and K_ℓ' are functions of $(\omega A^2/\nu)$ where ν is the kinematic viscosity, so that by measuring f_e the value of the viscosity of the fluid can be determined.

CHAPTER 2

THE PRESENT DEVELOPMENT - A BRIEF OUTLINE

2.1 INTRODUCTION

Various transducers using electromechanical resonators, developed in the past, for the measurement of physical variables such as fluid density, fluid pressure, temperature, force, viscosity, etc., have been reviewed in the previous chapter. The work described in this thesis is the result of an attempt to develop some improved versions of this type of transducer for measuring fluid density and force in the form of tension. Improvements in such factors as sensitivity, accuracy, robustness, simplicity and cost have been the aims. Some resonators of special structural configurations have been considered and studied for this purpose. The resulting designs have been used to achieve the improvements of the transducers. The basic operating technique adopted is that of frequency domain, as described in Chapter 1. This technique has been used for its various advantages, already discussed there.

2.2 A GENERAL VIEW OF THE RESONATORS

Figure 2.1 shows general designs of the resonators. 2.1(a) is a pair of clamped-free-free-free rectangular plates and 2.1(b) is a pair of circular disks clamped together at the centre by a post. These designs are for

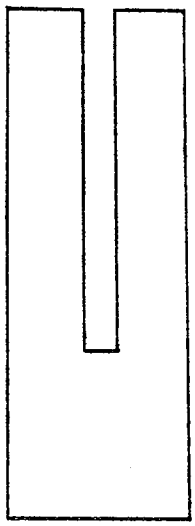

(a) A pair of clamped-free-free-free rectangular plates. (For fluid density transducer).

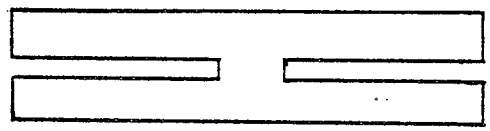

(b) A pair of circular disks clamped at the centre by a post. (Also for fluid density).

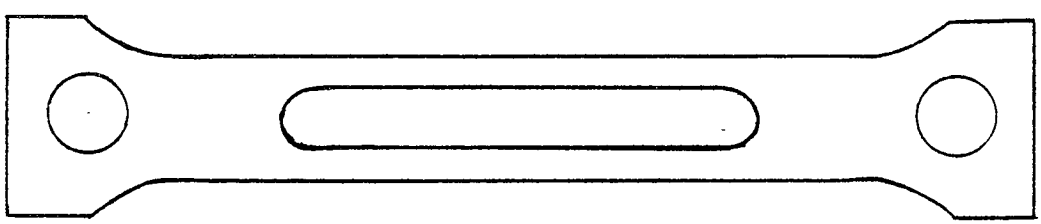

(c) A pair of clamped-free-clamped-free beams. (For tension transducer).

FIGURE 2.1 A general view of the resonators shown in section.

fluid density transducers. That for a tension transducer is a pair of clamped-free-clamped-free beams, as shown in 2.1(c). Considering structural configurations and their desired flexural mode of vibration, they may be classifield as a type of double resonators. In the literature, the most familiar double resonator is the tuning fork. It has a long history of various applications. Lord Rayleigh used an electrically maintained tuning fork to measure temperature. Where the accuracy requirement does not justify the higher cost of crystal controlled oscillators, tuning forks are widely used as frequency standards[37]. Other typical applications are in time and frequency measuring devices[38,39], fixed audio filters[40,41], and remote control systems[42]. In our laboratory much work had been done successfully to develop ultrasonic thermometers using specially designed double resonators[18-20] which may be taken as a type of tuning fork. A general view of a typical one of them is shown in Figure 2.2. From the view point of their desired mode of vibrations - flexure of the two members in anti-phase, the resonators used by the author may also be regarded as some types of tuning forks. For example the resonator of Figure 2.1(a) may be taken as a rectangular plate tuning fork, that of Figure 2.1(b) as a circular plate tuning fork, etc..

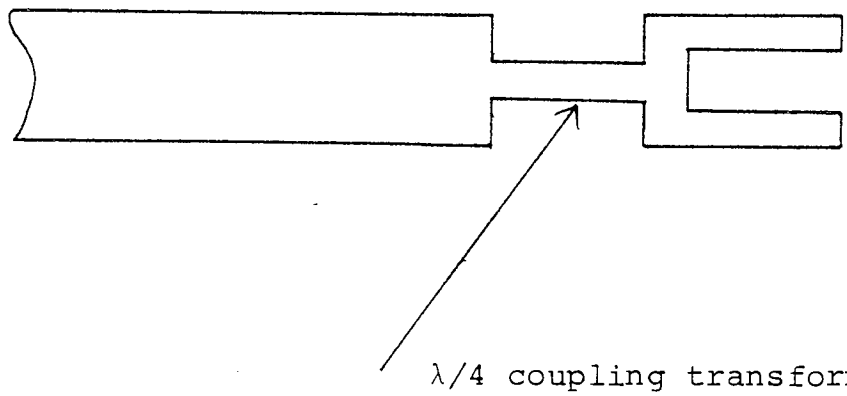

FIGURE 2.2 A double resonator used for ultrasonic thermometry

A brief outline of the properties of these double resonators, which are the basis of the proposed developments, is given in the following sections.

2.3 DOUBLE RESONATORS AND DYNAMIC CLAMPING

The use of mechanical resonators in the designs of transducers and also other practical situations, generally require one or more of the boundaries of the resonators to be clamped. This clamping condition is, however, difficult to realise practically but the use of double resonators gives a simply realisable method of approximating to this condition by the phenomenon of dynamic clamping. It is a situation created by the opposing motion of the two members of a double resonator vibrating in anti-phase. Thus at

the base of a tuning fork, because of the constraining effect one tine sets on the other, the angular momentum of one tine exactly balances that of the other. The static equivalent is the clamped reed, where it is assumed that the clamp is sufficiently massive to react to momentum changes without energy absorption. Consider the vibration of the resonator of Fig. 2.1(a) as shown in Fig. 2.3. When the two tines perform the kind of motion indicated, the very small displacement at point p will be in the x direction only, since the resultant

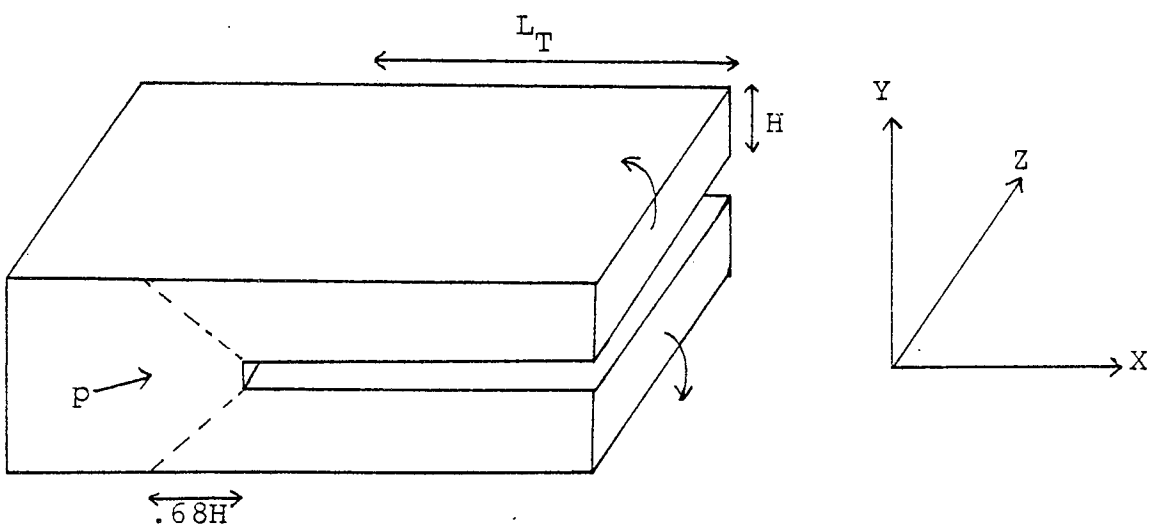

FIGURE 2.3 A Double Resonator in Tuning Fork-like Vibration

L_T is the tine length and 0.68H is the empirical correction of Karlmarczie.

of that in y direction will be zero. In addition, the

differential of the displacement in the Y direction will be zero. Therefore since

$$U_y = \frac{\partial U_y}{\partial x} = 0 \qquad (U_y \text{ is displacement in y direction}) \tag{2.1}$$

at y=0, it seems reasonable to assume that the kind of boundary condition that exist should be related to that of clamped. However, because of the complexity of the problem, theoretical solutions are not readily obtainable to locate the position of p on x-axis. Karlmarczie[43] depending on experimental results, made an empirical approach to solve the problem. He compared the natural frequencies of the tines of the double resonator with that of a statically C.F.F.F. plate, by developing a dimensionless frequency factor. Thereby he concluded that the tines may be taken in C.F.F.F. state by assuming an apparent increase in length L_T by a factor proportional to thickness H. He also found that this proportionately factor C depends on the particular mode of vibration. He determined the values of C for first and second modes of tuning fork like vibration, approximately, as 0.68 and 1.14 respectively.

Similar conditions may be assumed for the other resonators of Figure 2.1, as have been verified experimentally in Chapters 4 and 6. Thus it can be seen that the problem of clamping in designing transducers with mechanical resonators, is made considerably easier

by using this type of double resonator.

2.4 DOUBLE RESONATORS AND FLUID DENSITY TRANSDUCERS

A general view of the particular structures of the double resonators designed for fluid density transducers has been shown in Figures 2.1(a) and 2.1(b). A significant feature of these resonators is that a thin layer of fluid is trapped between the vibrating members. This feature may be taken as a main criterion for the proposed improved versions of density transducers.

When a vibrating body is immersed in a fluid medium, there are changes in the dynamics of the body due to loading effects of the fluid. This interaction may be used as a good basis for designing density transducers. In the past several such transducers were built with different structures of resonators giving various degrees of success , as already discussed in Chapter 1. While based on the same fundamental principle, the present structures have been designed with an aim to have a significant improvement in sensitivity of the transducers. At the same time improvements in robustness, simplicity, cost, etc., have also been looked for.

Fluid loading effect on a resonator may be split up into three main divisions

(a) reactive loading

(b) sound radiation loading

(c) viscous loading.

Of these the first one has the effect of changing the natural frequencies of the resonator, while due to the other two its vibrations are damped. Therefore in designing frequency domain transducers utilising fluid loading effects, a normal attempt is a maximisation of reactive loading with possible minimums of the other two. Reactive loading may be expressed by an equation of the form

$$\omega^2 = (S_e + \Delta S)/(M_e + \Delta M) \qquad (2.2)$$

where ω is a natural frequency of a resonator, S_e is the stiffness and M_e is the mass of its corresponding in vacuum equivalent lumped circuit. ΔS and ΔM are the effective changes in stiffness and mass respectively due to the loading. From equation 2.2 it can be seen that ΔM, which arises from the additional kinetic energy stored by the resonator in its surrounding fluid, lowers the natural frequency. On the other hand ΔS - due to compression of the fluid raises the natural frequency. The resultant change depends upon the relative values of ΔM and ΔS. ΔM is the one which is normally related directly with the density of the fluid. Thus a predominant mass effect (negligible stiffness effect) is usually the desirable criterion for designing density transducers. Conditions under which compression, hence stiffness effect is negligible, can be found in the literature. A main one is that the wavelength of sound in the fluid should be

considerably larger than the geometrical dimensions of the vibrating body[44,45]. In view of the above comments and also of supporting results of preliminary experiments, the double resonators were designed to operate at low frequencies (typically below 5kHz). Low frequency also increases the magnitude of the mass effect. The interpretation given by Junger[46] is that at high frequencies, the resonator vibrates with such rapidity that the disturbance does not travel far before the action is reversed; whereas with low frequency the resonator tends to accelerate larger quantities of fluid. Again this low frequency helps to keep the unwanted loss due to sound radiation loading at a low value.

The literature indicates that at low frequencies mass effect is normally highest at the fundamental flexural mode of vibration of the resonator[47]. This being the lowest frequency mode also favours geometrical designs. Another practical advantage of this mode is its good isolation from other modes. This generally helps in the design of the associated electrical circuits for maintaining the vibration of the resonators in this mode (see Chapters 4 and 5).

Initial experiments with the double resonators support the above discussed criteria of fluid-vibrating body interaction. In fact in those experiments it was found that these resonators at low frequency fundamental flexural mode, are a very convenient type of structure to obtain pre-

dominant mass effect of high values. This initiated further practical and theoretical investigations with them for the proposed development. Theoretical analysis has been discussed to a detail in Chapter 3; while experimental verifications and thereby practical designs for gas density and liquid density transducers have been discussed in Chapters 4 and 5 respectively.

To have a preliminary idea, added mass ΔM for the double resonator of Figure 2.1(b) (analysed in Chapter 3 as an approximate model of two disks in piston like motion at low frequencies) has been found to be

$$\Delta M = \frac{3\pi\rho_f R^4}{20\ h_o} \qquad (2.3)$$

where ρ_f = fluid density

R = radius of the disks

$2h_o$ = initial gap between the disks.

Added mass for a single disk in piston like motion at low frequencies (in an infinite baffle) is given by[48]

$$\Delta M = \frac{8\rho_f R^3}{3} \qquad (2.4)$$

It can be seen that ΔM of equation 2.3 is greater than that of equation 2.4 by a multiplication factor of $.18(R/h_o)$. For the rectangular plate double resonator a similar multiplication factor W/h_o, where W is the width of the plates, has been found. In a practical design for a gas

density transducer (liquid density will be discussed separately, later on in this section, for reasons stated there) R or W, as the case is, can be made much larger than h_o. In typical designs as shown in Figures 2.4(a) and (b), R or W is about two hundred times larger than h_o. This gives high values of sensitivity even with such robust structures as shown in those figures. The sensitivity of the resonator of Figure 2.4(a) results in a 20% change of frequency for density change from 0 to 20 kg/m^3. That of the resonator of Figure 2.4(b) is about a 20% change of frequency for density change from 0 to 10 kg/m^3. Simplicity of structure, particularly the rectangular one, is also a virtue of the present design. Moreover this type of structural configurations makes it very convenient to maintain the oscillation of the resonators by a considerably simple and more reliable electrical circuit (Chapter 4). In addition to the conventional uses of a gas density transducer, the present design has been found to have potentiality of being developed for special uses such as a detector stage of a gas chromatographic system. This has been discussed in Chapter 4.

Typical geometrical dimensions of a practical design of the double resonator for a liquid density transducer are as shown in Figure 2.5. It may be noted that while all other dimensions are of same orders as for a gas density transducer, the gap $2h_o$ between the

two vibrating members is relatively wider. This has been done from the practical point of view, of allowing free movement of the liquid surrounding the resonator. Due to this required wider gap the rectangular one of the resonators has been found to be more practical from the manufacturing point of view, as discussed in Chapter 5. Though a wider gap lowers the multiplication factor, the retained sensitivity is quite high considering the relatively higher densities of liquids. The sensitivity of the typical unit of Figure 2.5 is about a 55% reduction in frequency for a density span of 1000 kg/m^3 (i.e. vacuum to water). All the other virtues of the gas density transducers - dynamic clamping, robustness, simplicity, low cost, are also present in the liquid one.

2.5 DOUBLE RESONATORS AND TENSION TRANSDUCERS

Changes in stiffness of a mechanical body may be arranged to be a direct effect of changes in tensile stress applied on it. Resonant frequencies of the mechanical body are functions of its stiffness. Thus they can be good measures for the applied tensile force. On this basic principle there are, as mentioned in Chapter 1, a number of developments using such mechanical bodies as wires, beams, etc.. However in these designs much difficulty was encountered regarding an important requirement - efficient clamping arrangements for the resonators. With an aim to overcome this problem, the type of double

resonators, shown generally in Figure 2.1(c) and in typical geometrical dimensions (for a range 0-5kN) in Figure 2.6 has been designed. As already discussed in Section 2.3, dynamic balancing in this type of resonator makes the problem of clamping easier. Development of a tension transducer using this type of resonator has been discussed in detail in Chapter 6.

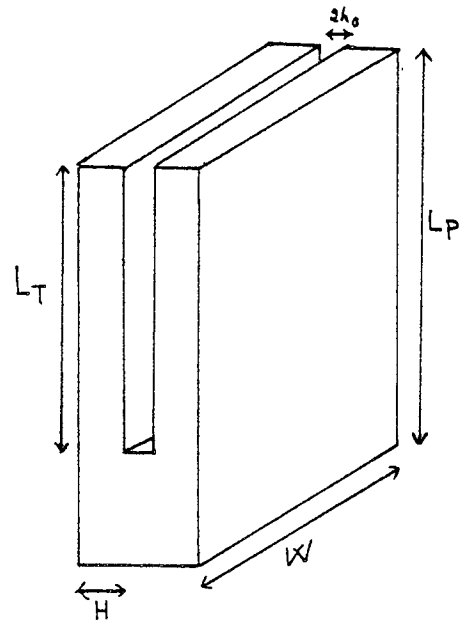

(a) Rectangular plate tuning fork.

Dimensions (m x 10^2):

L_p	: length of the plates	= 3.8
L_T	: length of the tines	= 2.54
W	: width of the tines	= 2.54
H	: thickness of the tines	= .254
$2h_o$	: gap between the tines	= .04

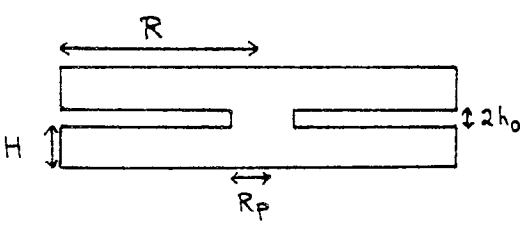

(b) Circular plate tuning fork

Dimensions (m x 10^2):

R	: radius of the disks	= 2.54
R_p	: radius of the post	= .237
H	: thickness of the disks	= .254
$2h_o$	: gap between the disks	= .04

FIGURE 2.4 Typical geometrical dimensions of the resonators for gas density transducers. The gap between the vibrating members is very small in comparison to width or radius (as the case is) of the resonator.

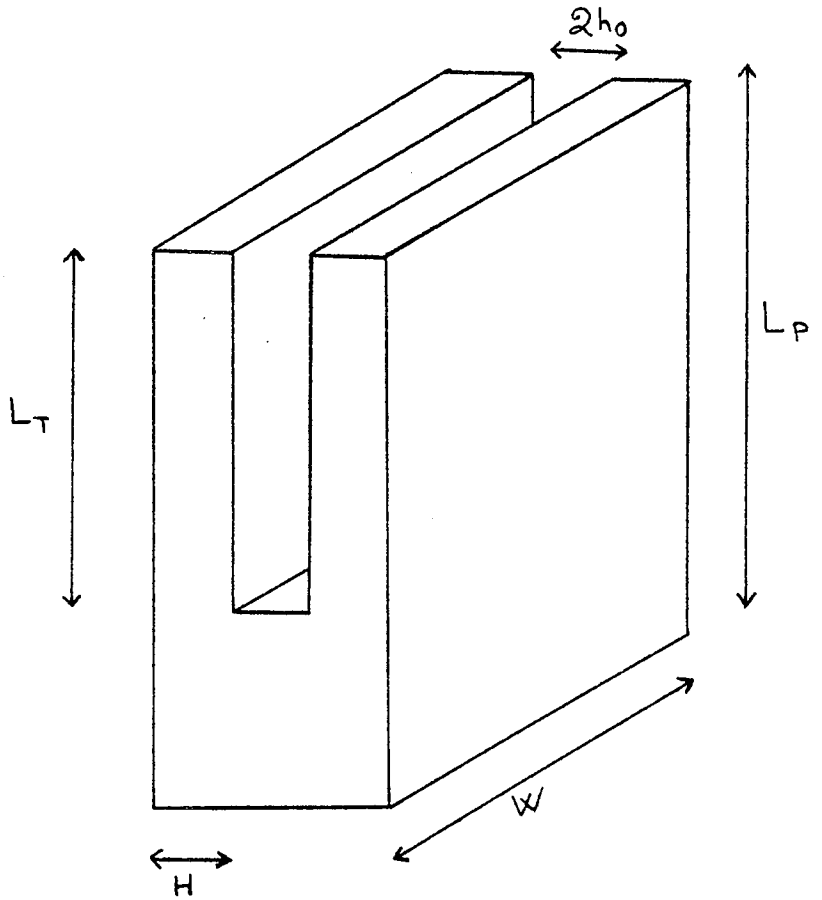

L_p : length of the plates = 3.8×10^{-2}m

L_T : length of the tines = 2.54×10^{-2}m

W : width of the tines = 2.54×10^{-2}m

H : thickness of the tines = 2.54×10^{-3}m

$2h_o$: gap between the tines = 2.54×10^{-3}m

FIGURE 2.5 Typical geometrical dimensions of the resonator for the liquid density transducer. The gap between the tines is wider in comparison to that for the gas density transducer.

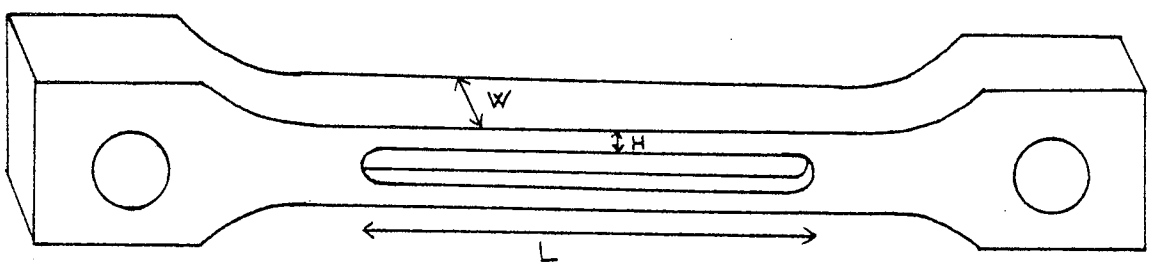

L : Length of beams = 5.39×10^{-2}m

H : thickness of the beams = 0.13×10^{-2}m

W : width of the beams = 0.6×10^{-2}m

FIGURE 2.6 Typical geometrical dimension of the resonator for the tension transducer for a range of (0-5) kN.

It can be seen that the holes by which the force is applied are remote from the vibrating members.

CHAPTER 3

VIBRATING BODY - FLUID INTERACTION

3.1 INTRODUCTION

An elastic structure vibrating in a fluid medium experiences loadings due to its interaction with the fluid, which results in the modifications of the forces acting on it. Thereby the in-fluid dynamic characteristics of the structure may differ considerably from its characteristics in vacuo. This phenomenon being the basis of the density transducers, as already mentioned previously, an analytical investigation of it is presented in this chapter. Firstly, a general outline of the loading effects has been given followed by a discussion of some common approaches and techniques of analysis found to be in use in the literature. Thereafter a brief review of the cases of some structures of vibrating bodies, comparable with the present resonator, has been given. Finally the present resonator has been analysed revealing some features of it, significant for the improvements in aim.

3.2 AN OUTLINE OF THE PHENOMENON

There are three main classifications that may be given to the loading effects on a structure due to the interaction:

(a) The vibrating body sets the fluid into motion and thus stores additional kinetic energy in it. This has an inertial reaction on the resonator dynamics which effectively is an apparent increase in the mass of the body. This mass loading causes a lowering in the resonant frequency of the body. While normally there is always this mass loading, there could be a stiffness loading, due to compression of the fluid, which raises the resonant frequency. The net effect of the two reactive loadings depends upon their relative values.

(b) Energy is radiated away from the body in the form of sound. This has a damping effect on the body which causes its free vibration to decay in amplitude. In general the radiation of sound decreases as the ratio of resonator size to acoustic wavelength in the fluid decreases.

(c) By virtue of the motion of the structure in the fluid, viscous drag forces are produced on the structure. This also has a damping effect on the body.

The magnitudes of the above mentioned effects depend on such factors as geometrical dimensions and structural configurations of the body, mode of vibration, frequency of resonance, and physical properties of the fluid. As already mentioned in Chapter 2, a predominated mass loading of significant value is a good basis for designing

a fluid density transducer. The analysis of the present resonator (section 6 of this chapter) shows a very convenient way of achieving this.

3.3 APPROACH - ACOUSTIC vs HYDRODYNAMIC

The vibrating body-fluid interaction is quite an old and vastly studied phenomenon in the literature. Dubut in 1786 and Bessel in 1826, while studying the sources of errors in pendulums, found that it was necessary to attribute to an oscillating sphere in a fluid a virtual mass greater than that of the body alone (i.e. the mass effect). The vast study of the phenomenon can be found in various literature such as Acoustics, and Hydrodynamics. Some main concerns regarding it in Acoustics, are its effects on such phenomena as the radiation and the scattering of sound. A good reference is the book by Junger and Feit[45]. Its influences on drag force on the body, lift on the body, flow of the fluid are some main topics of interest in Hydrodynamics. Books by Lamb[49], Landau and Lifshitz[50] are good references. Though dealings with the interaction problem in both Acoustics and Hydrodynamics are mainly in their own domains of interest, a useful amount of information about the loading effects (on which the present density transducer is based), is also available there. Thus the mass loading is found to be dealt with in both Acoustics and Hydrodyanmics, while usually, radiation loading is dealt in the former and viscous loading in the latter.

A rigorous theoretical analysis of the interaction problem taking all the involving factors into account, is too difficult if not impossible. Thus a normal procedure in the literature is to solve a particular case under some consistent assumptions and approximations, thereby simplifying the situation. In the words of Cottrell[51], (from hydrodynamical approach), - "the general equations are formidable but fortunately many simplifying concepts can be introduced, e.g streamline flow, irrotational flow, representation of velocity in terms of potential, which when combined with various approximations, e.g. neglect of viscosity and compressibility, enables a variety of problems to be solved". Von Karman[52], in 1954, stated, "looking back on fifty years of aerodynamic research, it appears to me most remarkable that the crude approximation which considers the air as an incompressible fluid has proved itself so valuable in solving many practical problems of aircraft design".

There is no sharp line of demarcation between the hydrodynamic and acoustic approaches. Usually, when the body is in steady or accelerated motion (an approximation of low frequency oscillation), the former approach is more suitable. Oscillatory motions, particularly in high frequency range, are best dealt with by the latter approach. Thus two important usual assumptions in the former approach are to take the fluid as incompressible and to ignore the radiation of sound. In the latter

approach a common assumption is to take the fluid as inviscid. This simplifies the problem significantly as then only normal loading on the body comes into account. The two approaches may be related by examining the results which show that as frequency of oscillation $\omega \to 0$, normally acoustic solutions tend to those of hydrodynamic. This will be more clear in Section 3.5, where some specific cases will be discussed.

Again another simplifying approach is to consider the various effects separately as if the others were absent. Then the net performance is approximately the sum of the separate effects.

3.4 TECHNIQUES OF ANALYSIS

For the analysis of the interaction problem, various techniques are found in the literature. Two widely adopted and suitable, particularly for finding the loading effects on the body (which are of primary concern in the present work) are

(a) Impedance method

(b) Energy method.

The present analysis being also based on these two techniques, a brief discussion of them follows:

(a) Impedance method: the concept of mechanical impedance of a system has been borrowed from electrical circuit theory. In the latter case the impedance is defined as voltage divided by current flow. By analogy

mechanical impedance is taken as force divided by velocity. Thus in the present case of interaction, the loading effects on the resonator may be expressed by an impedance which is the ratio of the excess pressure at its surface to its velocity. Various names of this impedance such as radiation impedance, mechanical impedance of the fluid load, are found to be in use in the literature. The latter one seems to be more appropriate for the present case. Normally the impedance, expressed in complex notation, will have a real term R_L and an imaginary term X_L corresponding to the in phase and quadrature components respectively, of pressure and velocity. Thus mechanical impedance of the fluid load Z_L is

$$Z_L = \frac{\text{excess pressure at the surface}}{\text{velocity of the surface}} = R_L + jX_L$$

In parallel to electric circuit theory, R_L is the ohmic part and thus represents the energy dissipated by the resonator. The reactive part X_L represents the amount of energy fluctuating between the resonator and the medium. Thus positive X_L stands for the mass effect and negative X_L for the stiffness effect. The magnitudes of the effects can be found from the values of R_L and X_L. For example, in case of a harmonic vibration of angular frequency ω, the added mass (i.e. the apparent increase in the mass of the resonator) ΔM is given by

$$\Delta M = \frac{X_L}{\omega} \qquad (3.1)$$

(b) Energy method: This is based on the fundamental principle of the conservation of energy. Thereby an equation can be obtained relating the change in energy of the system and the work done on it. Information regarding the loading effects may be found from this equation. For example, the change in resonant frequency of the body due to the inertial loading can be found from a resultant expression of the energy equation of the form

$$\frac{f_f}{f_o} = \frac{1}{\sqrt{1+T_{fm}/T_{om}}} \qquad (3.2)$$

where f_o = in-vacuo resonant frequency of the body

f_f = in-fluid resonant frequency of the body

T_{om} = in-fluid maximum kinetic energy of the body

T_{fm} = Maximum kinetic energy of the fluid.

Though comparatively simpler than the impedance method, a drawback of the energy method is that it often requires more idealized assumptions to be solved readily.

3.5 A BRIEF REVIEW OF THE LOADING EFFECTS ON SOME STRUCTURES

Because of the complexity of the problem, generally in the literature, analytical solutions are found for simple structures of resonators such as spheres, ellipsoids and circular pistons. Moreover, for simplification, normally they are analysed under some assumptions and approximations,

as discussed in section 3.3. A review of some of them is given in order to have a comparative idea between them and the present resonator (whose analysis will be given in Section 3.6). It will also help in making consistent assumptions for simplifying the analysis of the present resonator.

Predominant mass effect being the basis of the density transducer, there is an emphasis on it in the review. Some important assumptions common to all the cases discussed are

(a) the oscillation is harmonic,

(b) strains are small enough in both the structure and the fluid, so that they are linearly related to the excitation.

(c) both the solid and the fluid media are homogeneous.

3.5.1 An Oscillating Sphere

It is a sphere whose radius remains constant while the sphere executes a movement of translation as a function of time. This case is found to be dealt with extensively in both hydrodynamic and acoustic literatures[50,53,54]. In the hydrodynamic approach usually the frequency of oscillation is taken to be zero (an approximation of low frequencies), i.e. the body is in unidirectional accelerated motion. Thus compressibility of the fluid is ignored and for an inviscid fluid the drag force F on the sphere is given by

$$F = \frac{2}{3}\pi R^3 \rho_f \frac{dU}{dt} \qquad (3.3)$$

where R = radius of the sphere

ρ_f = density of the fluid

U = velocity of the sphere, assumed to be low, so that no turbulence is produced

t = time

As force is mass multiplied by acceleration, the added mass ΔM due to the fluid loading is

$$\Delta M = \frac{2}{3}\pi R^3 \rho_f \qquad (3.4)$$

Taking viscosity of the fluid into account, the drag force F is given by

$$F = \frac{2}{3}\pi \rho_f R^3 \frac{dU}{dt} + 6\pi R\mu U \qquad (3.5)$$

where μ = viscosity of the fluid

and all other notations have the same meanings as in equation (3.3).

The first term of the right hand side of equation (3.5) gives the same value of ΔM, as given by considering the fluid inviscid. The other expression being related to the velocity gives the dissipation of energy of the body due to the viscous loading (the famous Stokes' formula).

From the acoustical approach, in which the radiation of sound is taken into account while viscous loading is neglected, the mechanical impedance of the fluid load Z_L is given by

$$Z_L = \frac{4\pi R^2 \rho_f c}{3} \left| \frac{K^4R^4 + j(2KR + K^3R^3)}{4 + K^4R^4} \right| \qquad (3.6)$$

where R = radius of the sphere

ρ_f = density of the fluid

c = velocity of sound

$K = \frac{\omega}{c}$, where ω is the angular frequency of oscillation of the sphere

$j = \sqrt{-1}$

As already mentioned (section 3.4), the expression with j gives the reactive part X_L (being positive it is mass effect) and that without j gives the resistive part R_L (i.e. the damping effect due to sound radiation). They are plotted in Figure 3.1 from which it can be seen that at low values of KR (i.e. approach to hydrodynamic case) the mass effect is predominant with very low value of damping due to sound radiation.

For KR << 1, i.e. approach to hydrodynamic case, from equation (3.6)

$$\Delta M \equiv \frac{\text{Reactive part of } Z_L}{\omega} \simeq \frac{2}{3} \pi R^3 \rho_f \qquad (3.7)$$

the same as given by hydrodynamic approach (see equation 3.4). It is worth noting from the above expression that in the hydrodynamic region ΔM is almost independent of frequency of oscillation of the body. This is a significant criterion for the resonator of the density transducer.

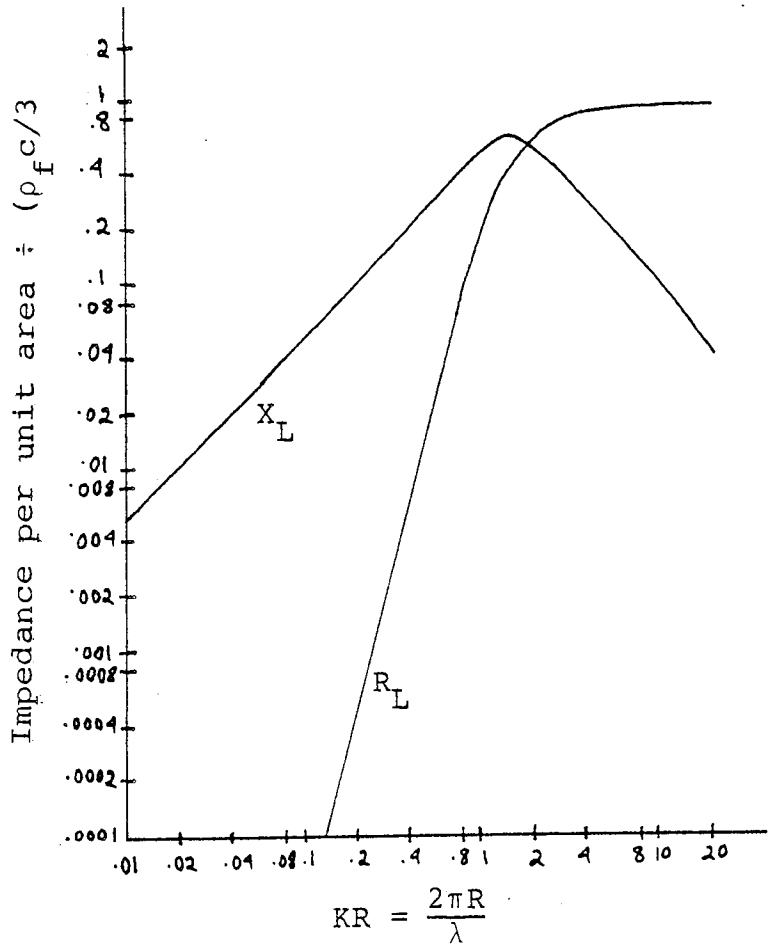

FIGURE 3.1 The resistive part R_L and the reactive part X_L of the mechanical impedance of the fluid load of an oscillating sphere. At low values of KR, R_L is negligible, i.e. damping due to radiation of sound can be ignored when wavelength of sound in the fluid medium is much larger than the radius of the sphere.

3.5.2 A Pulsating Sphere[54]

It is a sphere whose radius increases and decreases with time. The motion of the fluid around the sphere will, like the motion of the sphere itself, take place only in radial direction (assuming non-turbulence).

From acoustical approach(with the same assumptions as in the previous case) the mechanical impedance of the fluid load Z_L is given by

$$Z_L = 4\pi R^2 \rho_f C \left| \frac{(KR)^2 + jKR}{1+(KR)^2} \right| \qquad (3.8)$$

where all the notations have the same meanings as in equation (3.6).

As before the expression with j (being positive) corresponds to the mass loading and that without j corresponds to the radiation loading. They are plotted in Figure 3.2(a) which shows the predominated mass effect at low values of KR (with negligible radiation loss).

From equation (3.8), the added mass ΔM is

$$\Delta M \equiv \frac{\text{Reactive part of } Z_L}{\omega} = \frac{4\pi R^3 \rho_f KC}{\omega \left| 1+(KR)^2 \right|} \qquad (3.9)$$

For $KR \ll 1$, i.e. when the situation tends to hydrodynamic, the value of the predominant added mass is

$$\Delta M \simeq 4\pi R^3 \rho_f \qquad (3.10)$$

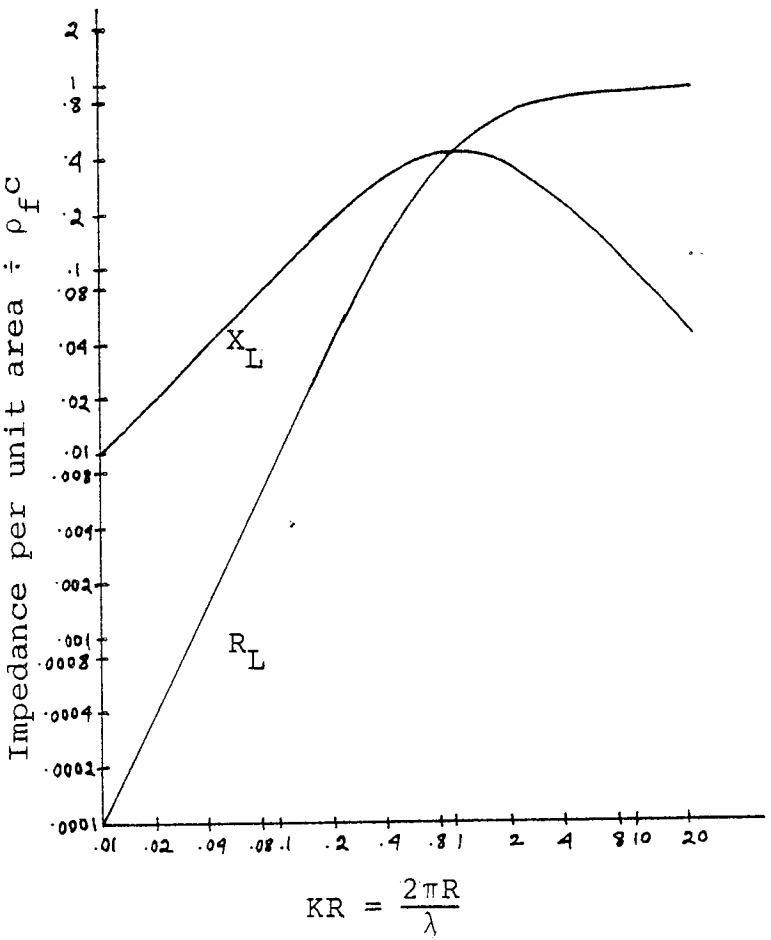

FIGURE 3.2(a) The reactive part X_L and resistive part R_L of the mechanical impedance of the fluid load of a pulsating sphere. At low values of KR i.e. when wavelength λ of sound in the fluid medium is much larger than the radius of the sphere, loss due to sound radiation is negligible and reactive (mass) loading is predominant.

which is independent of frequency (same as the previous case). Values of ΔM as given by equation (3.10) are plotted in Figure 3.2(b), which also shows the hydrodynamic region. The increasing value of ΔM as KR decreases is also apparent from this figure.

3.5.3 A Circumferentially Clamped Circular Plate With Fluid On One Side

This was originally studied by Lamb[44]. He assumed the dynamic deflection curve of the plate of the form

$$W(r) = A'(1 - \frac{r^2}{R^2})^2 \qquad (3.11)$$

where $W(r)$ = normal displacement of the plate at r

r = distance from the centre

R = radius of the plate

A' = a function of time

He also assumed the fluid as incompressible and ignored viscosity loading. With these assumptions he adopted the energy method (see Section 3.4b). Thus he calculated the kinetic energy of the plate T_o from the formula

$$T_o = \pi \rho_m H \int_0^R (\frac{\partial W}{\partial t})^2 \, r \, dr \qquad (3.12)$$

where ρ_m = density of the plate material

H = thickness of the plate

and all other notations have got the same meaning as in equation (3.11).

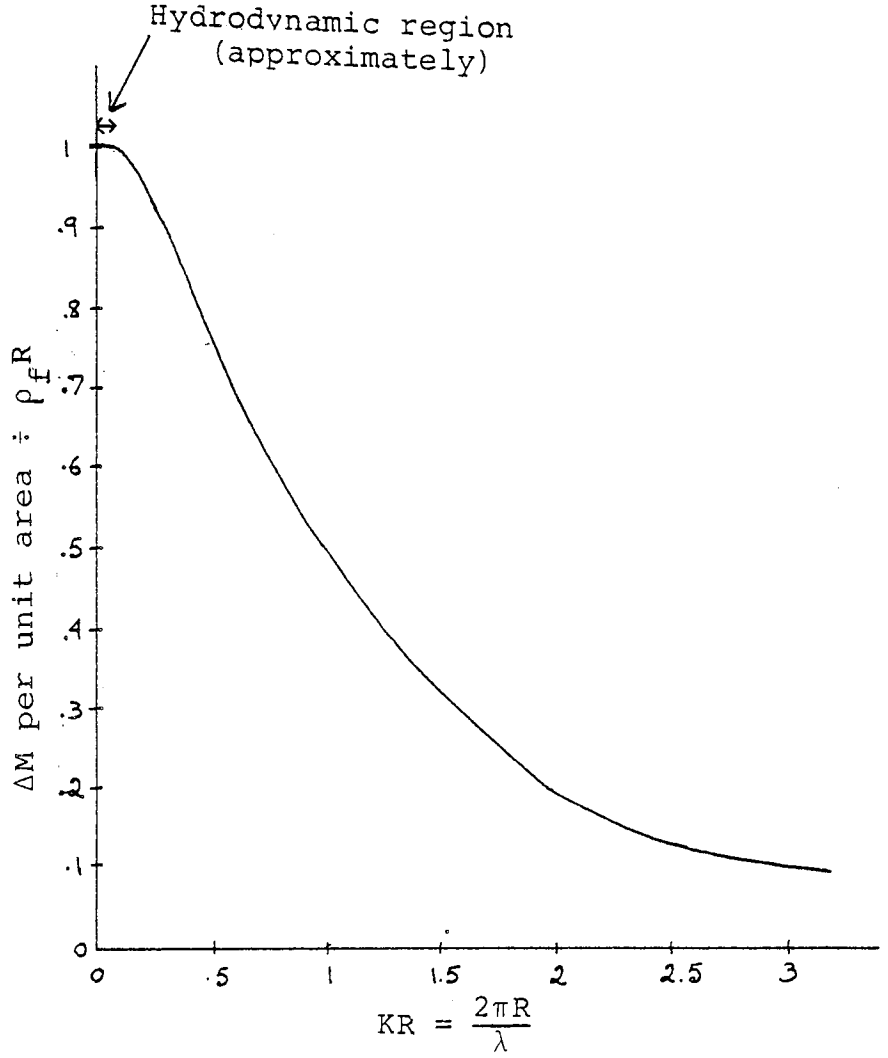

FIGURE 3.2(b) Added mass ΔM per unit area (which is equal to X_L/ω, see Figure 3.2(a)) of a pulsating sphere. In the hydrodynamic region, ΔM is largest and almost independent of KR, hence of the frequency of oscillation.

He then worked out the velocity potential of the fluid at the surface of the plate and with it the kinetic energy of the fluid T_f by the use of the formula.

$$T_f = \frac{1}{2} \rho_f \int\int \phi \frac{\partial \phi}{\partial n} \, ds \qquad (3.13)$$

where ρ_f = density of the fluid

$\frac{\partial \phi}{\partial n}$ = normal velocity of the surface (as no slip condition is assumed at the interface between the plate and the fluid medium)

ds = elemental area of the plate.

From the maximum values of T_o and T_f, he then calculated the change in frequency of the plate, by using the relation of equation (3.2) and found to be

$$\frac{f_f}{f_o} = \frac{1}{\sqrt{1+.6689 \frac{\rho_f}{\rho_m} \frac{R}{H}}} \qquad (3.14)$$

where f_o = frequency in vacuum

f_f = frequency in the fluid

It may be mentioned here that in terms of added mass ΔM the change in frequency is given by the formula

$$\frac{f_f}{f_o} = \frac{1}{\sqrt{1+ \frac{\Delta M}{M}}} \qquad (3.15)$$

where M = dyanmic mass of the plate.

A more rigorous analysis than that by Lamb was carried out by Lax[47]. He dropped the assumption of incompressibility and solved the problem by the impedance method. The added masses evaluated for various symmetrical modes of flexural vibrations are shown in Figure 3.3. An important feature which is of much help for the analysis of the resonator of the present transducer, can be found from the figure. Thus it is seen that at low KR (which is the region of interest in the present work),the added mass at fundamental mode is by far greater than that at other modes. Other common features of mass loading (at fundamental mode), e.g. its almost independency of frequency in hydrodynamic region and largest value at this region, can also be seen.

3.5.4 A Vibrating Circular Piston in an Infinite Baffle

This case being directly comparable with the model via which the resonator of the present density transducer has been analysed (section 3.6), a detailed discussion of it is given. Various analytical procedures of this case using different approaches and techniques can be found in the literature. The one discussed here is through acoustical approach and following Stephens and Bate[48].

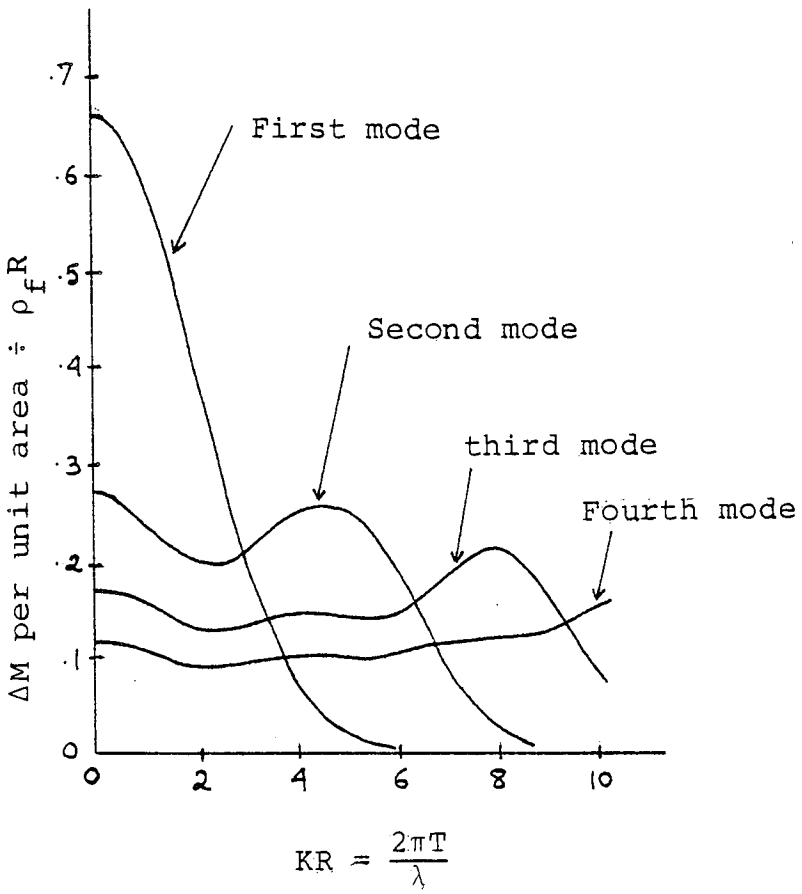

FIGURE 3.3 The added mass ΔM per unit area of a circumferentially clamped plate with fluid loading on one side only. Data for the first four symmetrical flexural modes is given. At low values of KR, hence at low frequency, the fundamental mode gives the highest loading.

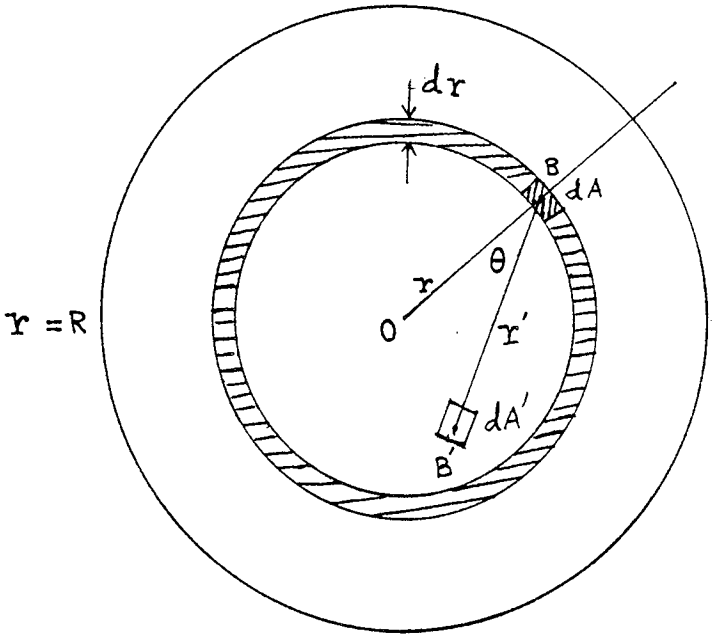

FIGURE 3.4 RADIATING FACE OF THE PISTON

It is assumed that the rigid circular piston is vibrating in an infinite baffle and that each point on the plane surface may be considered as a source of hemispherical waves.

In Figure 3.4, B is any arbitrary point on the circular piston face at which is located the small elementary area dA. Suppose that α is the amplitude of the velocity potential produced per unit area of the vibrating surface at unit distance away (the vibrating element being considered to be vanishingly small). O is the centre of the circular radiating face, and through it is drawn the axis of a system of polar

co-ordinates with the pole located at B. Velocity potential at B due to elementary area dA' at B', distant r' from B is

$$\Delta\phi_B = \alpha \frac{dA'}{r'} e^{j(\omega t - Kr')} \qquad (3.16)$$

where ω = angular frequency of the harmonic vibration.

t = time

$k \equiv \frac{\omega}{c}$ = wave number

c = velocity of sound in the fluid.

Therefore total velocity potential at B is

$$\phi_B = \alpha e^{j\omega t} \int \frac{e^{-jKr'}}{r'} dA' \qquad (3.17)$$

α can be evaluated by considering the source of hemispherical waves at B' to be a pulsating hemisphere of radius r_o, which is finally to be made vanishingly small. This gives

$$\alpha = \dot{\eta}_o/2\pi \qquad (3.18)$$

where $\dot{\eta}_o$ = velocity amplitude of the piston.

At any point the acoustic excess pressure $p = \rho_f \frac{\partial \phi}{\partial t}$, where ρ_f is the equilibrium density of the fluid. Hence from equation (3.17) and (3.18)

$$p_B = \frac{j\omega\rho_f\dot{\eta}_o}{2\pi} e^{j\omega t} \int \frac{e^{-jkr'}}{r'} dA \qquad (3.19a)$$

Noting that $dA' = r' dr' d\theta$ and that the maximum distance

in the direction θ from dA to any point within the circle of radius r is $2r\,\mathrm{Cos}\theta$, then equation (3.19a) may be rewritten as

$$p_B = \frac{j\omega\rho_f \dot{\eta}_o}{2\pi} e^{j\omega t} \int_{-\pi/2}^{+\pi/2} d\theta \int_0^{2r\mathrm{Cos}\theta} e^{-jKr'} dr' \qquad (3.19b)$$

The total force exerted on the shaded ring by all elementary sources such as dA' within the circular area of radius r is

$$df_R = 2\pi r dr p_B$$

$$= j\omega\rho_f \dot{\eta}_o e^{j\omega t} r dr \int_{-\pi/2}^{+\pi/2} d\theta \int_0^{2r\mathrm{Cos}\theta} e^{-jKr'} dr' \qquad (3.20)$$

To obtain total force f_R on the piston, the forces on the rings are summed up, integrating from r=0 to r=R, and multiplying by 2 (because every pair of elements such as dA and dA' will appear twice, once as an elementary receiver and the other as an elementary source).

Hence

$$f_R = 2j\omega\rho_f \dot{\eta}_o e^{j\omega t} \int_0^R r dr \int_{-\pi/2}^{+\pi/2} d\theta \int_0^{2r\mathrm{Cos}\theta} e^{-jKr'} dr$$

$$= \pi R^2 \rho_f c \dot{\eta}_o e^{j\omega t} \left| 1 - \frac{J_1(2KR)}{KR} + j \frac{K_1(2KR)}{2K^2R^2} \right| \qquad (3.21)$$

where J_1 and K_1 are Bessel functions of first order of first kind and second kind respectively. Therefore mechanical impedance of the fluid load

$$Z_L \equiv \frac{f_R}{\text{velocity of the piston}}$$

$$= \pi R^2 \rho_f c \left| 1 - \frac{J_1(2KR)}{KR} + j\frac{K_1(2KR)}{2K^2R^2} \right| \qquad (3.22)$$

As before the real term represents the dissipation of energy due to radiation of sound and the imaginary term represents the mass loading. They are plotted in Figure 3.5(a), from which the predominant mass loading and negligible radiation loading at low values of KR are apparent.

From equation (3.22), the added mass

$$\Delta M \equiv \frac{\text{Reactive part of } Z_L}{\omega}$$

$$= \frac{\pi \rho_f c \, K_1(2KR)}{2K^2\omega} \qquad (3.23)$$

In Figure 3.5(b) ΔM is plotted against KR, from which the increasing value of ΔM as KR decreases is apparent. It also shows that at low KR (i.e. hydrodynamic region) the effective mass tends to a constant value, independent of frequency.

From equation (3.23), this effective mass

$$\Delta M \simeq \frac{8}{3} \rho_f R^3 \qquad (3.24)$$

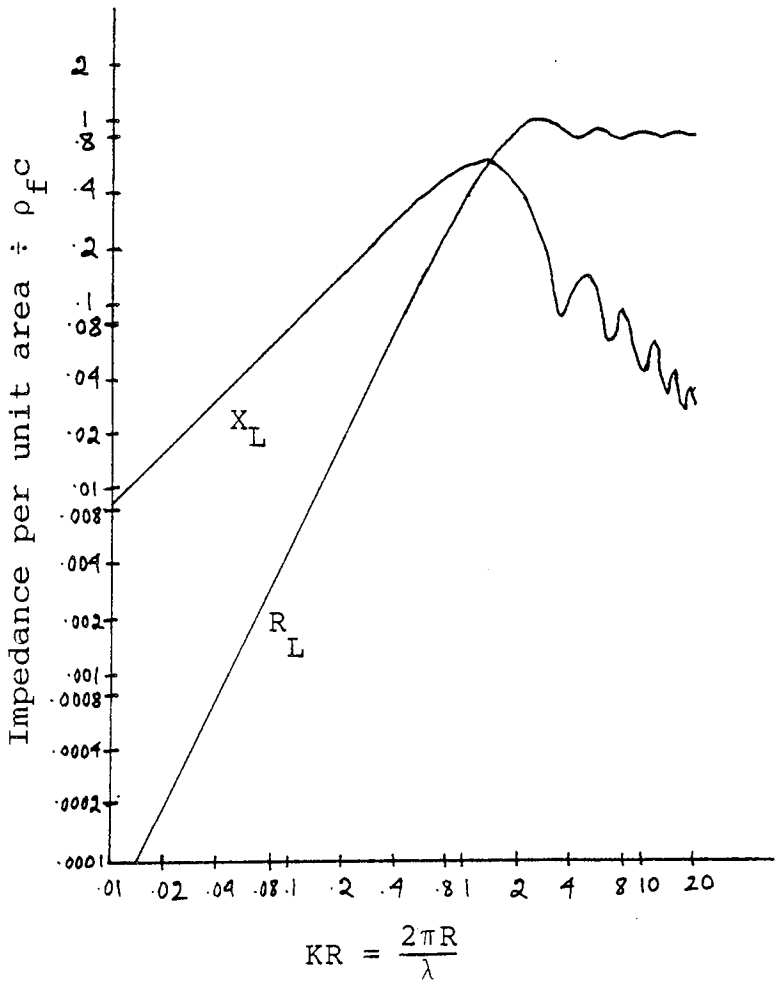

FIGURE 3.5(a) The reactive part X_L and resistive part R_L of the mechanical impedance of the fluid load of a circular piston in an infinite baffle. Radiation of sound is very negligible at low value of KR i.e. at low frequency or for small piston area. Reactive (mass) loading is predominant at this condition.

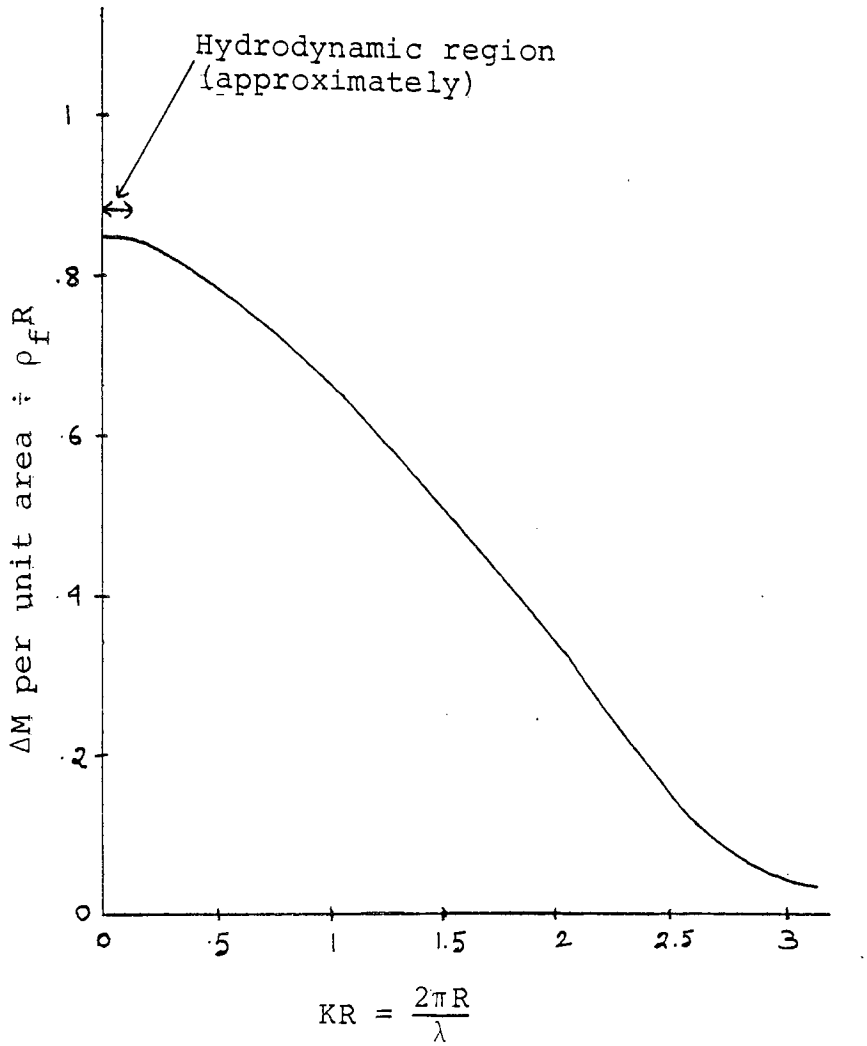

FIGURE 3.5(b) Added mass ΔM per unit area of a circular piston vibrating in an infinite baffle. At low KR (hydrodynamic region) ΔM is largest and almost independent of KR and hence of frequency.

3.6 THE FLUID LOADING EFFECTS ON THE PRESENT RESONATOR

The geometrical configurations and typical dimensions of the structure of the present resonator have already been shown in Chapter 2 (Figures 2.1, 2.4, 2.5). Of the two versions i.e. the circular plate tuning fork and the rectangular plate tuning fork theoretical analysis has been carried out for the former one. This is because of the fact that the symmetry in that one helps much to solve the problem, while the lack of symmetry makes the analysis of the rectangular one extremely difficult. However formulation for the latter case can be found by analogy with the former one, supported by experimental results.

The complexity of the problem of fluid loading and hence the normal procedure generaly found in the literature for simplifying it by consistent assumptions and approximations, have already been discussed in section 3.3. Some exemplary indications have also been given in the review in section 3.5. The present case being also a very complicated one, some assumptions and approximations have been made to simplify it. Analysis has been carried out by both impedance and energy techniques, with an emphasis on mass loading, an optimisation of this being the primary object.

3.6.1 An Analysis By Impedance Technique

As already discussed in section 3.4, basically this

method involves the calculation of the excess pressure at the surface of the body. Then the quotient obtained by dividing this pressure by the velocity of the surface gives the mechanical impedance of the fluid load, from which the reactive and the resistive loadings can be calculated.

The assumptions and approximations made in this procedure are

(a) The frequency of oscillation is low (typically below 5 kHz) so that the wavelength λ in the fluid is much greater than the goemetrical dimensions of the resonator. Thereby the compressibility of the fluid is negligible and the situation tends to that of hydrodynamics where the mass loading is predominant, highest and almost independent of frequency. The loss due to radiation of sound also is negligible at low frequencies. Thus the analysis has been carried out taking only the mass and the viscous effects into account. The validity of the above assumptions and approximations is quite evident from the discussions of sections 3.3 and 3.5, and also has a support from experimental results (see Chapter 4).

(b) Bearing in mind the results of Lax for circumferentially clamped disk (see section 3.5) and also supported by experimental results, it is assumed that at low frequencies the mass effect is greatest at fundamental flexure mode. So the analysis has been carried out only for this mode, as it enables to simplify the complex

situation due to the actual vibration of the resonator, by an approximate model of two disk vibrating in antiphase in piston-like motion. The actual resonator and the model have been shown in Figure 3.6.

(c) It is sufficient to consider the loading due to the thin layer of fluid between the disks only (this being much greater than the loadings on other faces of the disks, as will be shown later in this analysis).

(d) The vibration is harmonic with amplitude, much much less than the gap between the disks. Both the solid and the fluid medium are homogeneous.

NOMENCLATURE

r, θ, z = cylindrical polar co-ordinates

$2h_o$ = initial separation between the disks

R = radius of the disks

H = thickness of the disks

ρ_m = density of the material of the disks

ω = angular frequency of oscillation of the disks

A = αh_o = amplitude of oscillation

V_o = ωA = velocity amplitude of the disks

t = time

U_r = fluid radial velocity, $U_r(r,z,t)$

U_z = fluid axial velocity, $U_z(z,t)$

p = fluid pressure, $p(r,z,t)$

ρ_f = fluid density

μ = fluid viscosity

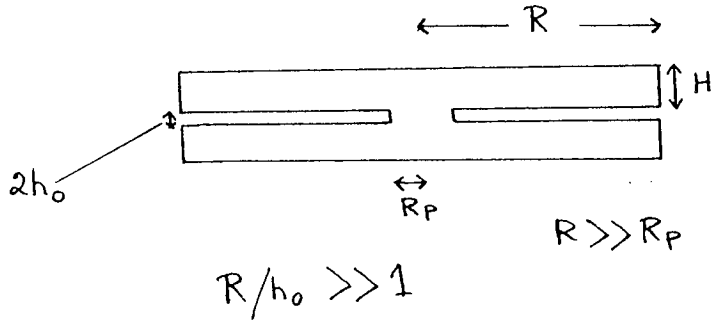

(a) The actual resonator; two circular disks clamped at the centre by a post. Vibration is harmonic at fundamental flexural mode with amplitude much much less than h_o.

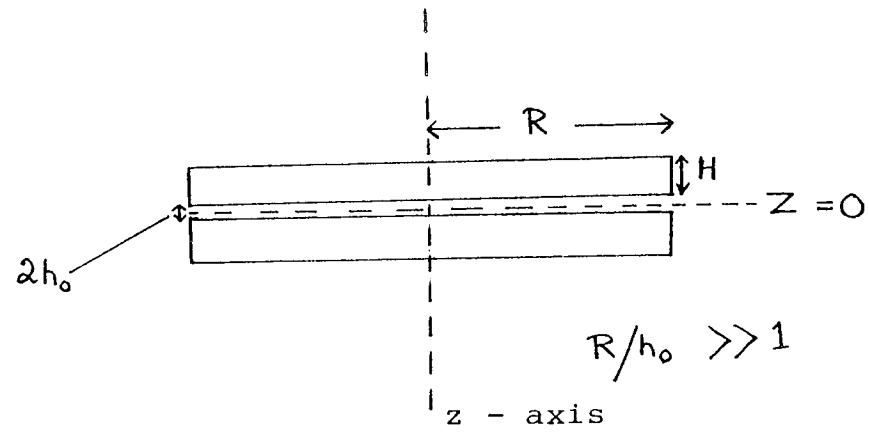

(b) The two piston model: two circular disks vibrating harmonically in anti-phase in piston-like motion along z-axis. Amplitude is much much less than h_o.

FIGURE 3.6. The actual resonator and its model for simplification of the analysis.

$R_e = \frac{\omega h_o^2 \rho_f}{\mu}$ = typical Reynolds number

f_o = in vacuum frequency of oscillation of the disks

$f_f = \frac{\omega}{2\pi}$ = in fluid frequency of oscillation of the disks.

$j = \sqrt{-1}$

Cylindrical polar co-ordinates r, θ, z are so chosen that the mid-plane between the two oscillating disks is situated at z=0 (see Figure 3.6b). The position of the upper disk at any subsequent time is $z = h_o(1+\alpha \mathrm{Sin}\omega t)$, (because of the symmetry about the plane through z=0, it is sufficient to consider any one of the two disks). Hence the boundary conditions are

$$\begin{aligned} &\text{at } z=0, \quad U_z = 0 = \frac{\partial U_r}{\partial z} \\ &\text{at } z=h_o(1+\alpha \mathrm{Sin}\omega t), \quad U_r = 0 \\ &\qquad\qquad\qquad\qquad\qquad\qquad U_z = h_o \alpha \omega \mathrm{Cos}\omega t \end{aligned} \tag{3.25}$$

The boundary conditions on U_z suggest that it is independent of r, that is $U_z = U_z(z,t)$. Under this condition and assuming the flow axially symmetric, Navier-Stokes equations for the fluid (only that between the disks are considered, as already discussed in the assumption "c") are

$$\rho_f\left(\frac{\partial U_r}{\partial t} + U_r\frac{\partial U_r}{\partial r} + U_z\frac{\partial U_r}{\partial z}\right) = -\frac{\partial p}{\partial r} + \mu\left(\nabla^2 U_r - \frac{U_r}{r^2}\right) \tag{3.26}$$

$$\rho_f\left(\frac{\partial U_z}{\partial t} + U_z\frac{\partial U_z}{\partial z}\right) = -\frac{\partial p}{\partial z} + \mu\nabla^2 U_z \tag{3.27}$$

where $\nabla^2 = \frac{\partial^2}{\partial r^2} + \frac{1}{r}\frac{\partial}{\partial r} + \frac{\partial^2}{\partial z^2}$

(in the above equations absence of body forces are assumed).

The equation of continuity is

$$\frac{1}{r}\frac{\partial}{\partial r}(rU_r) + \frac{\partial U_z}{\partial z} = 0 \qquad (3.28)$$

Differentiating equation (3.27) with respect to r

$$\frac{\partial^2 p}{\partial r \partial z} = 0 \qquad (3.29)$$

From equation (3.28)

$$U_r = -\frac{1}{2} r \frac{\partial U_z}{\partial z} \qquad (3.30)$$

From equations (3.26), (3.29) and (3.30)

$$\rho_f \left(\frac{\partial^3 U_z}{\partial z^2 \partial t} + U_z \frac{\partial^3 U_z}{\partial z^3}\right) = \mu \frac{\partial^4 U_z}{\partial z^4} \qquad (3.31)$$

Introducing the following dimensionless variables

$$U = U_z/(h_o \alpha \omega), \quad T = \omega t, \quad \beta = z/|h_o(1+\alpha \mathrm{Sin}\omega t)| \qquad (3.32)$$

and taking $\alpha R_e << 1$ (which is the condition in the present work) equation (3.31) reduces to

$$\frac{\partial^4 U}{\partial \beta^4} = R_e \frac{\partial^3 U}{\partial \beta^2 \partial T} \qquad (3.33)$$

Under the transformation of (3.32), the boundary conditions (3.25) become

$$\text{at} \quad \beta=0, \qquad U=0 = \frac{\partial^2 U}{\partial \beta^2} \qquad (3.34)$$

$$\text{at} \quad \beta=1, \qquad U=\mathrm{Cos}T, \ \frac{\partial U}{\partial \beta} = 0$$

With these boundary conditions the solution of equation (3.33) can be shown as (see Appendix 1)

$$CU = \left| \frac{2\beta \text{Cosh} K}{K} - \frac{2 \text{ Sinh } K\beta}{K^2} \right| e^{jT} \qquad (3.35)$$

where $c = \frac{2 \text{ Cosh } K}{K} - \frac{2 \text{ Sinh } K}{K^2}$

$$K = \sqrt{jR_e}$$

Applying the transformation (3.32) in equation (3.26) and neglecting terms of order αR_e

$$\frac{\partial p}{\partial r} = \frac{1}{2} \frac{\mu\alpha\omega r}{h_o^2 (1+\alpha \text{Sin} T)^3} \left| R_e \frac{\partial^2 U}{\partial\beta\partial T} - \frac{\partial^3 U}{\partial\beta^3} \right| \qquad (3.36)$$

Substituting for U from equation (3.35)

$$\frac{\partial p}{\partial r} = \frac{\mu\alpha\omega r \text{ K Cosh K}}{Ch_o^2 (1+\alpha \text{Sin} T)^3} e^{jT} \qquad (3.37)$$

On the assumption that the variation of p with z is very negligible (this is a common approximation in hydrodynamic literature for problems similar to the present one), integrating equation (3.37) with respect to r yields the pressure p_r on the disk at a point distant r from the centre as

$$p_r \simeq p_o + \frac{\mu\alpha\omega K(r^2-R^2) \text{Cosh K}}{2Ch_o^2} e^{jT} \quad \left| \because \alpha << 1 \right| \qquad (3.38)$$

where $p_o = p_r$ at $r = R$.

Excess pressure dF_r, on a circular ring of radius r and width dr of the oscillating disks is

$$dF_r = 2\pi r\, dr\, (p_r - p_o) \tag{3.39}$$

Substituting for $(p_r - p_o)$ from equation (3.38) in equation (3.39) and then integrating with respect to r, from O to R yields the excess pressure F on the disks as

$$F = \frac{\pi\mu\alpha\omega R^4\ K\ \text{Cosh}\ K}{4Ch_o^{\,2}}\ e^{jT} \tag{3.40a}$$

Expanding C and Cosh K in power series

$$F \simeq \left| \frac{3\pi\mu A\omega R^4}{8h_o^{\,3}} + j\ \frac{3\pi A\omega^2\rho_f R^4}{20\ h_o} \right| e^{j\omega t} \tag{3.40b}$$

Therefore mechanical impedance of the fluid load

$$Z_L = \frac{F}{V_o e^{j\omega t}}$$

$$= \frac{3\pi\mu R^4}{8h_o^{\,3}} + j\frac{3\pi\omega\rho_f R^4}{20\ h_o} \tag{3.41}$$

As before, the real term represents the energy loss due to viscous loading and the imaginary term, being positive, represents the mass loading.

Therefore the value of the added mass

$$\Delta M = \frac{\text{imaginary part of equation (3.41)}}{\omega}$$

$$= \frac{3\pi\rho_f R^4}{20\ h_o} \tag{3.42}$$

In the case of piston-like motion the dynamic mass of the

disk is equal to its static mass.

So,

$$M = \pi R^2 H \rho_m$$

Therefore finally,

$$\frac{f_f}{f_o} = \frac{1}{\sqrt{1+\frac{\Delta M}{M}}}$$

$$= \frac{1}{\sqrt{1+\frac{3\rho_f R^2}{2O\rho_m H h_o}}} \qquad (3.43)$$

3.6.2 An Analysis By Energy Technique

As already mentioned in section 3.4(b), more idealized assumptions are often required for a simplified analysis by the energy technique. Thus in order to enable to solve the present case (the two piston model of Figure 3.6) in a simplified way, the following assumptions in addition to those of "(a) to (d)" of the previous procedure, have been made:

(a) The fluid is inviscid and so only the mass loading is present. Thereby the analysis will give a formulation only for the change in frequency of the resonator (which is, of course, the primary object of the present work). In reality there is strong viscous effect (see equation (3.41) of the previous analysis). However, it can be ignored while evaluating the change in frequency, on the basis of the principle (discussed in section 3.3)

that the consideration of the various effects separately as if the other were absent, gives a good approximation of the real situation. Assumption of the fluid as inviscid, makes the radial velocity of the fluid U_r independent of z (see Figure 3.7).

(b) Both the amplitude of the vibration and the gap between the disks being very small, the calculation of the kinetic energy of the fluid taking into account only the radial velocity U_r (neglecting axial velocity U_z) of the fluid, is a good approximation.

With the above assumptions the change in resonant frequency of the disks have been formulated from their maximum kinetic energy and the maximum kinetic energy of the fluid, as outlined in section 3.4(b).

Let the sinusoidal vibration of the disks be of angular frequency ω and amplitude A. At any time t, the gap h_t between the disks (considering squeezing) will be

$$h_t = 2(h_o - A \sin\omega t) \tag{3.44}$$

where $2h_o$ = initial gap

After a very short time dt the gap will be squeezed to

$$h_{t+dt} = 2(h_o - A\sin\omega t - A\omega \cos\omega t\, dt) \tag{3.45}$$

The volume of the fluid within the radius r (see Figure 3.7), at time t is

$$V_t = \pi r^2 h_t$$
$$= 2\pi r^2 (h_o - A \sin\omega t) \tag{3.46}$$

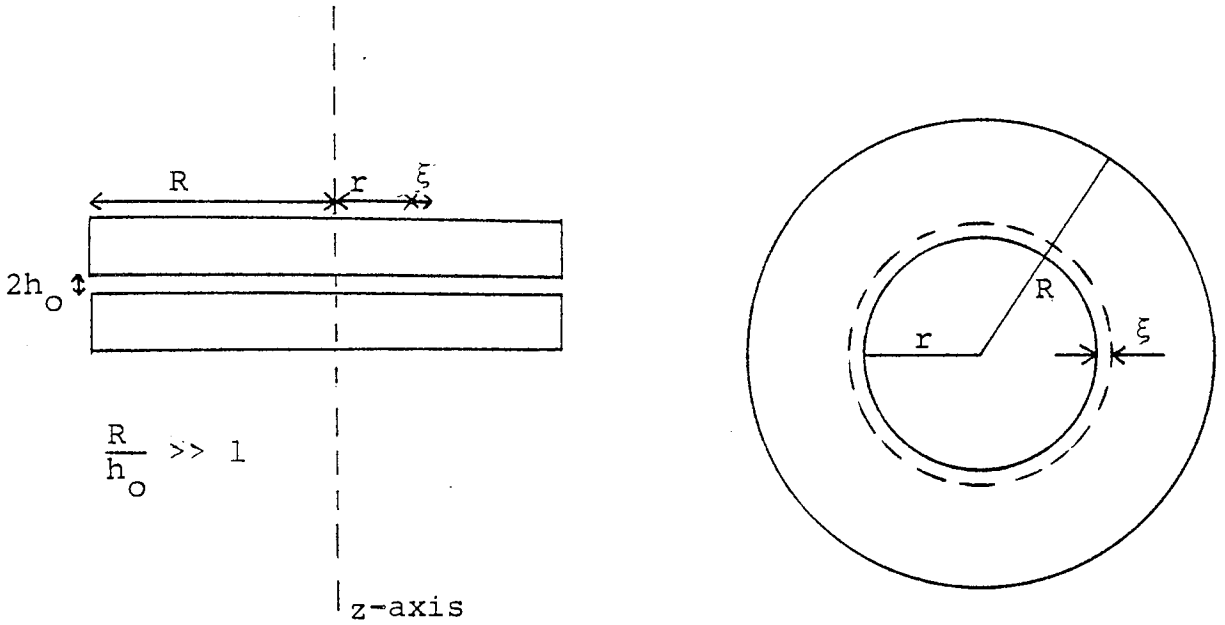

(a) View in section (b) View from the top.

FIGURE 3.7 The two piston model (same as Figure 3.6(b)). The two pistons are vibrating harmonically in anti-phase, in piston like motion along z-axis.

At the time (t+dt), this fluid will occupy the volume

$$y_{t+dt} = (\pi r^2 + 2\pi r\xi)h_{t+dt} \qquad (3.47)$$

where ξ = distance moved by the fluid at r in the time dt.

As the fluid has been assumed as incompressible,

$$V_t = V_{t+dt}$$

Or, $2\pi r^2 (h_o - A\sin\omega t) = 2(\pi r^2 + 2\pi r\xi)(h_o - A\sin\omega t - A\omega\cos\omega t\ dt)$

(3.48)

Neglecting the very small term $(4\pi r\xi A\omega\cos\omega t\ dt)$, equation (3.48) gives

$$2(h_o - A\sin\omega t)\xi = rA\omega\cos\omega t\ dt \qquad (3.49)$$

Therefore velocity of the fluid at r is

$$U_r = \frac{\xi}{dt} = \frac{rA\omega\cos\omega t}{2(h_o - A\sin\omega t)} \qquad (3.50)$$

As $A << h_o$, maximum value of U_r is

$$U_{r\ max} = \frac{rA\omega}{2h_o}$$

Therefore the maximum kinetic energy of the fluid is

$$T_{fm} = \int_o^R \frac{\pi\rho_f A^2\omega^2 r^3 dr}{2h_o} \qquad (3.51)$$

where R = radius of the disks

ρ_f = density of the fluid.

Carrying out the integration of equation (3.51)

$$T_{fm} = \frac{\pi\rho_f A^2\omega^2 R^4}{8h_o} \qquad (3.52)$$

The maximum kinetic energy of the disks is

$$T_{om} = \pi R^2 H\rho_m A^2\omega^2 \qquad (3.53)$$

where H = thickness of the disks

ρ_m = density of the disk material.

From equation (3.52) and (3.53) the change in frequency of the system (see equation (3.2)

$$\frac{f_f}{f_o} = \frac{1}{\sqrt{1+\frac{T_{fm}}{T_{om}}}}$$

$$= \frac{1}{\sqrt{1+\frac{\rho_f R^2}{8\rho_m H h_o}}} \qquad (3.54)$$

where f_f = in fluid resonant frequency of the disks

f_o = in vacuo resonant frequency of the disks.

It is interesting to note that by both the techniques, identical (except the numerical constant) expressions have been obtained for the change in frequency of the resonator (equations (3.43) and (3.54)). The difference in the numerical constant reflects the various assumptions and approximations in the procedures. In fact in such a complicated problem as the present one, normally experimental determination seems to be the only way to find the constants. Thus Vennard and Street[55], while describing a viscometer, made the comment - "these conditions involve too many complexities to allow the constants of the viscometer to be calculated analytically, and they are therefore usually obtained by calibration with a liquid of known viscosity".

3.7 DISCUSSION

The mass loading on a vibrating body due to its interaction with the surrounding fluid is normally, predominant, highest and almost independent of frequency, at fundamental mode of flexural vibration of low frequencies (i.e. when $KR << 1$). Thus under these conditions it can be made a good basis of a transducer for measuring fluid density, which is directly related with it. The value of the added mass (under the above conditions) per unit area for the present resonator (as obtained by the analysis) and those reviewed in section 3.5, are gathered below for a comparative picture:

(a) The present resonator (analysed as two piston model, considering only the fluid between the disks). : $(\Delta M)_U = .15\rho_f R(\frac{R}{h_o})$

(b) A circular piston in an infinite baffle. : $(\Delta M)_U = .85\rho_f R$

(c) A circumferentially clamped circular plate with fluid on one side only. : $(\Delta M)_U = .67\rho_f R$

(d) A pulsating sphere immersed in a fluid medium. : $(\Delta M)_U = \rho_f R$

(e) An oscillating sphere immersed in a fluid medium. : $(\Delta M)_U = .16\rho_f R$

where $(\Delta M)_U$ = added mass per unit area (under the conditions stated above).

ρ_f = density of the fluid

R = radius of the resonator

$2h_o$ = gap between the vibrating numbers of the present resonator.

As R can be made much larger than h_o, an inspection of the above expressions reveals that the present resonator is a very convenient structure for the magnification in sensitivity of the fluid density transducer.

CHAPTER 4

THE GAS DENSITY TRANSDUCER

4.1 INTRODUCTION

The theoretical basis of the transducer for measuring fluid density has been reported in the previous chapter. The reasons for dealing with experimental work and thereby practical designs for the two phases of the fluid (gas and liquid) separately, have already been mentioned in Chapter 2. This will be more clear from the discussions of this and the next chapters which deal with the gas density and the liquid density respectively.

4.2 RESONATOR MATERIAL

From equations 3.43, 3.54 and from the discussion of Section 3.6, the relationship between f_g, the frequency in a gas medium and f_o in the vacuo frequency of the circular resonator can be expressed as

$$\frac{f_g}{f_o} = \frac{1}{\sqrt{1+K_c \frac{\rho_g R^2}{\rho_m H h_o}}} \qquad (4.1)$$

where K_c = numerical constant whose value is to be determined experimentally

ρ_g = density of the gas

ρ_m = density of the resonator material

R = radius of the disks of the resonator

H = thickness of the disks

$2h_o$ = gap between the disks

As will be discussed in section 4.7, by analogy with the above expression and supported by experimental results, the relationship for the rectangular resonator can be written as

$$\frac{f_g}{f_o} = \frac{1}{\sqrt{1+K_R \frac{\rho_g W^2}{\rho_m H h_o}}} \qquad (4.2)$$

where K_R = numerical constant whose value is to be determined experimentally

W = width of the resonator

amd all other notations have the same meanings as in equation 4.1.

From equations 4.1 and 4.2, it is quite evident that the lighter the resonator material, the more will be the sensitivity of the transducer. Preliminary experiments with resonators made of different materials such as aluminium, copper, steel have supported the feature. However, while choosing a light material, the consideration of its internal friction and temperature coefficient is very important. As will be discussed in

section 4.8 minimisation of the loss of the resonator is a vital criterion for the transducer. Thus a material with low internal friction is to be selected. Again to overcome the unwanted temperature effect, a material with very small thermal coefficient is desirable, otherwise a compensating circuit is to be incorporated. Under the above facts, the material fused quartz has been chosen for the present transducer. Fused quartz is made by heating high purity naturally occurring quartz crystal to a sufficiently high temperature to produce an amorphous condition. It is a light material (density: 2.7×10^3 Kg/m^3) with very low internal friction and virtually zero temperature coefficient. Due to these favourable properties it is found in use in various commercially available transducers. For example, Texas Instruments Limited[56] in one of their design of pressure gauge, utilizes this material. They describe its properties as - "the high degree of accuracy of the Precision Pressure gauge is attributable to the fused quartz Bourdon tube. The low internal friction of fused quartz makes it the most perfectly elastic material known. Bourdon tubes made of fused quartz exhibit lower hysteresis, creep or fatigue, than tubes made of any other known material".

Other suitable materials having the properties of low internal friction and low temperature coefficient

may also be used. For example Solartron Limited[6] uses Ni-Span-C902 for both their gas density and liquid density transducers.

However the above materials being rather costly, aluminium has been used in most of the initial experimental work. Aluminium has low density (near that of fused quartz), and low internal friction, but has a high thermal coefficient. However, as there was not much variation of temperature during the experiments, the results obtained are quite satisfactory for assessing final design parameters.

4.3 DRIVING TECHNIQUES

Various techniques can be found in the literature for driving (and pick up from) a mechanical system. Some most common methods are electromagnetic, piezoelectric and electrostatic. A particular technique has its merits and demerits, depending upon the particular situation. Coupling efficiency, effect on "Q" factor of the resonator and mechanical simplicity are some important features which generally influence the choice. A brief discussion of them in context to the present resonator follows.

(a) Coupling efficiency: It may be defined as the ratio of the power picked up from the resonator to the power utilized for driving it. Thus the more the coupling efficiency, the less is the power required (hence simpler

electronics) to maintain the oscillation. In this respect, the piezoelectric method seems to be the best. Artificially produced piezoelectric ceramics such as lead zicronate titanate (PZT) and barium titanate, have very high coupling efficiency. Vernitron Limited[57], a manufacturer of these ceramics, describe it as - "providing the structructure has a reasonably high mechanical Q factor, milliwatts of power is all that is normally required to produce quite large amplitude of resonant vibration". Moreover the higher the coupling efficiency, the better is the signal-to-noise ratio. Again piezoelectric couplings are not affected by stray electric or magnetic field, and have no mutual effect, even in close lay out.

(b) Effect on Q factor of the resonator: In this respect both electromagnetic and electrostatic methods are better than piezoelectric. As in the former two cases there are no mechanical contact with the resonator, its Q factor is little affected. On the contrary, in the latter case the piezoelectric elements are to be bonded mechnically with the resonator and thereby the Q factor is affected. However by using piezoelectric elements, very small compared with the resonator, this can be minimized.

(c) Mechanical simplicity: In this respect again the piezoelectric method seems to have advantages. The small drive and pick up elements can be bonded firmly on the

resonator. In case of the electromagnetic and the electrostatic methods, the drive and pick-up coil assembly requires much care and space for positioning.

Under the above discussed facts, the piezoelectric method has been chosen for the present transducer. PZT components manufactured by Unilator Technical Ceramics[58] have been used. For optimum coupling efficiency the piezoelectric elements are to be bonded in the position of maximum dynamic strain occurring within the vibrating body. Figure 4.1 shows such positions for the present resonators in the desired fundamental flexural mode and thereby various drive and pick-up systems used. In the case of the rectangular resonator two PZT plates (typical dimentions: length 5×10^{-3}m, width 2.5×10^{-3}m, thickness 5×10^{-4}m) have been bonded on the two tines at the positions of maximum dynamic strain, as shown in Figure 4.1(a). One has been used for exciting the resonator, and the other for picking up the vibration. This simple system can also be arranged as shown in Figure 4.1(b), for the circular resonator with PZT rings. Rings are needed for providing facility (i.e. nodal space), for making mounting arrangement for the resonator (see the Figure). However disks have been used as they are readily available. In this case, for ease of mounting facility, one disk has been used (Figure 4.1(c)). Both the tasks of drive and pick up are performed by the

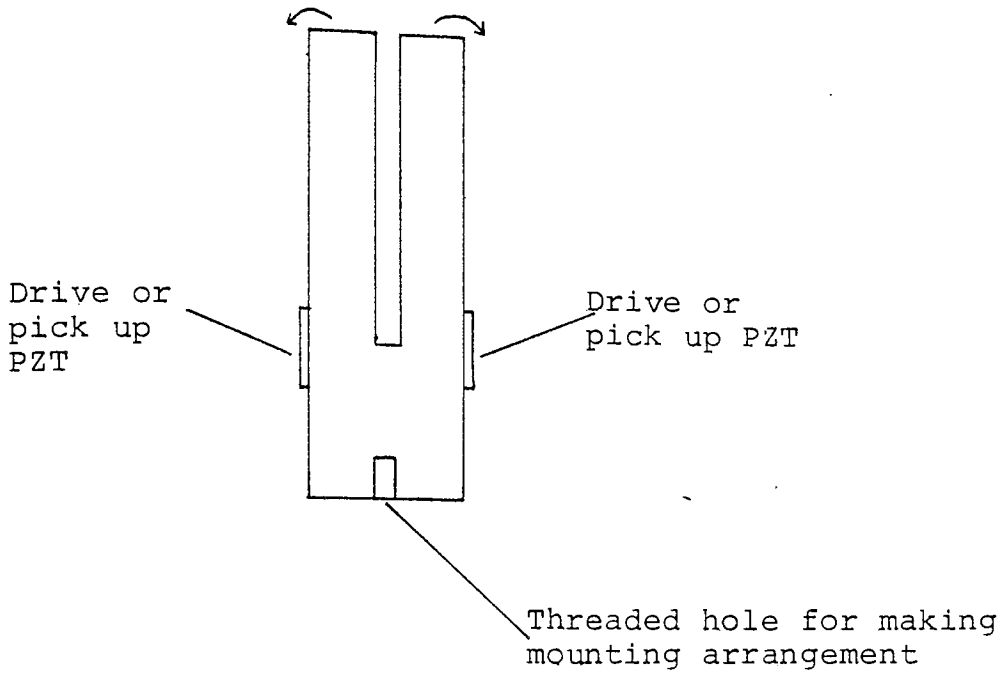

(a) Two PZT plates have been used, one for drive and the other for pick up.

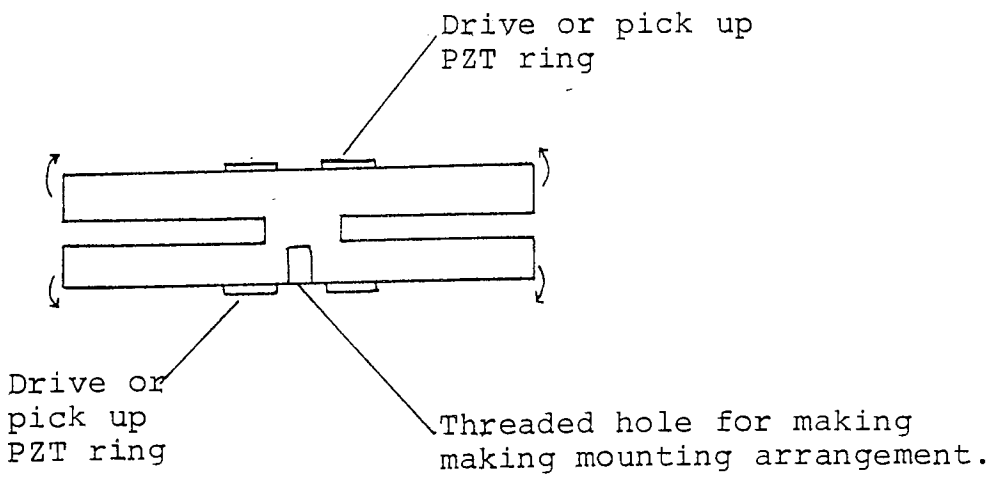

(b) Two PZT rings drive and pick up

FIGURE 4.1 (a) and (b) : Various drive and pick up techniques.

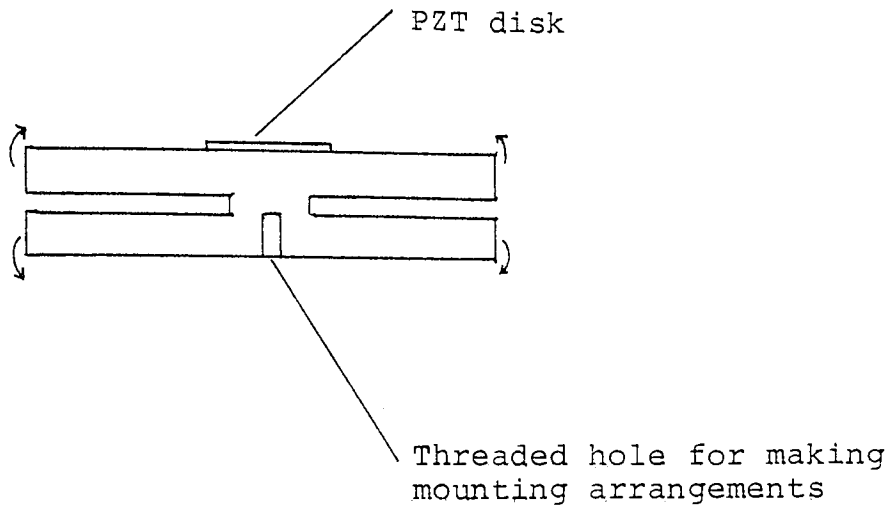

(c) Both drive and pick up are performed by a single PZT disk by placing it in one arm of an active bridge (Figure d).

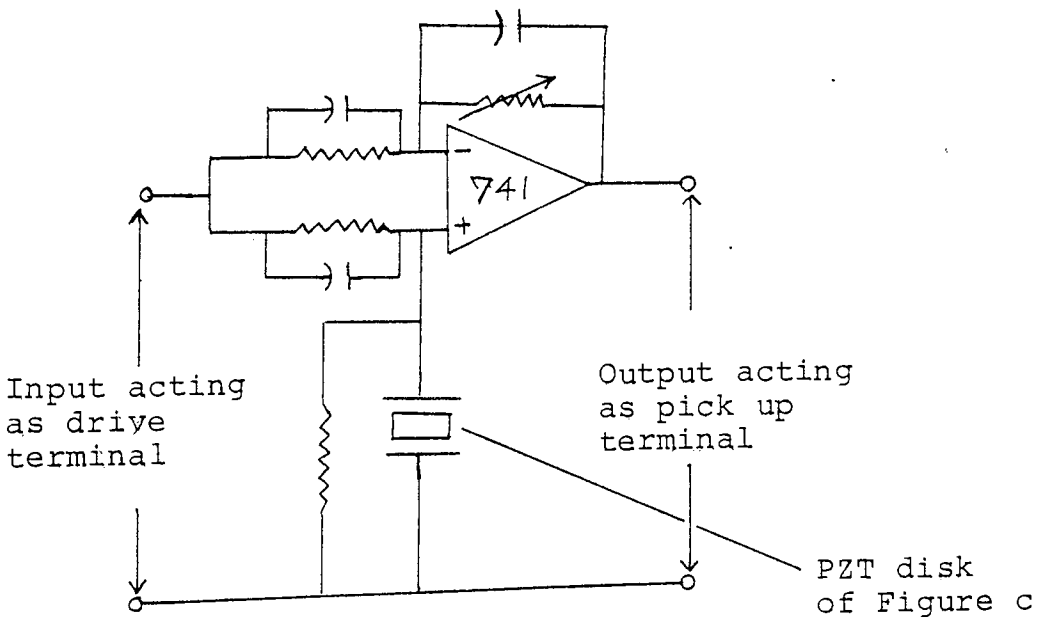

(d) An active bridge

FIGURE 4.1 (c and d) : Various drive and pick up techniques.

single disk by placing it in one arm of an active bridge as shown in Figure 4.1(d). The input and the output of the bridge serve as the drive and the pick-up terminals respectively.

In all the above arrangements, in manual operation, the resonator is excited with a signal from a variable frequency oscillator. By observing the pick-up signal on an oscilloscope the resonant frequency is determined. At resonance the pick-up signal is maximum and there is a phase difference of $\pi/2$ between it and the drive signal (as discussed in Section 1.2).

Various designs for automation will be presented later in Section 4.10.

4.4 EXPERIMENTAL SET-UP

For obtaining variation of density of the gas, the transducer has been located in a pressure vessel. This was constructed for a past project and for its suitability it has been used for the present work. Figure 4.2 shows the vessel and associated set-up. The length and the diameter of the vessel are 65×10^{-2}m and 10×10^{-2}m respectively. It can withstand pressure up to 17×10^{5} pascal. There are facilities for locating the transducer in different positions in the vessel (thereby effect of the wall can be examined), and for bringing out electrical connections. The vessel can be

FIGURE 4.2 The pressure vessel in which the transducer has been located for obtaining variations of densities of gases.

evacuated by a vacuum pump and there are provisions for controlled inlet and outlet of different gases. Investigations have been carried out with three gases having a wide density range, namely argon, nitrogen and helium. The pressure has been measured by a Bell and Howell strain gauge pressure transducer (type 4-306-0221-01MO). From the pressure the density of the gas has been calculated for calibrating the density transducer.

4.5 DYNAMIC CLAMPING

Ease of clamping of the resonator by the phenomenon of dynamic balancing is an important virtue of the transducer, as already discussed in Chapter 2. In this section is reported an experimental verification of this feature. According to Karlmarczie's solution (see Section 3 of Chapter 2), the tines of the rectangular resonator in the desired fundamental flexural mode, can be taken as clamped automatically at the boundary, as shown in Figure 4.3. The apparent increase in length of the tines is 0.68H, where H is the thickness of the tines.

Karlmarzie derived the solution by considering the tines of the resonator as plates. As for rectangular plates with boundary conditions other than simply supported, exact solutions are not known, to calculate the frequency, he had to use a numerical method which is quite an involved work. However, for the geometrical

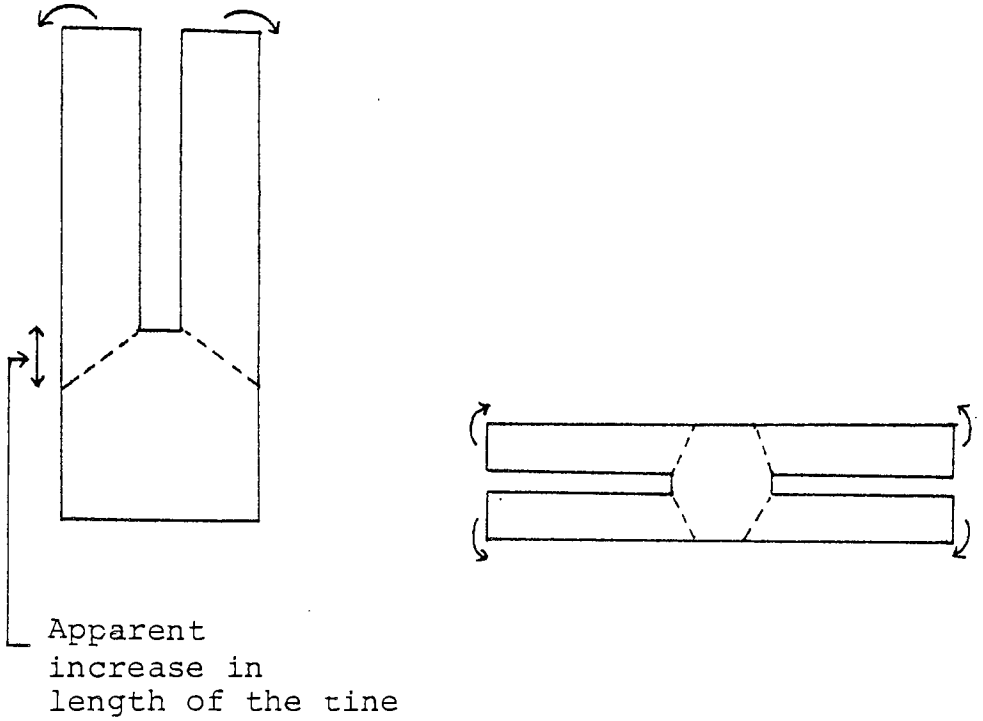

(a) Rectangular resonator. The vibration at the base is very small indeed.

(b) Circular resonator, analgous to the fork

FIGURE 4.3 The vibrating tines are in automatically clamped condition at the boundary shown by the dotted lines, by the phenomenon of dynamic balancing.

dimensions used in the present resonators, the two tines can be regarded, with a fair approximation, as rectangular bar. As in this case exact formulation is readily available, the solution is much simplified. The in vacuo fundamental natural frequency in flexural mode of a rectangular bar clamped at one end is given by[59]

$$fo = \frac{\pi}{2} \frac{(.597)^2}{L^2_T} \frac{H}{\sqrt{12}} C_o \qquad (4.3)$$

where L_T = length of the bar

H = thickness of the bar

$C_o \equiv \sqrt{\frac{E}{\rho}}$ = the rod velocity

E = Young's modulus

ρ = density

Resonators of different length and different thickness were made and their in vacuo frequencies were measured. The theoretical frequencies were calculated using equation 4.3 with and without Karlmarczie's correction of 0.68H. Some typical results are shown in Table 4.1. The fair agreement between the measured frequencies and those obtained theoretically with length correction, supports well the phenomenon of dynamic clamping. The small discrepancy may be due to:

(a) the very approximate approach to the problem,

(b) uncertainties in the measurement of the geometrical dimensions,

(c) slight dimensional differences (due to the limitation of machining) between the two tines.

Measurements with the circular version of the resonators also support well the phenomenon (see Figure 4.3b).

4.6 EXPERIMENTAL SUPPORTS FOR VARIOUS ASSUMPTIONS

(a) Mass effect vs stiffness effect: as already discussed in Chapters 2 and 3, of the two reactive effects, i.e.

Length of the tines ($m \times 10^2$)	Theoretical frequency (Hz)		Measured frequency (Hz)
	Without correction	With correction	
2.54	3308	2900	2975
2.00	5335	4520	4480
1.90	5911	4967	4860
1.70	7384	6085	6164

H : thickness of the tines = $.254 \times 10^{-2}$m
W : width of the tines = 1.905×10^{-2}m

Thickness of the tines ($m \times 10^2$)	Theoretical frequency (Hz)		Measured frequency (Hz)
	Without correction	With correction	
.254	3308	2900	2975
.300	3907	3347	3290
.356	4636	3964	4018
.400	5209	4250	4380

L_T : length of the tines = 2.54×10^{-2}m
W : width of the tines = 1.905×10^{-2}m

TABLE 4.1 Measured and theoretically calculated (with and without Karlmarczie's correction) frequencies of the rectangular resonator.

the mass effect and the stiffness effect, the former lowers and the latter raises the natural frequency of the resonator. The net effect depends upon their relative values. As the mass effect is directly related with the density of the surrounding gas, the conditions under which it is predominant (negligible stiffness effect) is desirable for the present transducer. In the analysis of the present resonator (Chapter 3), it was assumed that this is fulfilled at low frequencies (typically below 5 kHz).

A fluid medium can be taken as incompressible (i.e. the condition for negligible stiffness effect) when the following relations are satisfied[50]

$$V << C \tag{4.4a}$$

and

$$\lambda >> \text{geometrical dimensions of the body} \tag{4.4b}$$

where V = Velocity of the body

C = velocity of sound in the medium

λ = wavelength in the medium

The maximum value of V is $2\pi fA$, where f is the frequency and A is the amplitude of vibration. As in the present case A is less than a micron, a value of f below 5 kHz satisfies the condition 4.4a very well.

To verify the condition 4.4b a series of measurements

has been carried out. The relative values of λ and the geometrical dimension of the body can be varied by three factors:

(1) frequency of vibration of the resonator

(2) gases of different molecular weights

(3) geometrical dimensions of the resonator.

(1) Table 4.2a shows some typical results with the variation of frequency (obtained by varying radius or length of the resonators). From the table it is apparent that stiffness effect is negligible at low frequencies.

(2) Velocity of sound c in a gas medium is

$$c=\sqrt{\frac{P\gamma_c}{\rho}} \qquad (4.5a)$$

where P is pressure, γ_c is the ratio of specific heats and ρ_g is density. As $c = f\lambda$ and $\rho_g = \frac{PM}{RT}$ (assuming perfect gas) where M = molecular weight of the gas, T is absolute temperature and R is the gas constant, equation 4.5a gives

$$f\lambda=\sqrt{\frac{RT\gamma_c}{M}} \qquad (4.5b)$$

Thus for certain geometrical dimensions of the resonator there can be a net mass effect for a gas with low molecular weight but a net stiffness effect for a gas with higher molecular weight. This

Density of argon (Kg/m^3)	Frequency of the resonator (Hz)			
	L_T = 2.5cm	L_T = 1.8cm	L_T = 1.3cm	L_T = 1.1cm
0 (vacuum)	3274	6415	12360	17263
1.8	3229	6318	12395	17318
3.02	3199	6269	12448	17367
4.86	3146	6168	12470	17451
7.92	3075	6028	12540	17543
10.98	2999	5888	12601	17631
14.04	2939	5766	12665	17702
	Mass effect	Mass effect	Stiffness effect	Stiffness effect

$W = 1.8 \times 10^{-2}$m
$H = 3.2 \times 10^{-3}$m
$h_o = 1.27 \times 10^{-4}$m

TABLE 4.2a Mass effect vs stiffness effect. Some typical results (with rectangular version of the resonator) to show that the former is predominant at low frequencies.

interesting feature is demonstrated in the selected results of Table 4.2b. The effect is mass like for helium, while stiffness like both for argon and nitrogen.

(3) Table 4.2c shows some typical measurements from which it is apparent that stiffness effects become significant with the increase of geometrical dimensions of the resonator. The increases have been made in W (the width) rather than L_T (the length), thus keeping λ constant.

All the above experimental results support the assumption that at low frequencies the reactive loading is predominantly inertial.

(b) Fundamental mode and sensitivity

In Chapter 3, in the analysis of the present resonator, it was assumed that in flexural vibration the low frequency predominated mass effect is highest at the fundamental mode. In the case of a circumferentially clamped plate Lax has proved this feature theoretically, (see Section 3.5.3). However, for the present resonator, because of much complexity of the problem, only experimental results had to be relied on for this important feature. In fact it has been found that while for the fundamental mode the change of frequency is quite significant, at other modes the effects are very small. Table 4.3 shows such a typical set of results.

Helium		Nitrogen		Argon	
Density (Kg/m^3)	Frequency of the resonator (Hz)	Density (Kg/m^3)	Frequency of the resonator (Hz)	Density (Kg/m^3)	Frequency of the resonator
O(vacuum)	13160	O(vacuum)	13160	O(vacuum)	13160
.18	13142	1.25	13180	1.8	13174
.302	13126	2.10	13196	3.02	13185
.486	13105	3.37	13211	4.86	13204
.792	13083	5.50	13223	7.92	13221
1.098	13065	7.63	13236	10.98	13238
Mass effect		Stiffness effect		Stiffness effect	

$L_T = 1.27 \times 10^{-2}$ m
$W = 1.8 \times 10^{-2}$ m
$H = 3.2 \times 10^{-3}$ m
$h_o = 2.5 \times 10^{-4}$ m

TABLE 4.2b Mass effect vs stiffness effect. Some typical measurements (with rectangular version of the resonator) which show that for helium it is the former effect which is dominant, while for nitrogen and argon (having higher molecular weights) the latter effect becomes significant.

Density of argon (Kg/m^3)	Frequency of the resonator		
	W = 1.9 cm	W = 2.5 cm	W = 3.8 cm
O(vacuum)	5351	5340	5329
1.8	5260	5195	5347
3.02	5195	5106	5363
4.86	5119	4965	5380
7.92	4985	4752	5397
10.98	4864	4570	5412
14.04	4749	4402	5425
	Mass effect	Mass effect	stiffness effect

$L_T = 2 \times 10^{-2} m$
$H = 3.2 \times 10^{-3} m$
$h_o = 1.27 \times 10^{-4} m$

TABLE 4.2c Mass effect vs stiffness effect. Some typical measurements (with rectangular version of the resonator) which show that the latter effect becomes significant with the increase of geometrical dimension of the resonator.

Mode	FREQUENCY OF VIBRATION (Hz)	
	In vacuum	In air at atmospheric pressure
Fundamental	975	931
1st harmonic	4565	4562
2nd harmonic	14614	14614

TABLE 4.3 : Change of frequency due to reactive loading. The change is most significant at fundamental mode.

4.7 GEOMETRICAL DIMENSIONS AND SENSITIVITY

(a) The circular resonator:

As already mentioned, it is the geometrical configuration of the resonator by which a most significant virtue of the transducer, i.e. a high sensitivity with even a robust structure, has been achieved. The theoretical basis of this feature for the circular resonator has been presented in Chapter 3. From equation 4.1

$$\rho_g = \frac{\rho_m H h_o}{K_c R^2} \left| \left(\frac{f_o}{f_g}\right)^2 - 1 \right|$$

$$= \rho_o \left| \left(\frac{f_o}{f_g}\right)^2 - 1 \right| \qquad (4.6a)$$

where $\rho_o \equiv \frac{\rho_m H h_o}{K_c R^2}$ = scale factor (4.6b)

and all other notations have the same meanings as in equation 4.1.

From equation 4.6a, it is quite evident that the lower the ρ_o, the more is the sensitivity of the transducer. Thus this expression is the basis for obtaining optimum sensitivity within the limit of a practically realisable unit.

A series of measurements was carried out to verify the above theoretical expression. Figure 4.4a shows the variation of ρ_o with the variation of H (the thickness), for a typical set of values of other factors of the equation 4.6b. The experimental results agree well with the theoretical prediction that ρ_o should be a direct function of H. Thus sensitivity can be increased by reducing H to the limit set by the choice of having a robust structure.

The typical experimental results as shown in Figure 4.4b, supports the theoretical conclusion that ρ_o is a direction function of h_o. Thus with the decrease of the gap between the two tines of the resonator, the sensitivity increases. As already mentioned this is a main design criterion of the present transducer. However the sensitivity can be increased by this technique to the limit set by the loss of the resonator, which will be discussed in the next section.

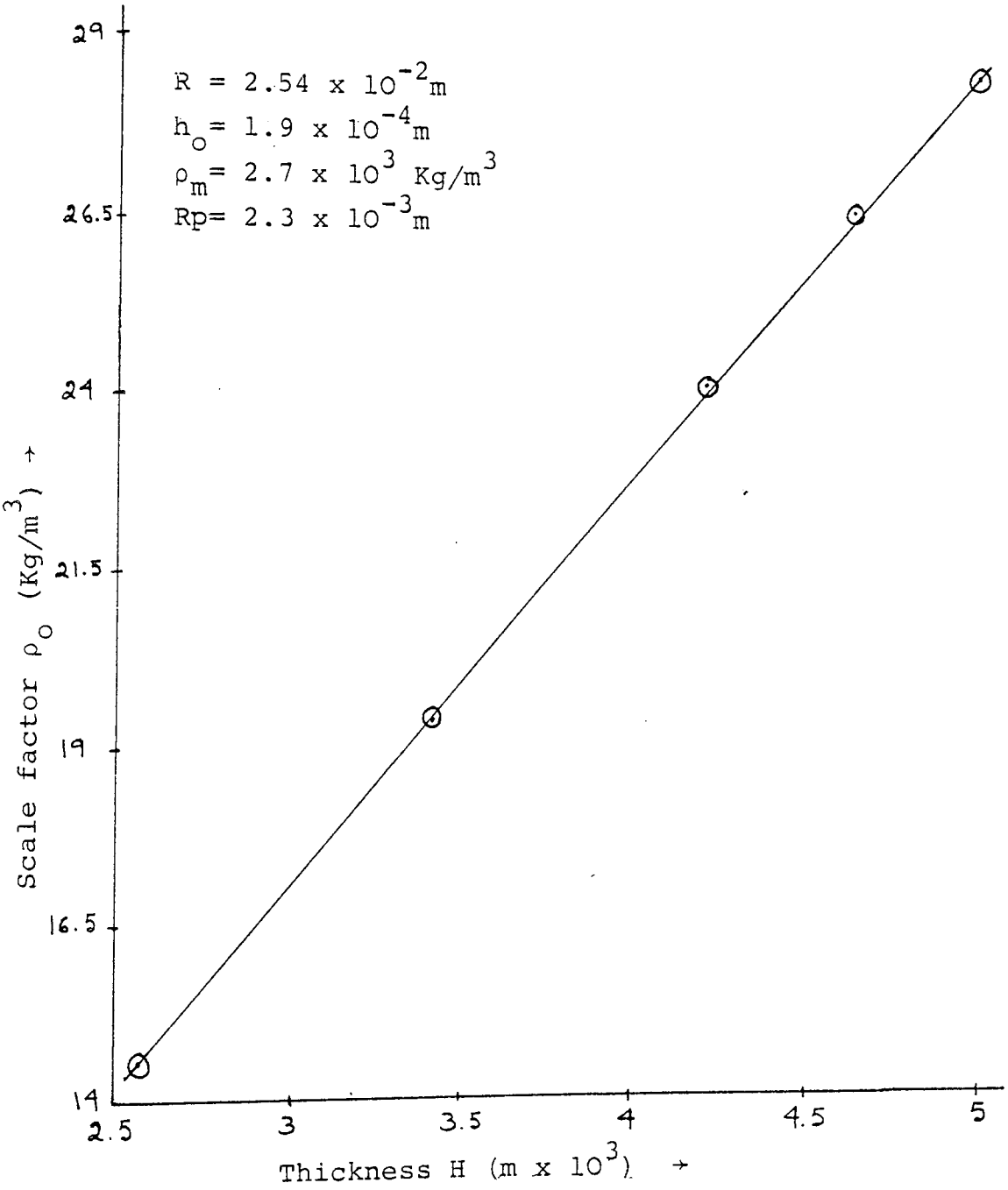

FIGURE 4.4a The variation of ρ_o, the scale factor as a function of H, the thickness of the disks of the circular resonator for a typical set of values of other parameters as shown.

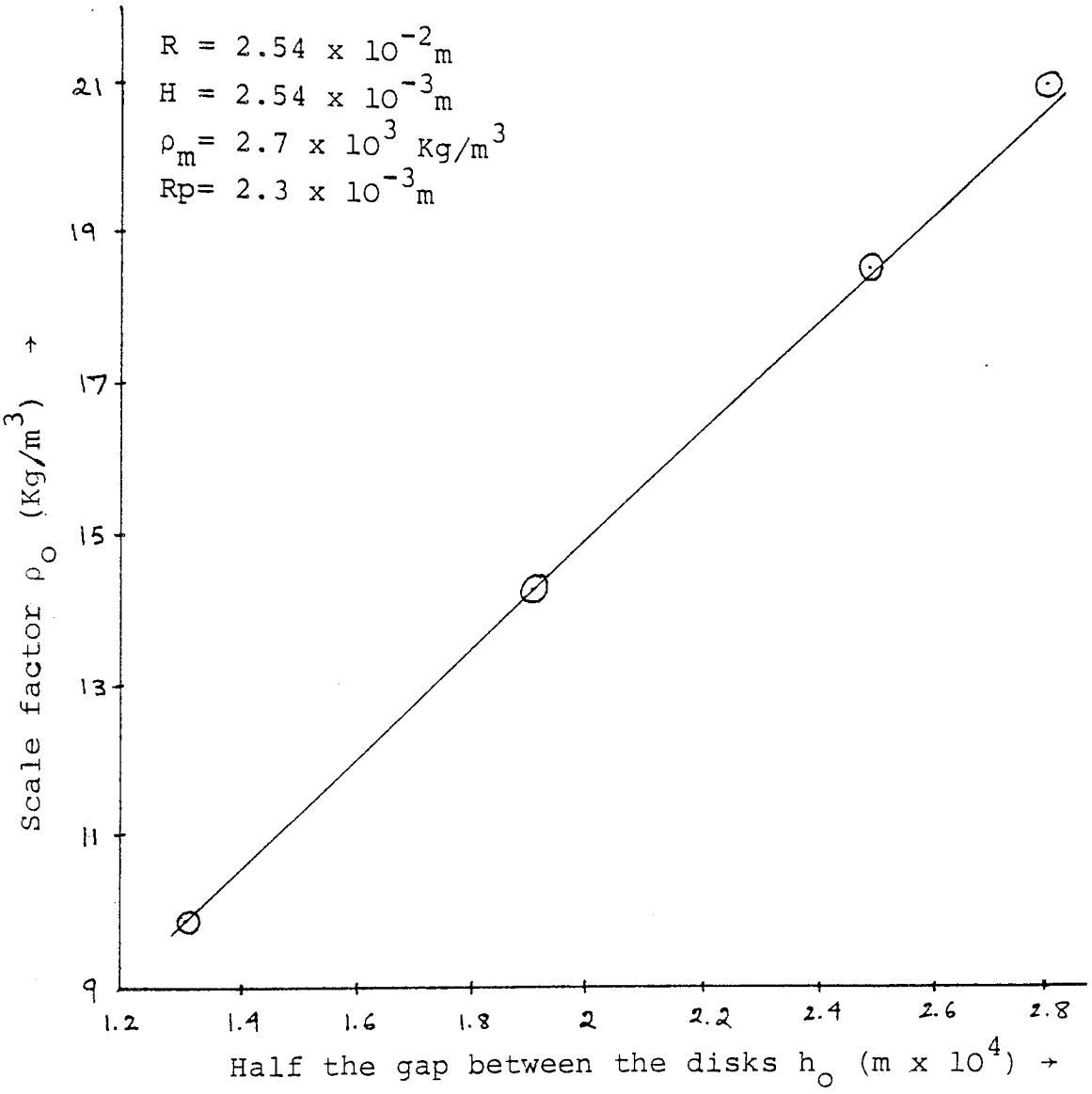

FIGURE 4.4b The variation of ρ_o, the scale factor, as a function of h_o, half the gap between the disks of the circular resonator, for a typical set of values of other parameters as shown.

According to the theoretical expression 4.6b, ρ_o should be an inverse function of R^2. The typical experimental results of Figure 4.4c agree well with this feature. Again this method of increasing the sensitivity by the increase of R, is limited by the loss of the resonator (see next section).

The role of ρ_m in ρ_o has already been discussed in Section 4.2.

The value of the numerical constant K_c, as calculated from experimental results is approximately .14. The theoretical analyses reported in Sections 3.6.1 and 3.6.2 gave the value as .15 and .125 respectively. The small discrepancy between the theoretical and experimental values reflects the approximate nature of the theoretical analysis.

(b) The rectangular resonator:

The difficulty for a theoretical solution for the rectangular resonator has already been mentioned in Chapter 3. However formulation for it can be done by analogy with the circular one, supported by experimental results. Thus a series of measurements has been carried out with different geometrical dimensions of the rectangular resonator.

As expected from the circular case H and h_o have similar effects on ρ_o.

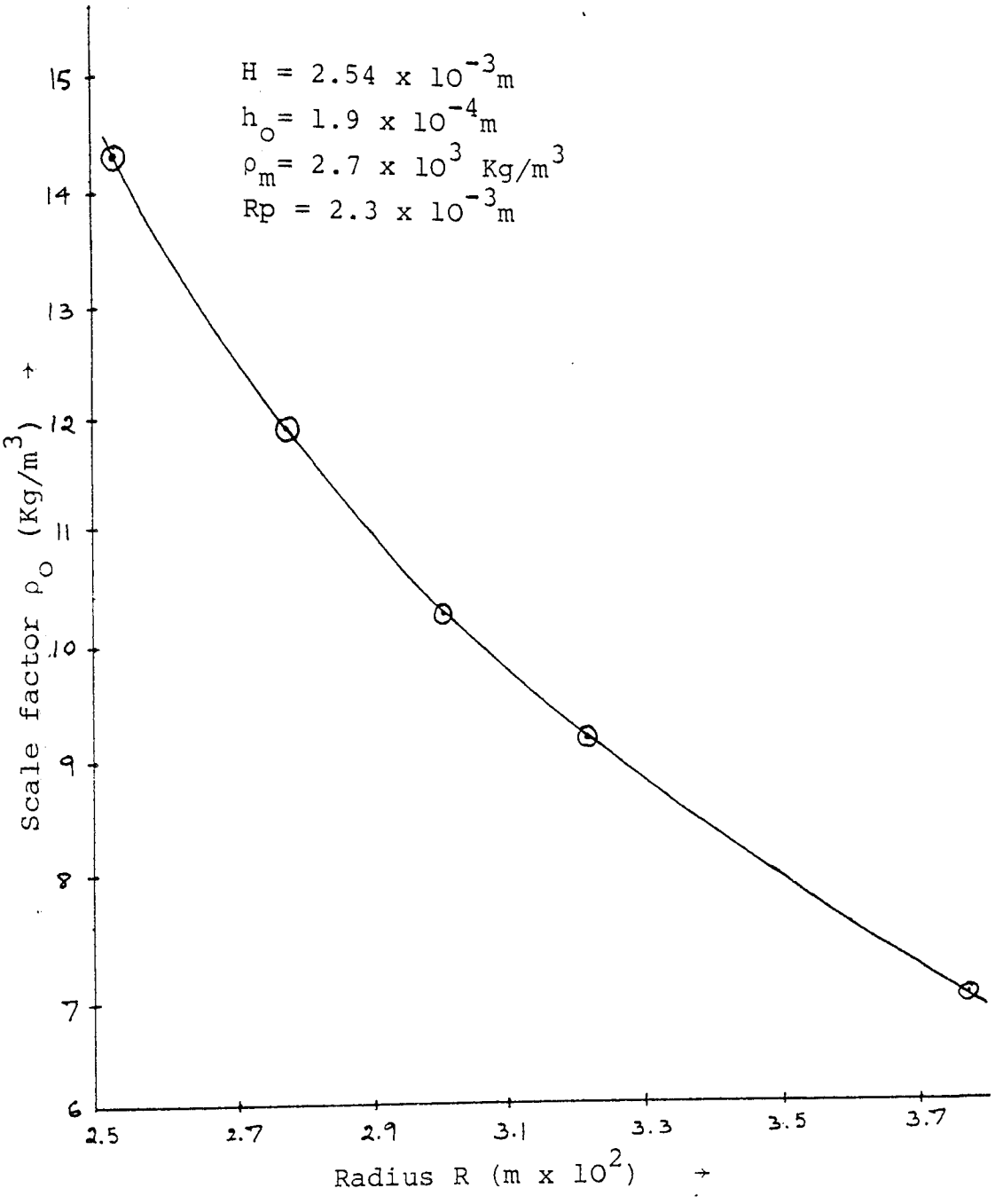

FIGURE 4.4c The variation of ρ_o, the scale factor, as a function of R, the radius of the disks of the circular resonator, for a typical set of values of other parameters, as shown.

The parameter L_T (the length of the tines) has been found to have no effect on ρ_o. Thus the size of the unit can be reduced by decreasing L_T, without affecting sensitivity. However this is limited by the stiffness effect which becomes significant with the increase of frequency due to the decrease of L_T (see Section 4.6).

Figure 4.5 is a typical plot of the variation of ρ_o with the variation of W (width of the resonator). It can be seen that ρ_o is an inverse function of W^2. Thus sensitivity can be increased by increasing W. Again this is limited by the stiffness effect as discussed in Section 4.6, and by the losses of the resonator as will be discussed in Section 4.8.

From the above experimental results and by analogy with the circular resonator, the formulation for the rectangular version can be expressed as

$$\rho_g = \frac{\rho_m H h_o}{K_R W^2} \left| \left(\frac{f_o}{f_g}\right)^2 - 1 \right| \qquad (4.7)$$

where K_R = numerical constant

W = width of the tines

and all other relations have the same meaning as in equation 4.1.

The value of the numerical constant K_R has been found to be approximately .06.

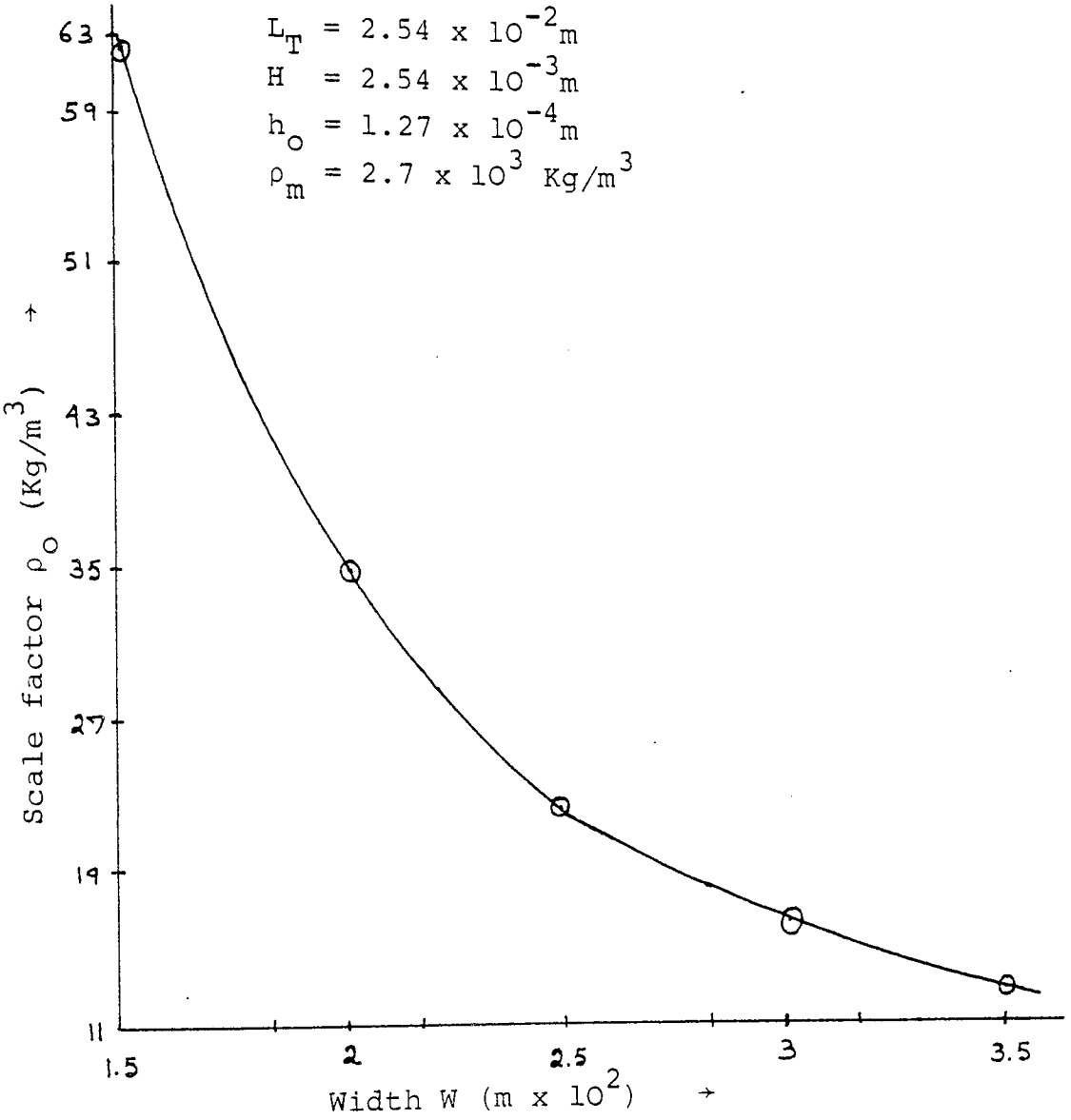

FIGURE 4.5 The variation of ρ_o, the scale factor as a function of W, the width of the plates of the rectangular resonator, for a typical set of values of other parameters, as shown.

4.8 LOSS AND Q FACTOR

The transducer is essentially an electronic oscillator using the mechanical resonator as the frequency controlling element. Therefore to keep the Q (a measure for sharpness of resonance) of the resonator at a reasonable value, (say more than 10), is an important factor in the design. An expression for Q is

$$Q = 2\pi \frac{\text{energy stored}}{\text{energy lost per cycle}}$$

Thus the lower the loss, the higher is the Q. The factors responsible for the loss may be classified into two broad divisions:

(a) Losses due to the presence of the gas

(b) Losses in the mechanical and electromechanical system.

(a) Losses due to the presence of the gas

There are two causes for this loss -

(1) loss due to acoustic radiation,

(2) viscous loss.

The former phenomenon has been widely studied in the literature. It is a well-established fact that the acoustic energy radiated by a resonator decreases as the ratio of its geometrical dimension to the wavelength of sound in the fluid decreases. As already mentioned,

this ratio has been designed to be small, making the losses minimal.

As a thin layer of gas is set into motion there is considerable viscous loss. In fact it has been found that this loss is a dominant factor in determining Q of the present resonators. The resistive part of equation 3.41 gives the theoretical expectation of the effects of different parameters on the viscous loss. For convenience the expression is repeated here:

$$R_L = \frac{3\pi\mu R^4}{8h_o^3} \qquad (4.8)$$

A series of measurements has been carried out to verify the above expression. The input of the active bridge (Figure 4.1d) has been supplied with a constant amplitude signal at the natural frequency of the resonator, from a variable frequency oscillator and the output amplitude has been measured by an oscilloscope. When there is no gas, i.e. in vacuum, there is no viscous loss. Thus the decrease of the output of the active bridge in presence of gas relative to that in vacuum, can be taken as a measure of the viscous loss (assuming negligible radiation loss).

In considering geometrical dimensions of the resonator, from equation 4.8, it is expected that the loss will increase directly with R^4 and inversely as h_o^3.

Resonators of different radii and gaps between the disks have been made and measurements with them agree fairly well with the above expectations.

Similar results have been obtained for the rectangular version of the resonator. The viscous loss increases with the increase of both W and L_T and decrease of h_o.

The effect of pressure on viscous loss is an interesting feature. From the kinetic theory of gases

$$\mu \simeq \frac{1}{3} \rho_g \bar{c} \ell \qquad (4.9)$$

where ρ_g is density of the gas, $\bar{c}$ is mean speed and ℓ is mean free path of the gas particles. For a particular gas, except at very low pressure (determined by the mean free path phenomenon[51]), $\bar{c}$ and the product $\rho_g \ell$ are constant at constant temperature. Hence from equations 4.8 and 4.9, it is expected that except at very low values, viscous loss should be almost independent of gas pressure. A typical experimental result is shown in Figure 4.6. The curve has been drawn automatically by an X-Y plotter. The circuit used is shown in Figure 4.7. The phase-locked loop and the active bridge maintain the resonator at the desired flexural fundamental natural frequency (details will be described in Section 4.10), which varies with the density of the gas due to variation in pressure. The output signal of PLL and hence input of the active bridge is constant in amplitude irrespective

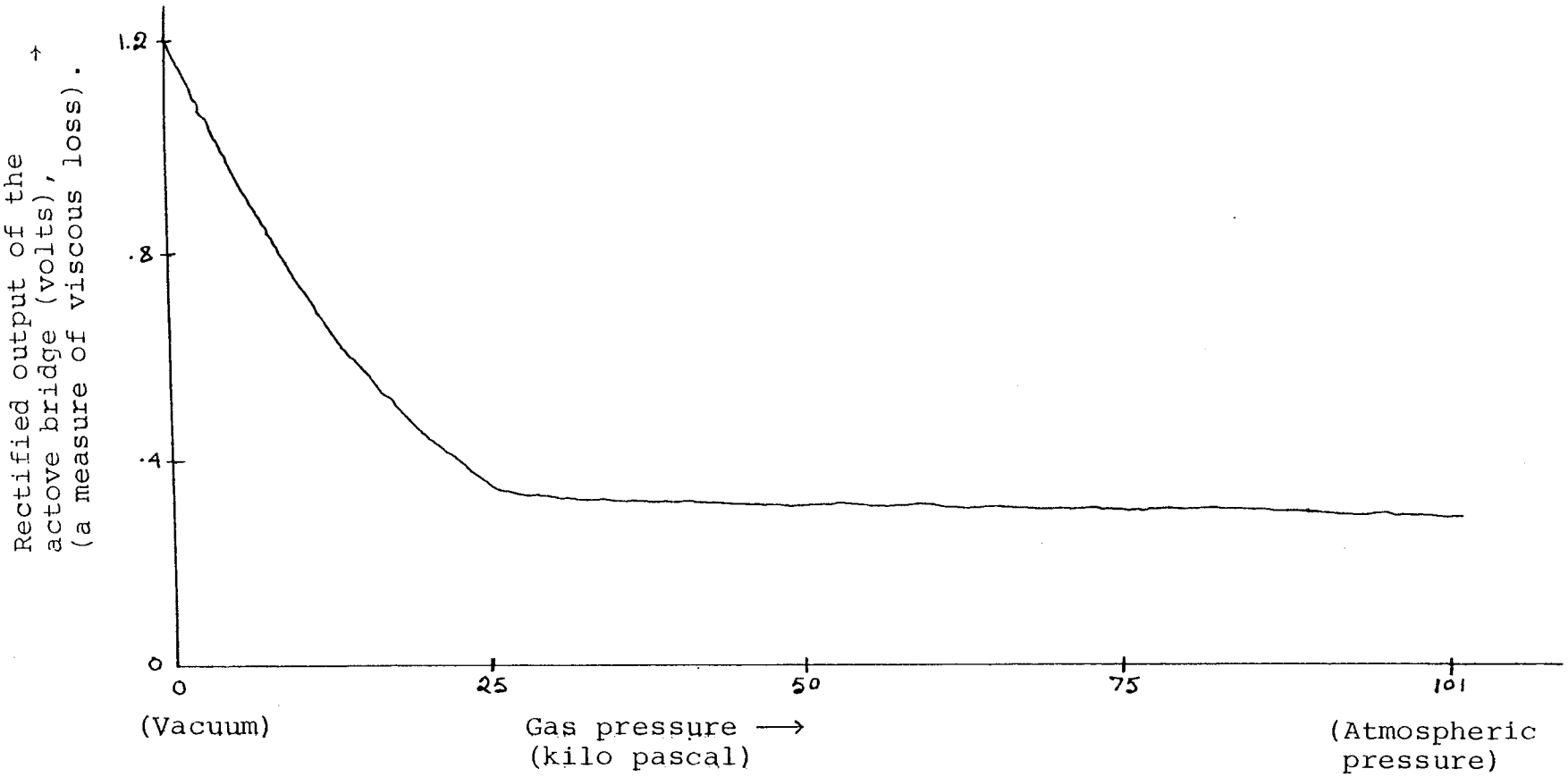

FIGURE 4.6 A typical variation of viscous loss with variation of pressure. At low range there is large variation but after that it is almost constant. The gas is argon.

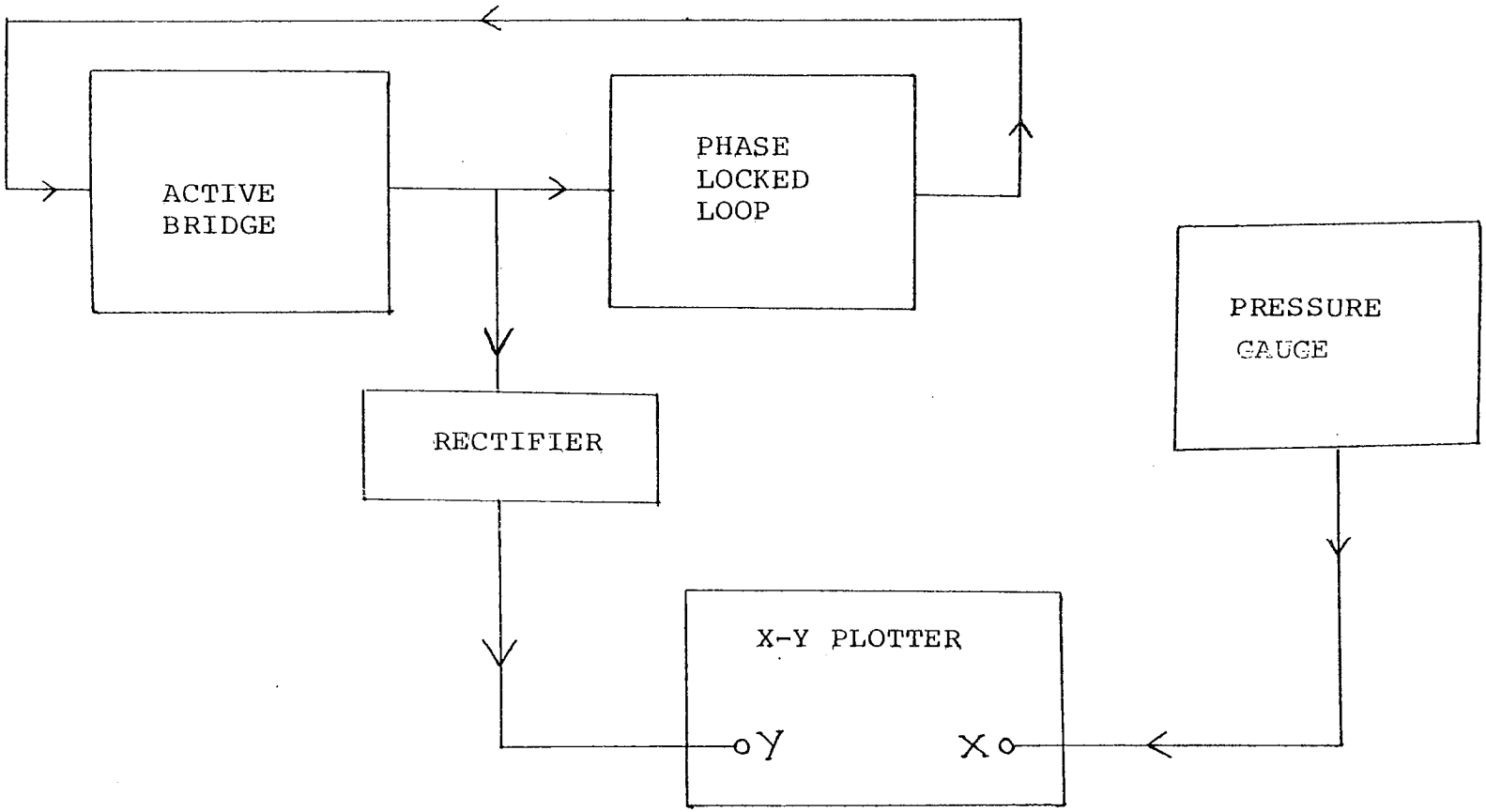

FIGURE 4.7 Block diagram of the circuit used for drawing the variation of the viscous loss as a function of pressure (the curve of Figure 4.6).

of the input of the PLL. Thus the resonator is excited by a constant amplitude signal and the output amplitude of the active bridge varies with the loss of the resonator. Thereby, as already explained, the output in the presence of the gas relative to that in vacuum can be taken as a measure of the viscous loss. The two inputs of the X-Y plotter are,

(1) the analog output of the pressure gauge (see Section 4.4) and

(2) the rectified output of the active bridge.

As can be seen from the plot, the experimental results agree well with the theoretical expectation. At very low pressure range there is large variation of viscous loss, but thereafter it is almost constant. The slight variation may be due to acoustic radiation loss (which increases with the increase of pressure).

(b) Losses in the mechanical and electromechanical systems:

These losses are due to

(1) the internal friction of the resonator material and the PZT elements,

(2) Signal loss due to coupling.

As already discussed in Section 4.2, materials with very low internal friction have been used in the designs, thus having negligible effect on the overall Q

factor. Different grades of PZT elements are available[58], with Q typically ranging from 60 to 1200. Thus loss due to internal friction of the PZT elements can be made small by choosing those of high Q and using gauges much smaller, compared with the resonator plates.

Signal loss due to coupling has been minimized by using piezoelectric drive and pick up as already discussed in Section 4.3.

4.9 OPTIMAL DESIGN AND CALIBRATION

The choice for a material of the resonator has already been reported in Section 4.2. From the discussions of Sections 4.7 and 4.8, the opposing conditions for maximization of sensitivity and maximization of Q are quite evident. Thus for an optimal design compromises are to be made in selecting geometrical dimensions of the resonator. By decreasing the gap ($2h_o$) between the two members of the resonator, sensitivity can be increased up to the limit set by a minimum satisfactory value of Q (say 10). By increasing radius (R) or width (W), as the case is, sensitivity can be increased, again limited by the above factor.

The thickness (H) of the members of the resonator can be decreased for increasing sensitivity, to the limit set by a choice for a robust structure. Again while choosing geometrical dimensions of the resonator, due

consideration is to be given to have the reactive loading in the predominated mass effect region, as discussed in Section 4.6.

Figures 4.8a and 4.8b show photographs of a final design of the rectangular version and a final design for the circular version respectively. Their geometrical dimensions are also shown in the Figures. The sensitivity of the former one is about a 25% change of frequency for density change from 0 to 20 Kg/m^3. For the latter one the corresponding change is about 35%. The Q of the former one, just above the mean free path phenomenon (see Figure 4.6) is about 72, the resonator being in argon (there are small variations of Q due to gases of different viscosities). (See equation 4.8). The value falls slowly (see Section 4.8), to 64 at a pressure of 17×10^5 pascal. This being well above the least satisfactory value, a high stability (about 1 in 10^5) of the transducer has been obtained. For the circular resonator Q (and hence stability) is of the same order.

Figures 4.9a and 4.9b show two calibration curves of the transducers using the resonators of Figures 4.8a and 4.8b respectively. In these manually drawn curves, three gases having a wide density range, namely argon, nitrogen and helium have been used. Variations of densities of the gases have been obtained by locating

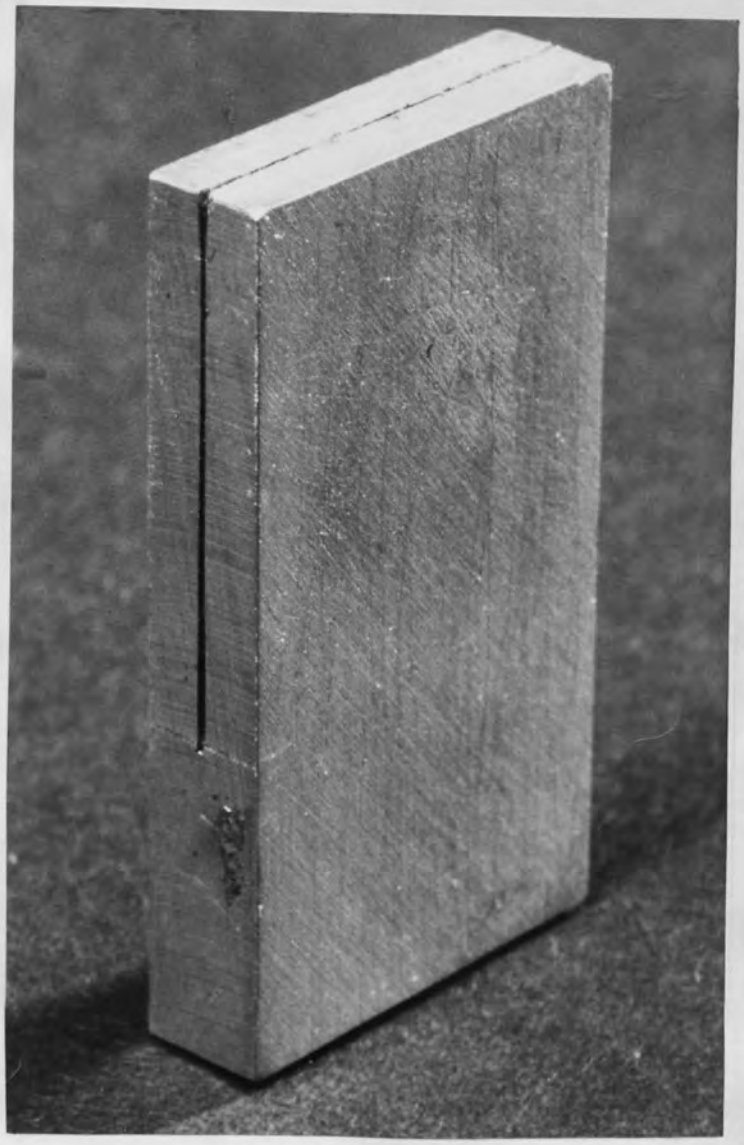

L_T : length of the tines = 2.54×10^{-2} m

W : width of the tines = 2.54×10^{-2} m

H : thickness of the tines = 2.54×10^{-3} m

$2h_o$: gap between the tines = 2.54×10^{-4} m

FIGURE 4.8a The photograph of a final design of the rectangular resonator for the gas density transducer. Calibration curve for it is shown in Figure 4.9a.

R : radius of the disks = 2.54×10^{-2} m

R_p : radius of the connecting post = 2.3×10^{-3} m

H : thickness of the disks = 2.54×10^{-3} m

$2h_o$: gap between the disks = 3.8×10^{-4} m

FIGURE 4.8b. The photograph of a final design of the circular resonator for the gas density transducer. Calibration curve for it is shown in Figure 4.9b.

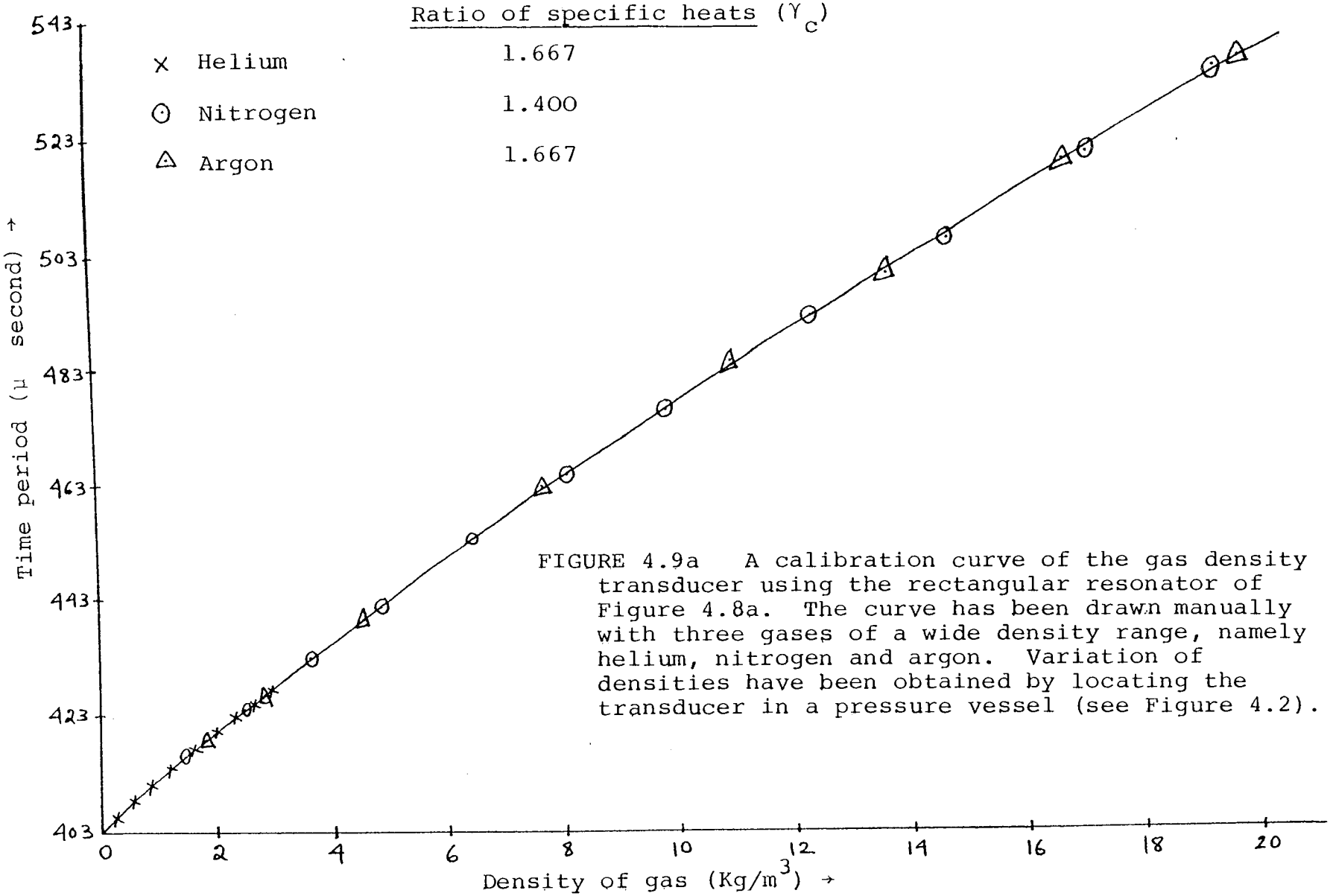

FIGURE 4.9a A calibration curve of the gas density transducer using the rectangular resonator of Figure 4.8a. The curve has been drawn manually with three gases of a wide density range, namely helium, nitrogen and argon. Variation of densities have been obtained by locating the transducer in a pressure vessel (see Figure 4.2).

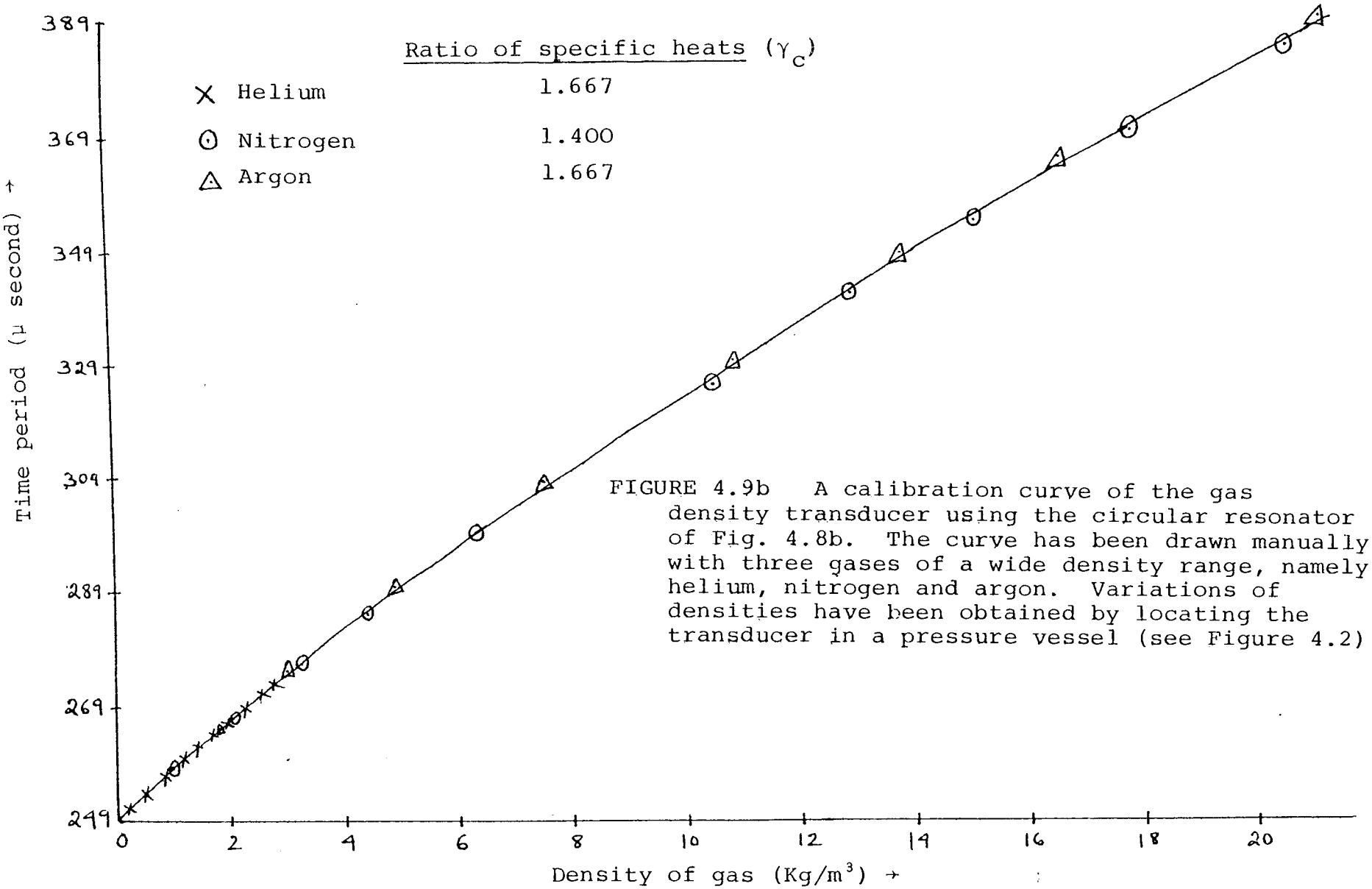

FIGURE 4.9b A calibration curve of the gas density transducer using the circular resonator of Fig. 4.8b. The curve has been drawn manually with three gases of a wide density range, namely helium, nitrogen and argon. Variations of densities have been obtained by locating the transducer in a pressure vessel (see Figure 4.2).

the transducer in a pressure vessel (see Section 4.4). Irrespective of γ_c the results for all the gases lie on the same curve. It may also be noted that time period (inverse of frequency) has been used, rather than frequency, because of its advantage of being measured more quickly[3,7] at these comparatively low frequencies. Figures 4.11a and 4.11b show two automatically drawn (using X-Y plotter) calibration curves for the transducer using the resonator of Figure 4.8a. The former is for the gas argon and the latter for helium. The arrangement used is shown in Figure 4.10. The two inputs of the X-Y plotter are

(1) the analog signal obtained by a D-A converter using the digital output (time period) of the transducer as input,

(2) the analog output of a pressure gauge which measures the pressure of the gas and from which the density was calculated.

Both the Figures have two overlapped curves - one traced with increasing density and the other with decreasing density. From the overlapping very low hysteresis of the transducer is quite evident.

4.10 ELECTRONIC SYSTEMS

The reliability and economy of the electronic circuitry, in which integrated components have been

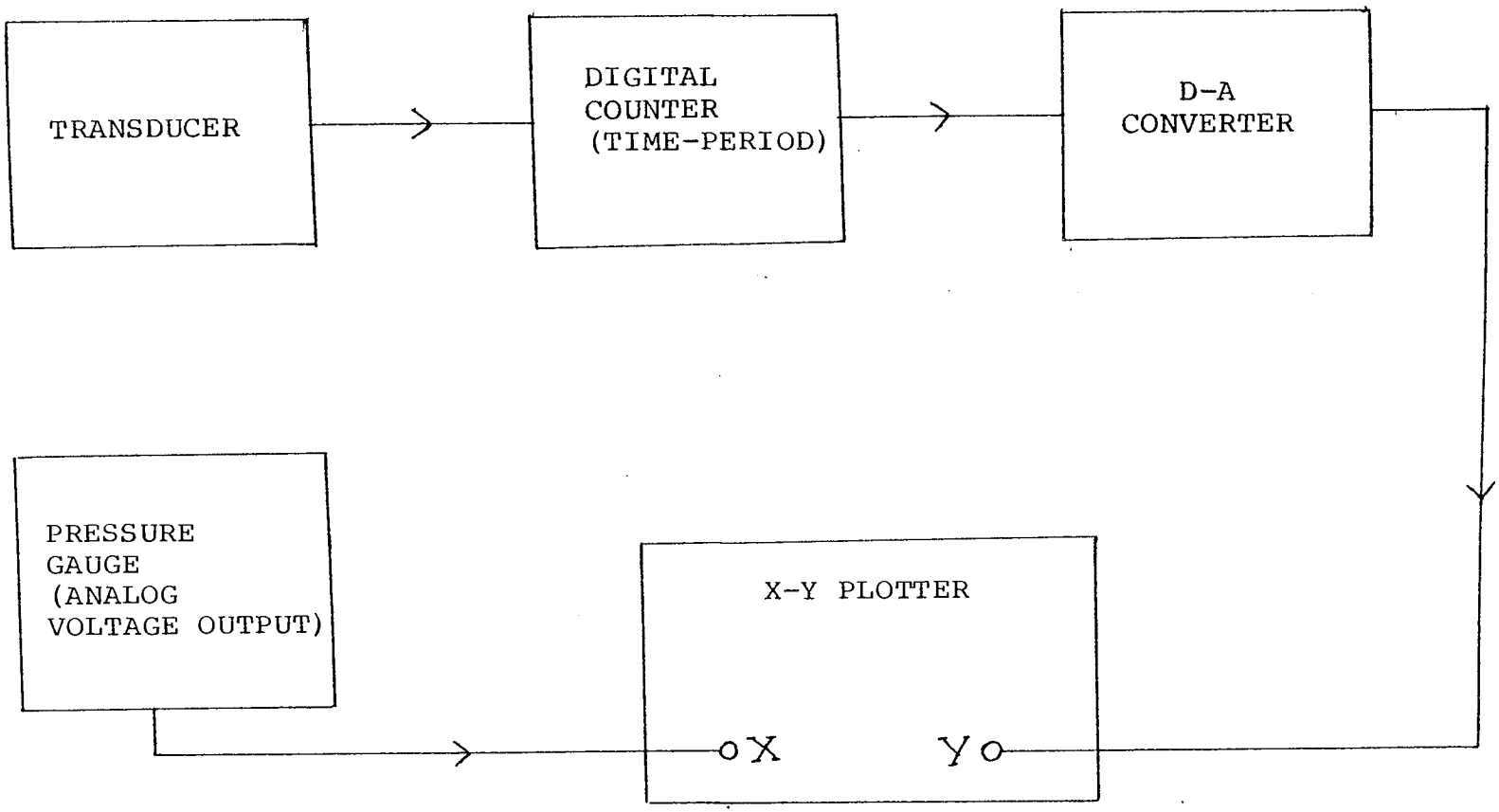

FIGURE 4.10 Block diagram of the arrangements used to draw the calibration curves of Figures 4.11a and 4.11b, by an X-Y plotter.

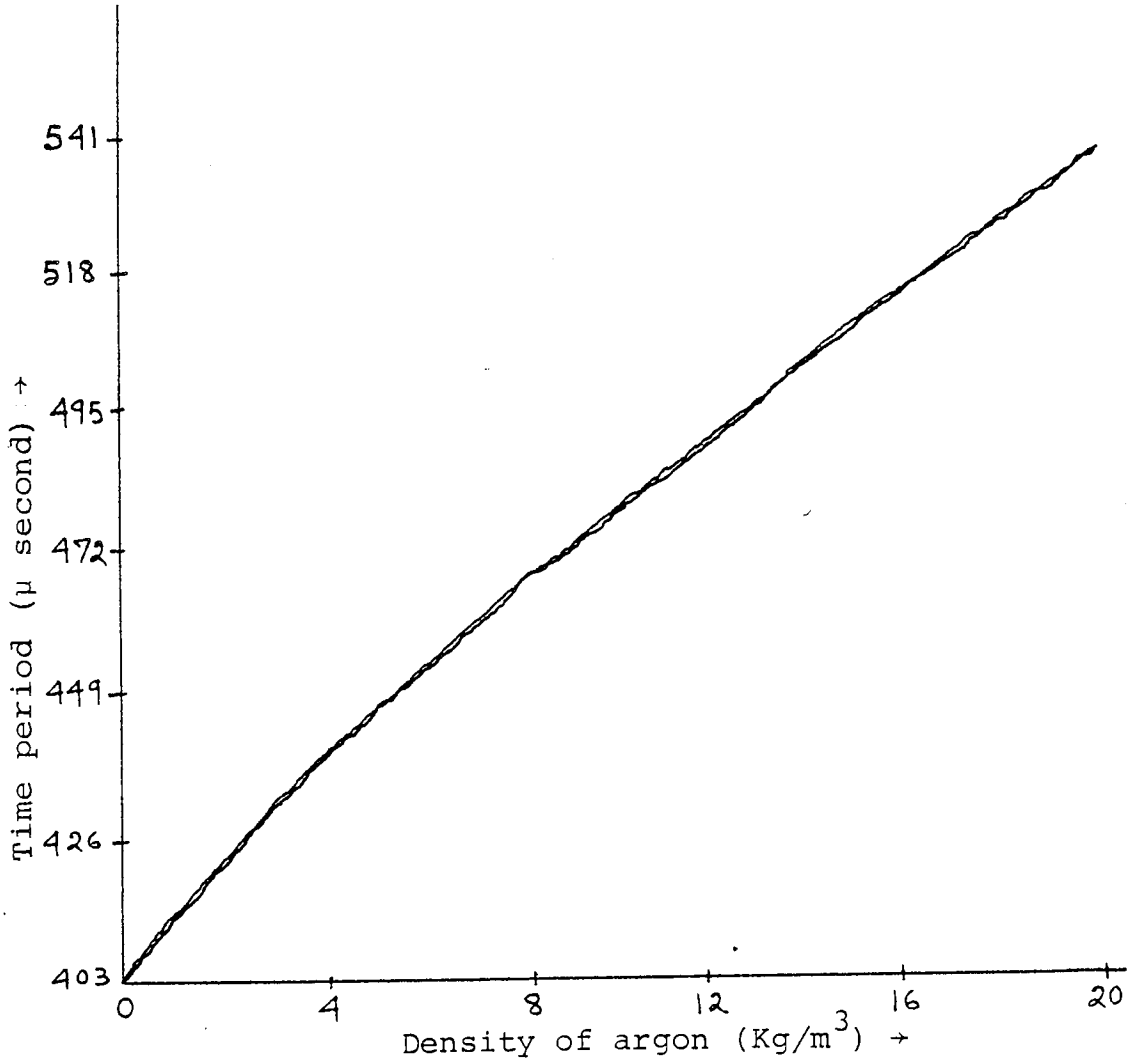

FIGURE 4.11a. A calibration curve drawn by a X-Y plotter (Figure 4.10) for the gas density transducer using the resonator of Figure 4.8a. The gas is argon and variation of its density has been obtained by locating the transducer in a pressure vessel. There are two overlapped curves - one with increasing density and the other with decreasing density. Very low hysteresis is quite evident from the overlapping.

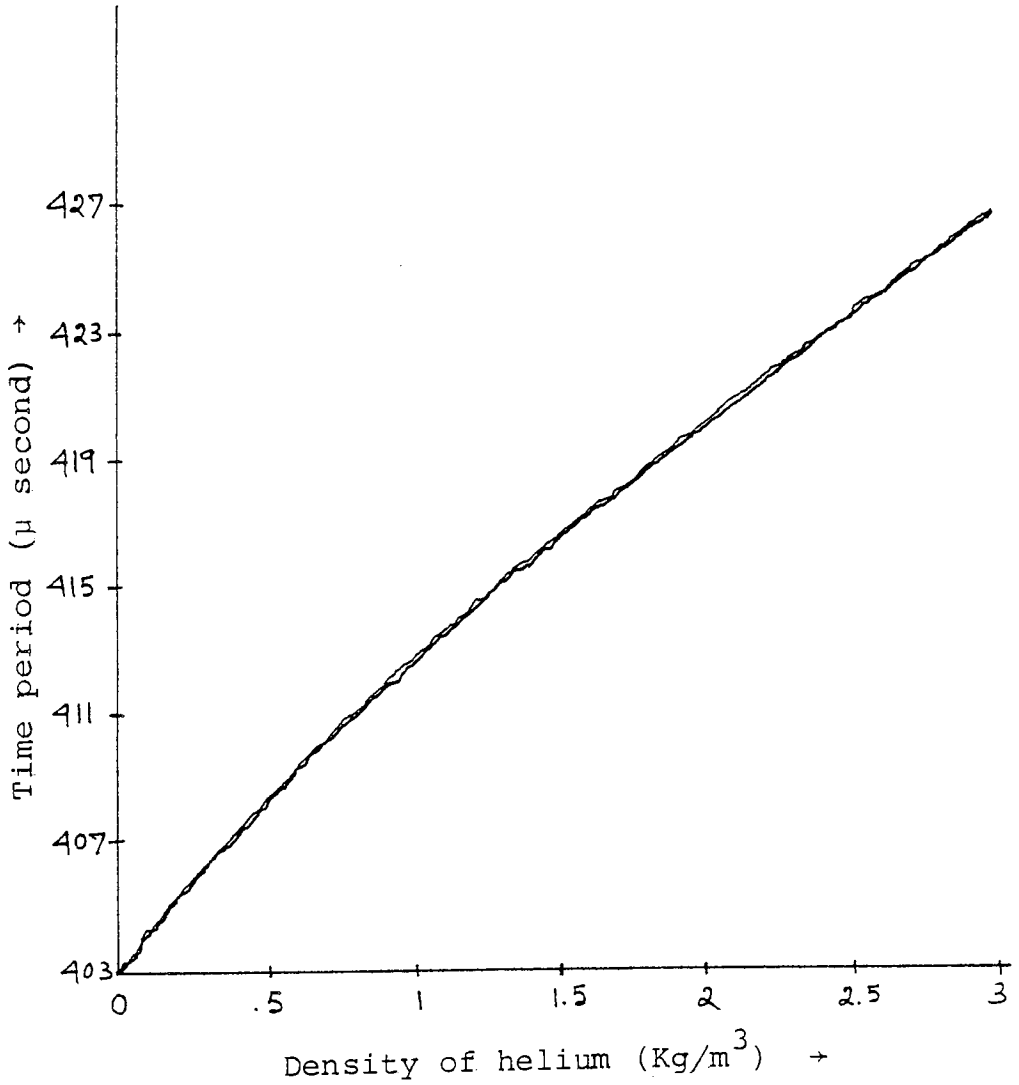

FIGURE 4.11b A calibration curve drawn by a X-Y plotter (Figure 4.10) for the gas density transducer using the resonator of Figure 4.8a. The gas is helium and variation of its density has been obtained by locating the transducer in a pressure vessel. There are two overlapped curves - one with increasing density and the other with decreasing density. Very low hysteresis is quite evident from the overlapping.

used throughout, is an important feature of the present density transducer. The drive and pick up arrangements of the resonator by highly efficient and mechanically very simple piezoelectric ceramics have already been dealt with in Section 4.3. Manual determination of the resonant frequency was also discussed there. Its automation is reported in this section. As the principles used are quite standard, only a brief outline is given.

Figures 4.12a and 4.12b show the block and detail circuit diagrams respectively, using the frequency tracking phenomenon of a phase locked loop. An excellent discussion of PLLs is given by Gardner[60] and by a number of integrated circuit manufacturers[61-63]. The one used here is the National LM 565. Basically the PLL has a free-running frequency determined by a timing resistor R_T and capacitor C_T. These components are so chosen that the desired (i.e. fundamental flexural) natural frequency of the resonator is within the capture range of the PLL. Then the PLL will lock onto the resonator frequency and thus will follow the density of the gas. Although a triangular waveform is used as the driving signal, because of the high selectivity of the resonator it responds only to the fundamental Fourier component of the driving signal[64].

An alternative circuit is shown in block and in detail in Figures 4.13a and 4.13b respectivly. Basically

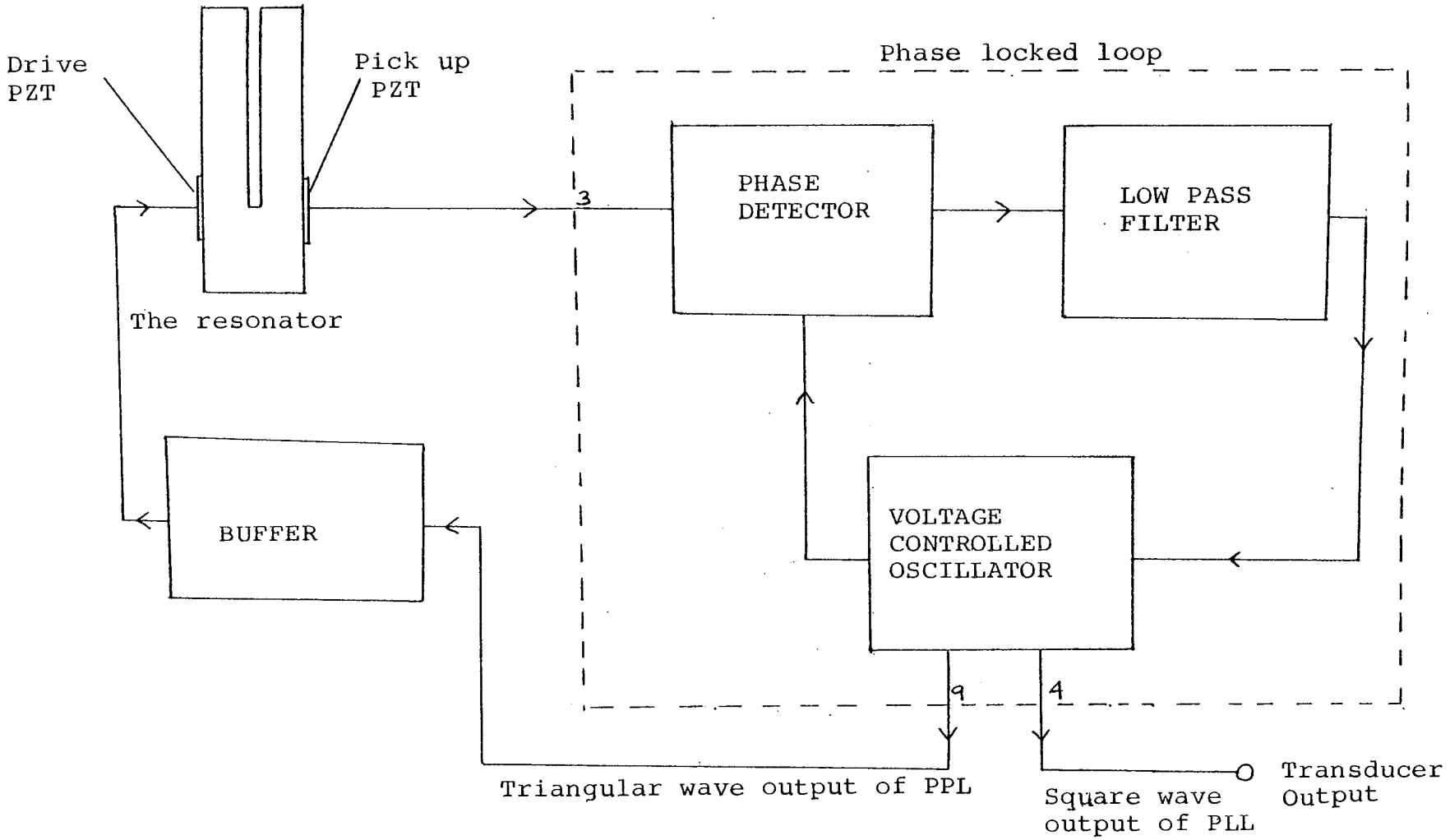

FIGURE 4.12a Block diagram of the gas density transducer using a phase locked loop.

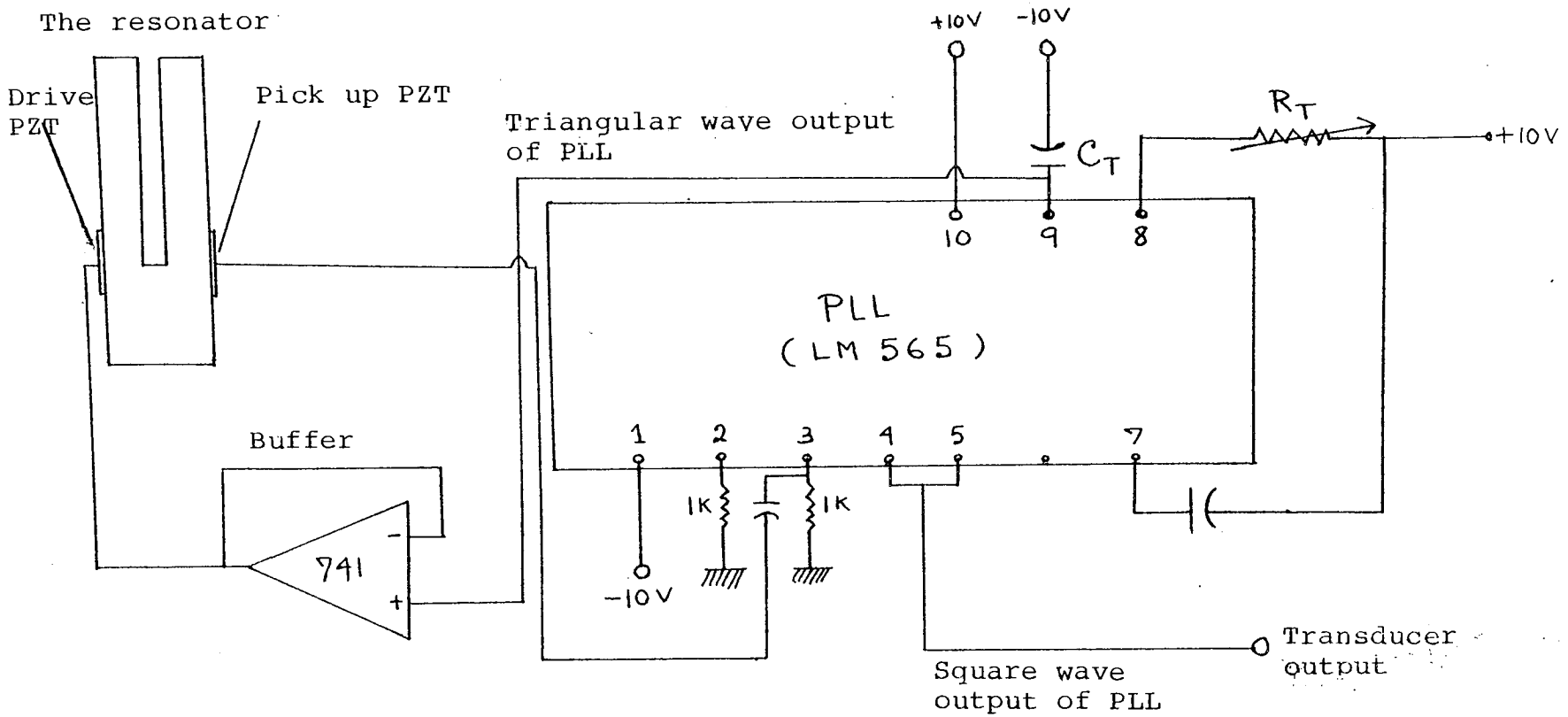

FIGURE 4.12b Detailed circuit diagram of the gas density transducer using a phase locked loop.

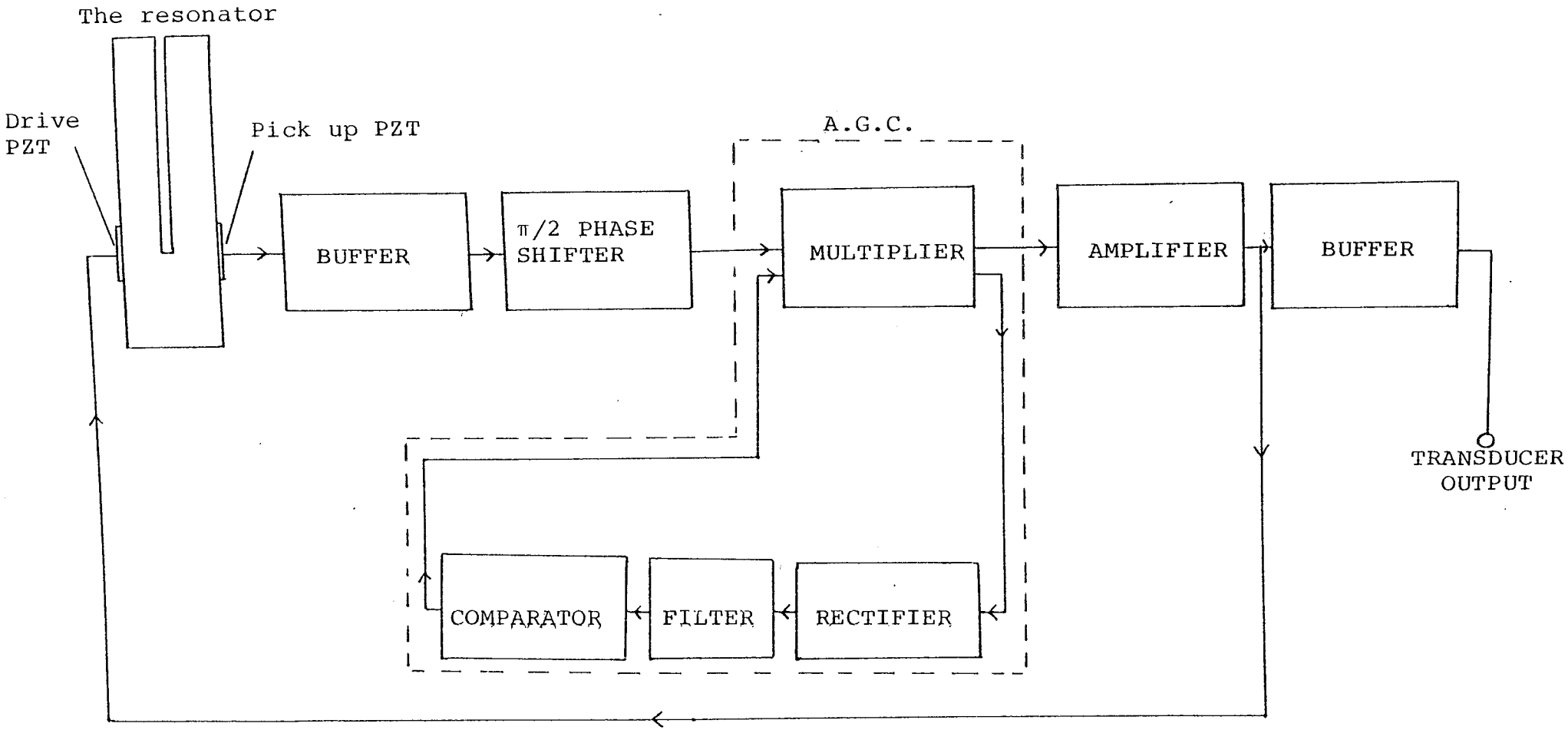

FIGURE 4.13a The block diagram of the gas density transducer using the technique of a feedback oscillator. The resonator acts as the frequency controlling element.

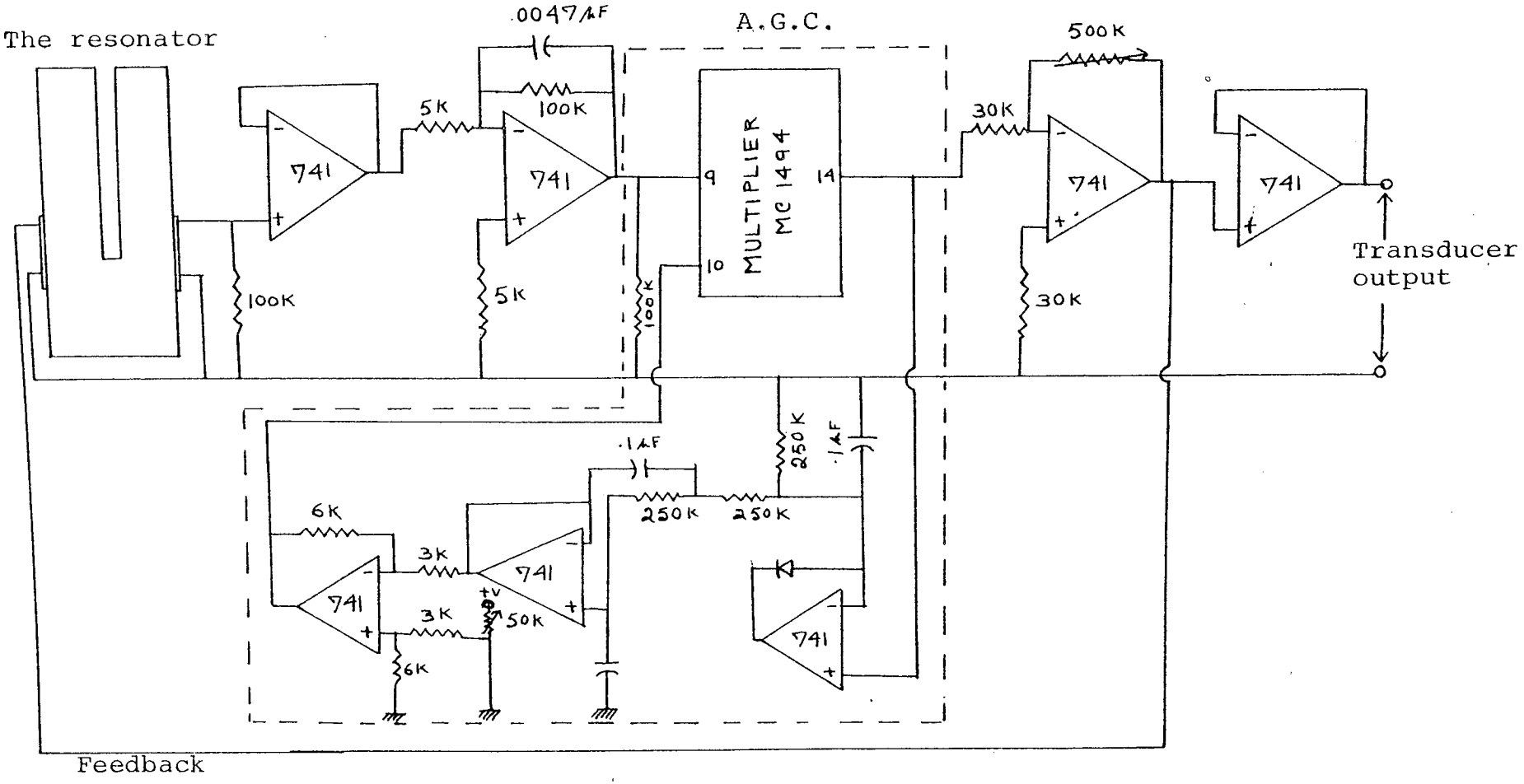

FIGURE 4.13b The detail circuit diagram of the gas density transducer using the technique of a feedback oscillator. The reasonator acts as the frequency controlling element.

it is a feedback oscillator where the resonator acts as the frequency controlling element. Thus the frequency of the oscillator follows the density of the gas. The fundamental flexural mode (i.e. the desired one) is well separated from other modes and the gain of the closed loop is sufficient to excite self oscillation only for this mode. The a.g.c. system is required to limit the amplitude of oscillation.

4.11 DISCUSSION

The thin layer phenomenon has made it possible to develop a high sensitive gas density transducer while retaining a robust structure of the sensor. Ease of clamping, virtual digital output, simplicity, compactness and moderate cost are also its advantages.

In addition to its conventional uses, it shows a promising development for a special use as the detector stage of a gas chromatographic system. Gas chromatography is an important technique which has applications in various fields such as process control, laboratory analysis of chemical compounds. This technique involves in anlysing a mixture of gases or vaporisable liquids by segregating it on a time basis into its components and measuring the concentration of each component. The detector stage carries out the latter function after the former is performed by the rest of the system which in a conventional unit comprises a controlled carrier gas supply, a sampler

and a column (Figure 4.14). Presently used detectors are based on complicated phenomena such as effect of gas on thermal loss of a hot wire, flame ionization and electron capature[65]. It is hoped that this density transducer being a highly sensitive absolute device for detecting very small change in gas density can be developed as a good simple detector stage. It will also have all the advantages of the frequency modulating technique. The rectangular sensor seems to be particularly suitable for this purpose. A schematic diagram of the proposed system is shown in Figure 4.14. The very narrow end of a conventional column can be made an integral part of the base of the sensor as shown in the figure. As in a conventional system carrier gas will continuously emerge at the end of the column and flow through the thin gap between the tines of the sensor. When segregated component gases will come out with the carrier gas, they will be detected by the sensor due to variation in densities. Preliminary experiments show a promising situation.

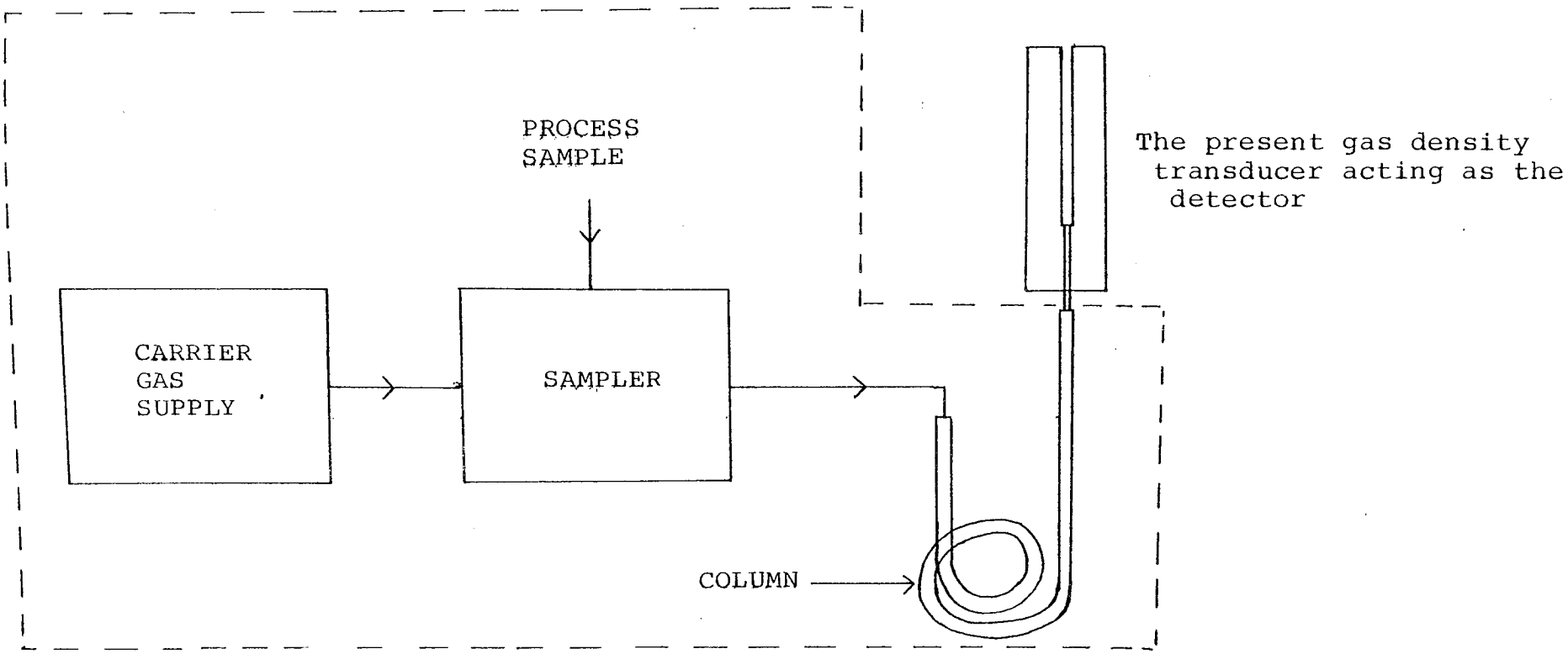

FIGURE 4.14 Proposed use of the gas density transducer as the detector stage of a chromatographic system.

CHAPTER 5

THE LIQUID DENSITY TRANSDUCER

5.1 INTRODUCTION

Typical geometrical dimensions of a practical design of the resonator for the liquid density transducer has been shown in Figure 2.5. An accuracy of about 1% was made the initial object. It can be seen that while all other dimensions are of the same order as for the gas density transducer, the gap between the two vibrating members is considerably greater. This feature gives the necessary practical requirement for the free movement of the liquid surrounding the resonator and also maintains a sharp resonance. Though the wider gap lowers the scale factor (see equations 4.6 and 5.8), the sensitivity is sufficiently high, considering the relatively higher densities of liquids. As based on the same principle and a similar structure of resonator, most of the design criteria for the case of gases (discussed in detail in the previous chapter) are also applicable to liquids. The particular considerations required for the latter case are dealt with in this chapter.

5.2 THEORETICAL CONSIDERATIONS

In the analysis of the two piston model (section 3.6), the added mass ΔM due to the loading effect of the thin layer of fluid was obtained as

$$\Delta M = \frac{3\pi}{20} \frac{\rho_f R^4}{h_o} \qquad (5.1)$$

where ρ_f = fluid density

R = radius of the disks

$2h_o$ = gap between the disks

The mass loading on the other face of a disk of the two piston model, can be taken approximately as that on a circular piston vibrating in an infinite baffle. This, as discussed in section 3.5.4, is

$$\Delta M = \frac{8}{3} \rho_f R^3 \qquad (5.2)$$

In the case of the resonator for the gas density transducer, only the added mass due to the thin layer was taken into account (neglecting that on the other face of the disk). From equations (5.1) and (5.2), it is quite evident that this is a reasonable approximation as (R/h_o) of the resonator for the gas density transducer is typically about two hundred. But due to the requirement of a wider gap, in the case of the liquid density transducer, ΔM of equation (5.2) becomes comparable to that of equation (5.1). Thus in calculating the change in frequency due to the mass loading of the surrounding liquid, both the expressions should be taken into account. By combining the two expressions, the added mass due to the loading of the surrounding liquid on a disk of the two piston model is

$$\Delta M = \frac{3\pi}{20} \frac{\rho_\ell R^4}{h_o} + \frac{8}{3} \rho_\ell R^3 \qquad (5.3)$$

where ρ_ℓ = density of the liquid

In the above expression, the effect due to the liquid circulating from one side of the disk to the other (making some contribution to ΔM) has been ignored. This has been done, as from the discussion of Chapter 3 it is quite evident that it is extremely difficult to include such a phenomenon in a theoretical analysis of vibrating body-fluid interaction. However, equation (5.3) gives useful information of the effects of different parameters for a practical design of the transducer.

From equations (5.3) and (3.15), the expression for the change of frequency of the two piston model, due to mass loading of the surrounding liquid is

$$\frac{f_\ell}{f_o} = \frac{1}{\sqrt{1 + \frac{\Delta M}{M}}}$$

$$= \frac{1}{\sqrt{1 + \frac{3\pi}{20} \frac{\rho_\ell R^2}{\rho_m H h_o} + \frac{8}{3} \frac{\rho_\ell R}{\rho_m H}}} \qquad (5.4)$$

where f_o = frequency in vacuum

f_ℓ = frequency in a liquid medium

ρ_m = density of the material of the disks

H = thickness of the disks.

From the fabrication point of view and also from other practical considerations such as the mounting and driving, the rectangular version of the resonator has been found to be more suitable. As discussed in Chapter 3 a complete theoretical analysis for this version is extremely difficult if not impossible, due to lack of geometrical symmetry. However, as in the case of the gas density transducer, formulation can be obtained by analogy with the circular version. Experimental results as discussed in Chapter 4, gave good support for this analogy. Thus following the procedure of section 4.4, the expression for change in frequency of the rectangular resonator can be written as

$$\frac{f_\ell}{f_o} = \frac{1}{\sqrt{1 + K_1 \frac{\rho_\ell W^2}{\rho_m H h_o} + K_2 \frac{\rho_\ell W}{\rho_m H}}} \qquad (5.5)$$

where W = width of the resonator

K_1, K_2 = numerical constants whose values are to be determined experimentally,

and all other notations have the same meanings as in equation (5.4).

From equation (5.5)

$$\rho_\ell = \frac{\rho_m H}{K_1 \frac{W^2}{h_o} + K_2 W} \left| \left(\frac{f_o}{f_\ell}\right)^2 - 1 \right|$$

Or,

$$\rho_\ell = \rho_o \left| \left(\frac{f_o}{f_\ell}\right)^2 - 1 \right| \qquad (5.6a)$$

$$\text{where } \rho_o \equiv \frac{\rho_m H}{K_1 \frac{W^2}{h_o} + K_2 W} = \text{scale factor} \qquad (5.6b)$$

5.3 EXPERIMENTS AND CALIBRATION

From equations (5.6b),

$$K_1 \frac{W^2}{h_o} + K_2 W = \frac{\rho_m H}{\rho_o} \qquad (5.7)$$

Thus measuring frequencies in vacuum and in a liquid of known density, of resonators having different widths (W) or gaps ($2h_o$), from equations (5.6a) and (5.7) the values of K_1 and K_2 can be obtained. With this object, two series of measurements - one with resonators of different widths, and the other with resonators of different gaps, have been carried out. The values of the constants have been found as

$$K_1 = .05 \text{ and } K_2 = .13 \text{ approximately.}$$

Putting these values in equation (5.6b),

$$\rho_o = \frac{\rho_m H}{.05 \frac{W^2}{h_o} + .13W} \qquad (5.8)$$

Equation (5.8) shows effects of different parameters on scale factor and hence sensitivity of the resonator.

Thus this expression is the basis for designing the transducer, guided by practical requirements. It can be seen that it is similar to the expression 4.6b for the gas density transducer, except the term (.13W) in the denominator. However this term also supports the feature that the scale factor should decrease with the increase of the width of the resonator. Therefore the design criteria as discussed in section 4.9 are also applicable to the present case. Experimental results support well this conclusion. Thus by decreasing the gap ($2h_o$) between the two plates of the resonator, sensitivity can be increased to the limit set by the requirement of free movement of the surrounding liquid. By increasing width (W), sensitivity can be increased limited by the decrease of quality factor Q (as discussed in section 4.8 for the case of the gas density transducer). The thickness of the plates (H) can be decreased for increasing sensitivity to the limit set by a choice for a robust structure. Again while choosing geometrical dimensions of the resonator, due consideration is to be given to have the reactive loading in the predominated mass effect region (similar to the case of the gas density transducer as discussed in section 4.6).

Under the above discussed criteria, a final design of the resonator is shown in the photograph of Figure 5.1. Its scale factor ρ_o is about 240. The frequency reduces by 55% from vacuum to water (i.e. for a density

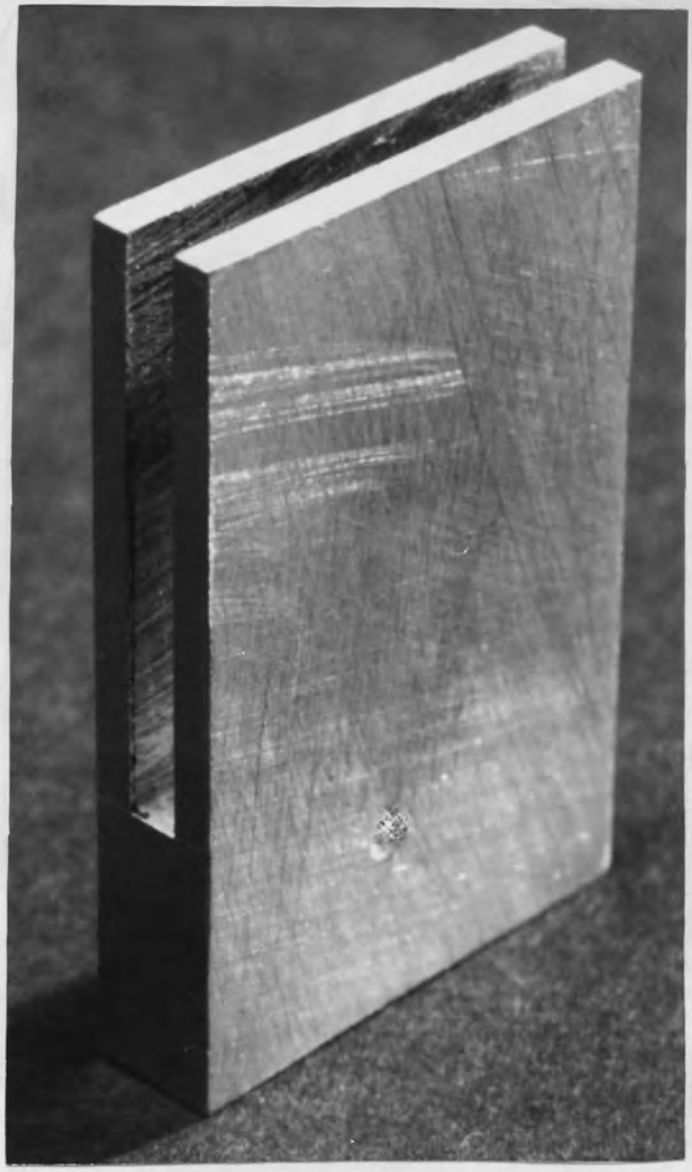

L_T : length of the tines = 2.54×10^{-2}m

W : width of the tines = 2.54×10^{-2}m

H : thickness of the tines = 2.54×10^{-3}m

$2h_o$: gap between the tines = 2.54×10^{-3}m

λ : wavelength in water (at the resonant frequency) = 1.28m (approx.)

FIGURE 5.1 The photograph of a final design of the resonator for the liquid density transducer. A calibration curve for it is shown in Figure 5.2.

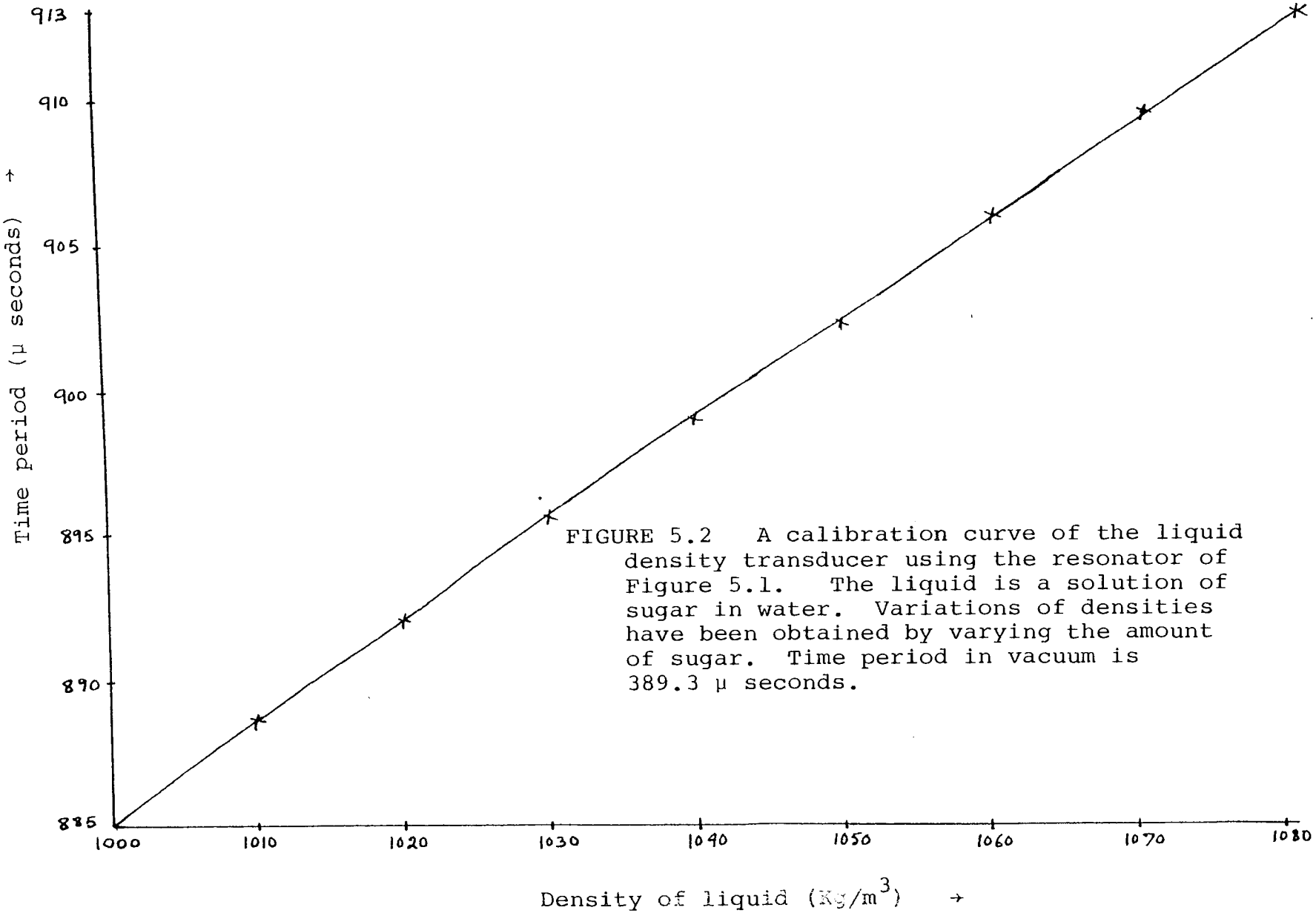

FIGURE 5.2 A calibration curve of the liquid density transducer using the resonator of Figure 5.1. The liquid is a solution of sugar in water. Variations of densities have been obtained by varying the amount of sugar. Time period in vacuum is 389.3 μ seconds.

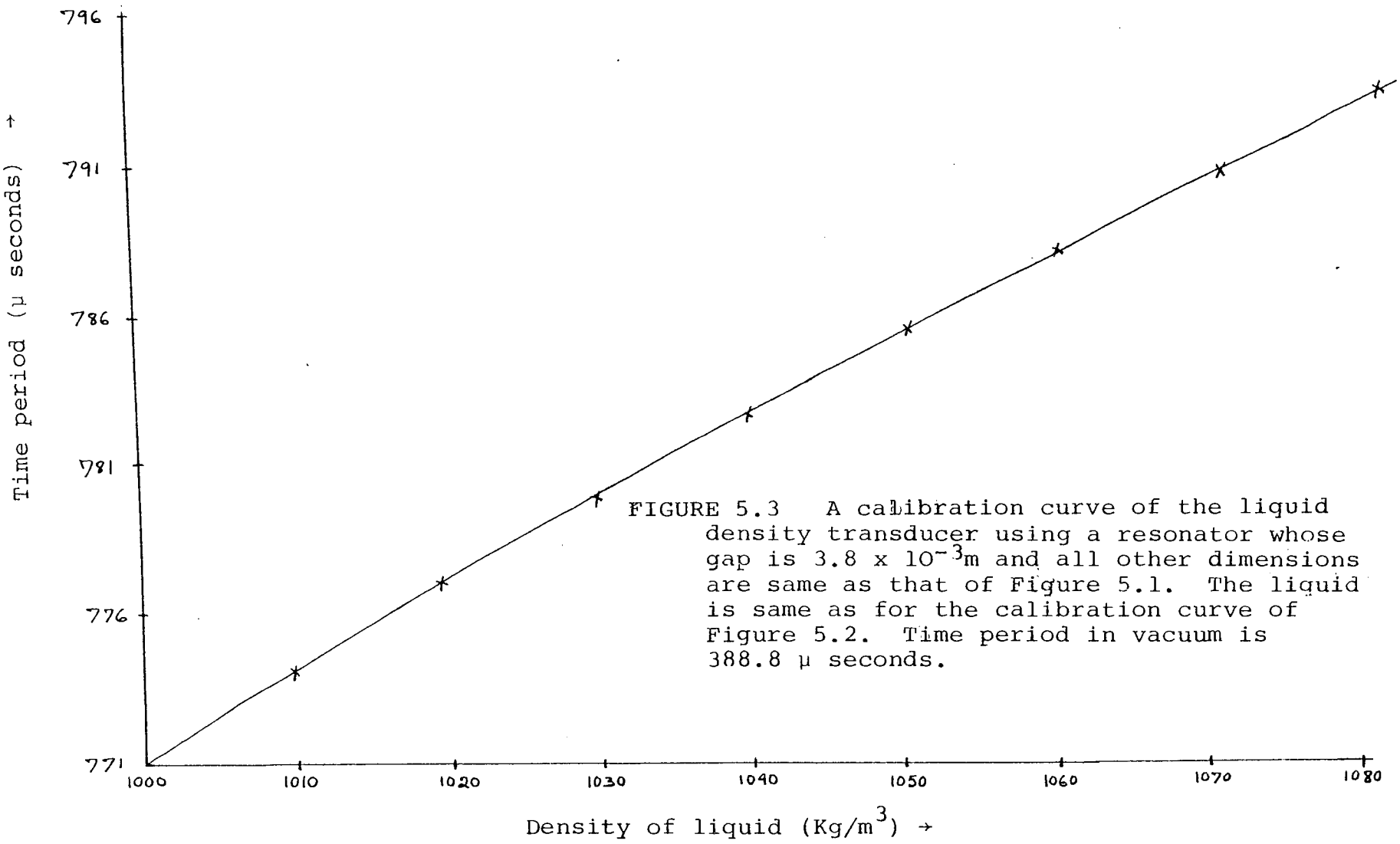

FIGURE 5.3 A calibration curve of the liquid density transducer using a resonator whose gap is 3.8 x 10^{-3}m and all other dimensions are same as that of Figure 5.1. The liquid is same as for the calibration curve of Figure 5.2. Time period in vacuum is 388.8 μ seconds.

span of 0-1000 Kg/m^3). The quality factor Q in water is about 50. This is well above the least satisfactory value (see section 4.8), giving a high stability (about 1 in 10^4). Figure 5.2 shows a calibration curve for the liquid density transducer using this resonator. The liquid is a solution of sugar in water. Variation of densities have been made by varying the amount of sugar. Again time period (inverse of frequency) rather than frequency has been used in the calibration as discussed for the case of the gas density transducer in section 4.9. Figure 5.3 shows a calibration curve for the liquid density transducer using a resonator whose gap is 3.8×10^{-3}m and all other dimensions are same as the resonator of Figure 5.1. Its scale factor is about 340.

5.4 DISCUSSION

Due to the relatively higher viscosity of a liquid (in comparison to a gas) the damping of the resonator is higher (see section 4.8). Thus a driving voltage amplifier is needed in the electronic system of Figure 4.9. Figure 5.4 shows such a system. The alternative circuit of Figure 4.10 can also be used.

Similar to the case of the gas density resonator, PZT plates have been used for drive and pick-up arrangements for the advantages discussed in section 4.3. Due to the very mechanical simplicity of this system, the present

transducer can be built in the form of a simple convenient probe (as shown in Figure 5.5) in addition to the conventional use of such a device in the pipe line of a process control unit. However a most significant consideration needed for the piezoelectric drive system, is the requirement for electrical insulation of the PZT plates. In the laboratory development, readily available insulating materials such as lacquer (aerosols), glue (araldite, super glue) have been used. These have given satisfactory results. However it is thought that in the case of commercial production of the transducer, a better method of insulation will be required. For example, during the manufacture of the PZT elements, a suitable insulating material can be sputtered on the surfaces (with connecting leads coming out). Literatures of PZT manufacturers[57,58] support this idea.

An alternative drive system is to use thin length of magnetostrictive metal sheets. This avoids the problem of insulation and has the advantage of removing the electrical drive from the liquid. This would require considerable effort to reach a good practical device.

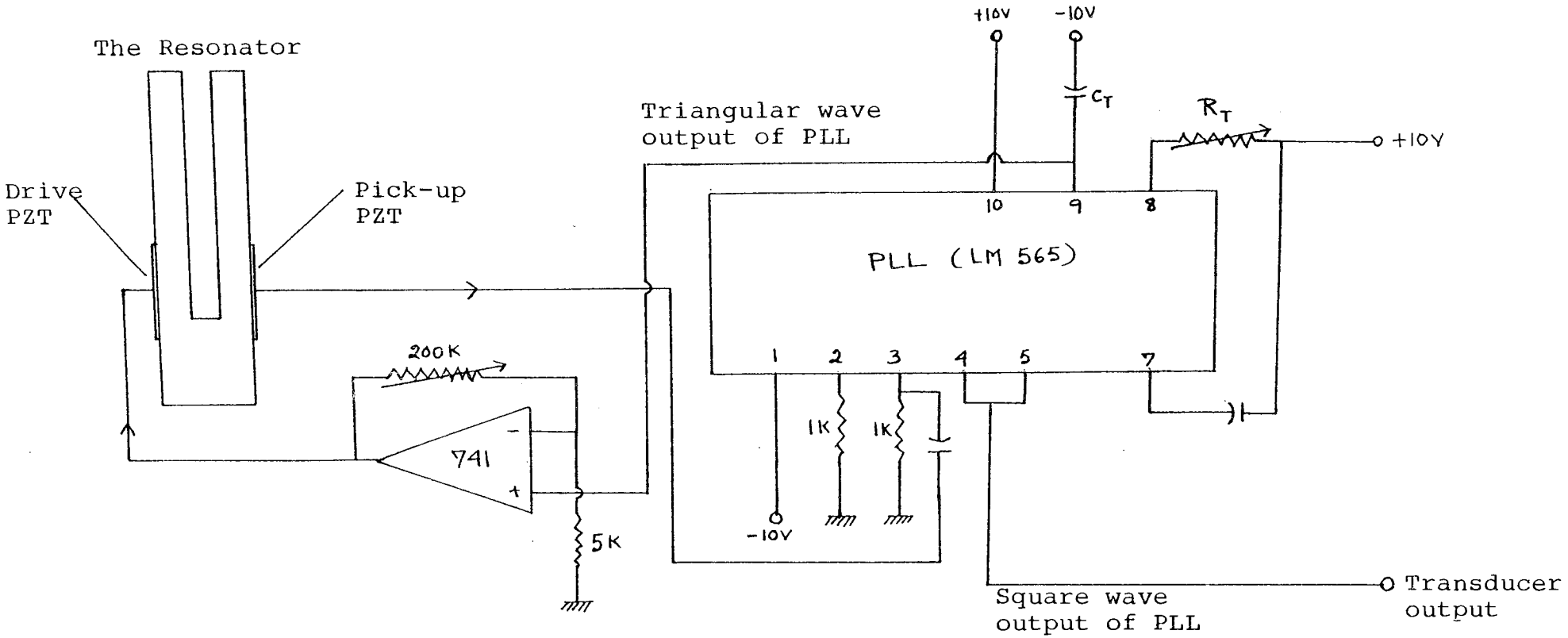

FIGURE 5.4 Detailed circuit diagram of the liquid density transducer using a phase locked loop.

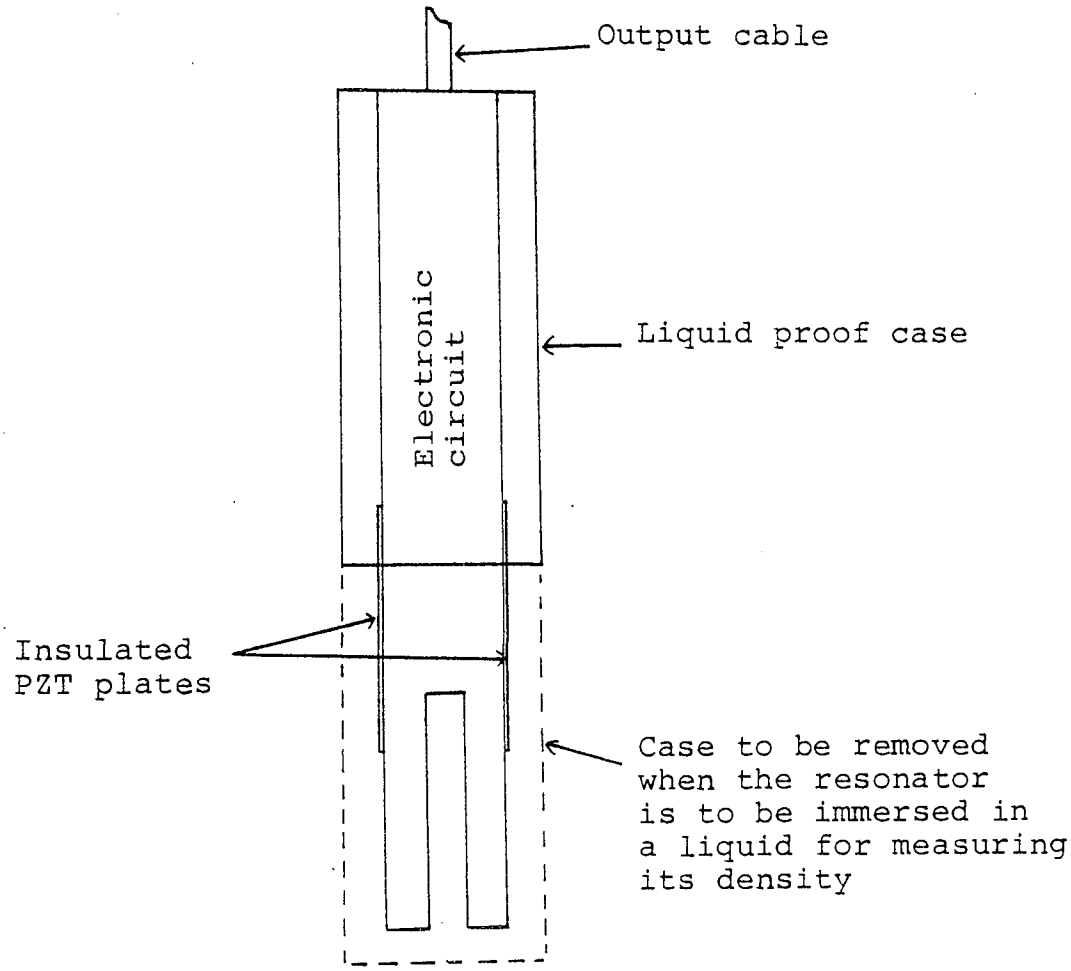

FIGURE 5.5 The liquid density transducer in the form of a convenient probe (view in section).

CHAPTER 6

THE TENSION TRANSDUCER

6.1 INTRODUCTION

In a simple beam a longitudinal stress will increase or decrease the stiffness depending on whether the stress is one of extension or compression. This will give rise to a corresponding increase or decrease in a natural resonant frequency of the beam. This principle is the basis of the tension transducer described here. With the increasing demand for digital instrumentation, this type of tension transducer having virtually a digital output is becoming widely used. A number of such devices have appeared within the last two decades[21-26]. Both wires and beams have been used as the sensing resonator. However in these designs major difficulties have been encountered regarding an important requirement, an efficient clamping arrangement for the resonator. Thus Wyman[21] in his force transducer says - "It is particularly important to terminate the wire efficiently, so that no relative movement exists between the wire and any part of the clamping arrangements. Furthermore no work hardening or embrittlement should occur at the termination".

In the case of the resonators for the fluid density transducers (discussed in Chapters 4 and 5) a successful

and easy clamping arrangement, using a type of double resonator giving dynamic balancing was achieved. The principal object here is to show that a similar double resonator can be used in a tension transducer to give an easy solution to this clamping problem. The double resonator, a pair of rectangular beams, designed for the purpose has been shown in Figures 2.1 and 2.6 (can also be seen in the photograph of Figure 6.3).

6.2 DYNAMIC CLAMPING

The basic principle of this phenomenon has been discussed in section 2.3. Its experimental verification for the case of the tuning fork like resonator for the fluid density transducer has been reported in section 4.5. The present resonator may be thought of two tuning forks end to end. Thus from the discussions of sections 2.3 and 4.5, it is expected that the two rectangular beams of this resonator in flexural vibration can be taken as in clamped state at the boundaries shown in Figure 6.1.

Because of the two clamped boundaries, the apparent increase in length should be double that of the tuning fork like resonator of the fluid density transducer.

Thus L, the length of the beams, in dynamic condition (in fundamental flexural mode of vibration), is

$$L = \ell + 2 \times .68H \qquad (6.1)$$

where ℓ = length in static condition

H = thickness

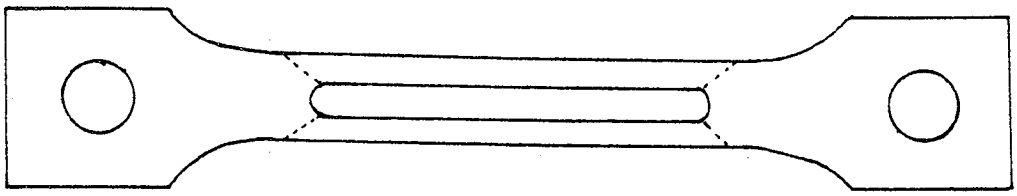

FIGURE 6.1 The two beams of the resonator while vibrating in flexure, are in clamped state at the boundaries shown by the dotted lines (view in section).

A series of measurements has been carried out to test this assumption. Resonators of different lengths and different thicknesses have been made and their resonant frequencies (in fundamental mode) under no tension have been measured. Theoretical values of these frequencies have been calculated from the formula[59]

$$f_{1O} = \frac{\pi}{2} \frac{(1.5056)^2}{L^2} \frac{H}{\sqrt{12}} C_o \qquad (6.2)$$

where f_{1O} = fundamental frequency in flexural vibration of a clamped-clamped beam under no tension.

L = length of the beam

H = thickness of the beam

$C_o \equiv \sqrt{\frac{E}{\rho}}$ = rod velocity

E = Young's modules

ρ = density of the material

A good agreement between the measured and theoretically calculated (with length correction as given by equation 6.1) frequencies has been found.

The dynamic clamping condition has also been verified by a vibration detecting magnetostrictive probe. By lightly touching a vibrating surface with the very sharp tip of this probe, the vibration can be observed on an oscilloscope (for a detailed description of the probe see reference 66). The beams have indeed been found in clamped state at the boundaries shown in Figure 6.1.

6.3 THEORETICAL FREQUENCY OF THE RESONATOR UNDER TENSION

A single beam of the resonator can be approximately represented as shown in Figure 6.2, below

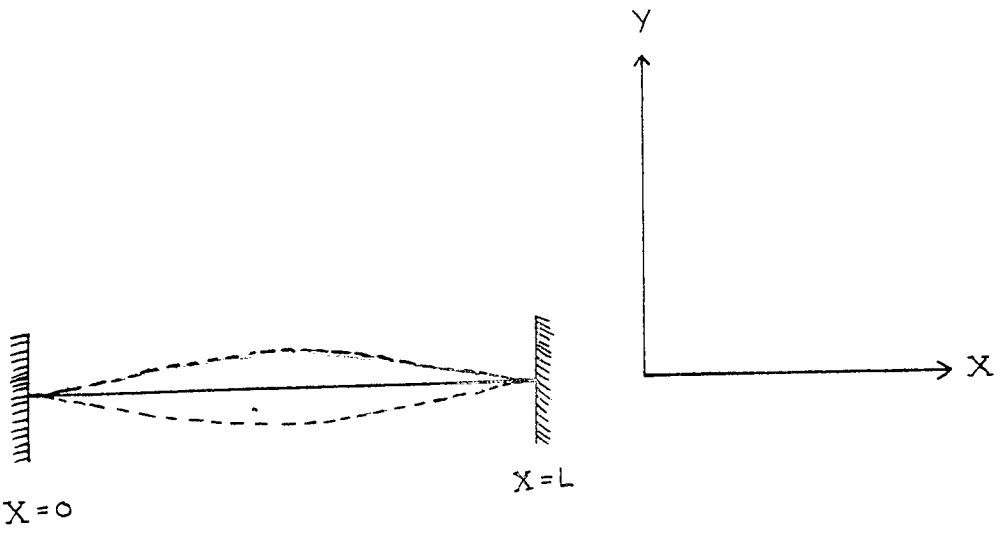

Figure 6.2

Under a tension T its equation of motion is[59)]

$$T\frac{\partial^2 y}{\partial x^2} - \frac{ESH^2}{12}\frac{\partial^4 y}{\partial x^4} = \rho S \frac{\partial^2 y}{\partial t^2} \qquad (6.3)$$

where $S \equiv WH$ = area of cross section

t = time

and all other notations have the same meanings as in equation 6.2.

Assuming a simple harmonic motion the frequency f_{nT} (where n=1 denote fundamental, n=2 first overtone and so on) is given by the equation

$$f_{nT} = \frac{\pi}{\sqrt{3}} C_o H \mu \sqrt{\mu^2 + 2\beta^2} \qquad (6.4)$$

where $\beta^2 = \dfrac{3T}{2\pi^2 ESH^2}$

and

for n=1, 3, 5 ...., μ is given by the equation

$$\mu \tan(\pi L \mu) = -\sqrt{\mu^2 + 2\beta^2}\tanh(\pi L\sqrt{\mu^2 + 2\beta^2}) \qquad (6.5)$$

for n = 2, 4, 6 ....., is given by the equation

$$\sqrt{\mu^2 + 2\beta^2}\tan(\pi L \mu) = \mu \tanh(\pi L\sqrt{\mu^2 + 2\beta^2}) \qquad (6.6)$$

To find f_{nT}, equations (6.4), (6.5) and (6.6) are to be solved numerically. Such a solution using a computer program is given in Appendix 2.

6.4 DESIGN CRITERIA

Though there is no explicit expression for the frequency f_{nT}, to show effects of different parameters in the design, an approximate equation can be fitted (for a certain range) using the numerical values. Thus equation (6.7) gives an approximate expression for the fundamental mode (for the range of $L\beta$ from 0 to .5).

$$f_{1T} \simeq \frac{1.015\ HC_o}{L^2} + \frac{.05}{L}\sqrt{\frac{T}{\rho WH}} \qquad (6.7)$$

From equation (6.7)

$$\frac{f_{1T}}{f_{1O}} \simeq 1 + .049L\sqrt{\frac{T}{EWH^3}} \qquad (6.8)$$

where f_{1O} = fundamental frequency under no tension

Equation 6.8 gives an approximate basis for designing the resonator within the limit of a practically realisable unit. Thus it can be seen that the sensitivity of the transducer will increase with the increase of length L. By choosing a material of lower Young's modulus E, sensitivity can be increased. However choice of material is limited by such factors as low temperature coefficient and low hysteresis (discussed later in this section). Equation (6.8) shows an interesting feature that for a certain cross sectional area WH (giving a certain maximum allowed stress and hence tension), sensitivity can be increased by decreasing

thickness H with the proportional increase of width W (to keep the certain value of WH). For the first overtone an expression corresponding to that of equation (6.8) for the fundamental mode, is

$$\frac{f_{2T}}{f_{20}} \simeq 1 + .027L \sqrt{\frac{T}{EWH^3}} \qquad (6.9)$$

where f_{2T} = frequency of first overtone under a tension T

f_{20} = frequency of first overtone under no tension.

Comparison between equations (6.8) and (6.9) shows that sensitivity is higher for the fundamental mode. In fact this mode has the highest sensitivity.

Under the above discussion, a resonator designed for the range of 0 to 5 kN is shown in Figure 6.3. Its calibration curve (at fundamental mode) is shown in Figure 6.4. Choice of material for the resonator of such a frequency domain tension transducer mainly depends on such factors as

(a) Low temperature coefficient
(b) Low hysteresis
(c) High eleastic limit

A low temperature coefficient is generally achieved by choosing a material in which the elastic changes can be balanced against dimensional changes over a specified temperature range[6,23]. Some favourable materials are titanium, steel P18, ground stock steel, steel GK40, steel 35 khGSA.

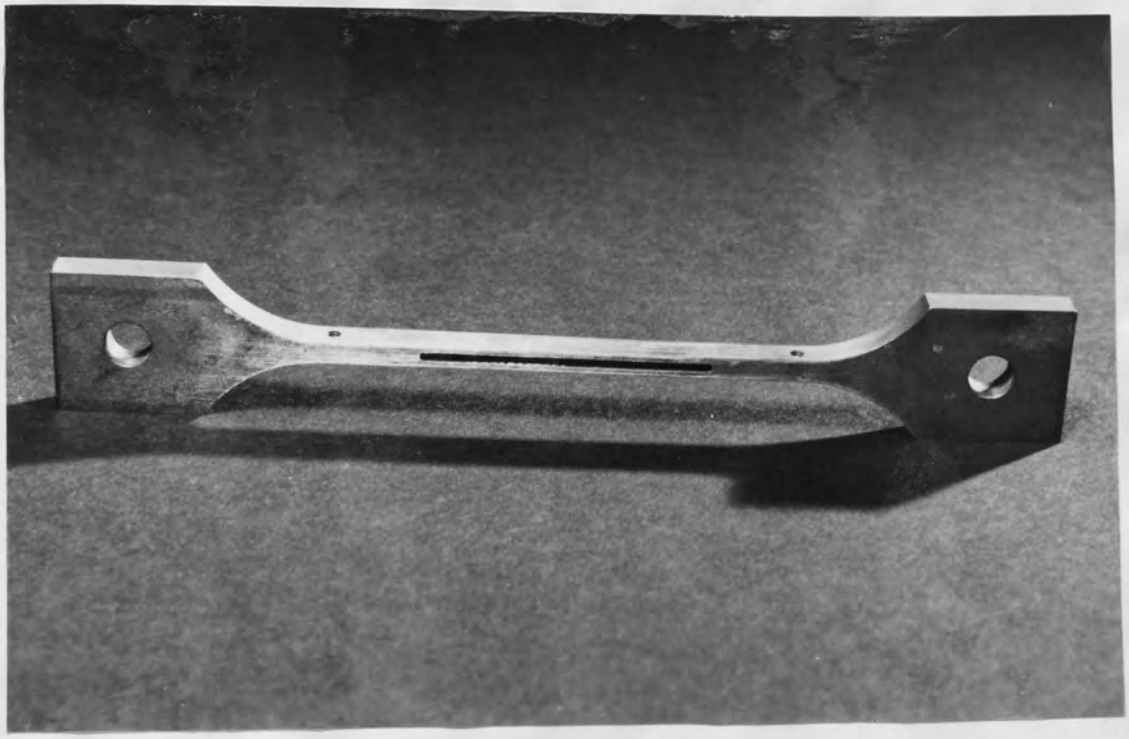

L : length of the beams = 5.39×10^{-2} m

H : thickness of the beams = 0.13×10^{-2} m

W : width of the beams = 0.6×10^{-2} m

FIGURE 6.3 The photograph of the resonator designed for the tension transducer for a range of 0-5 kN. Its calibration curve is shown in Figure 6.4.

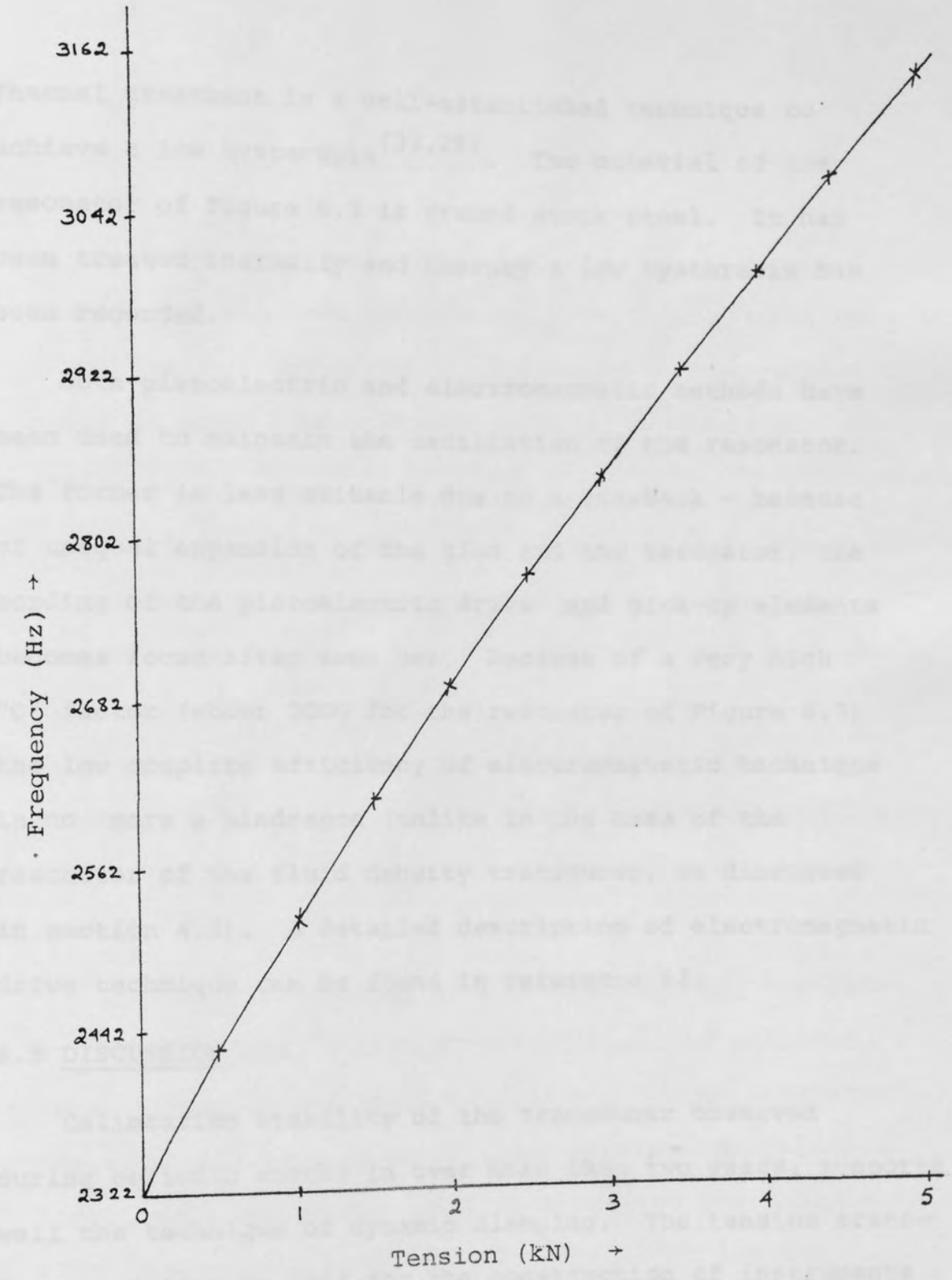

FIGURE 6.4 A calibration curve of the tension transducer using the resonator of Figure 6.3.

Thermal treatment is a well-established technique to achieve a low hysteresis[23,26]. The material of the resonator of Figure 6.3 is ground stock steel. It has been treated thermally and thereby a low hysteresis has been recorded.

Both piezoelectric and electromagnetic methods have been used to maintain the oscillation of the resonator. The former is less suitable due to a drawback - because of unequal expansion of the glue and the resonator, the bonding of the piezoelectric drive and pick-up elements becomes loose after some use. Because of a very high "Q" factor (about 2000 for the resonator of Figure 6.3) the low coupling efficiency of electromagnetic technique is no more a hindrance (unlike in the case of the resonator of the fluid density transducer, as discussed in section 4.3). A detailed description of electromagnetic drive technique can be found in reference 67.

6.5 DISCUSSION

Calibration stability of the transducer observed during periodic checks in over more than two years, supports well the technique of dynamic clamping. The tension transducer can also be used for the construction of instruments for measuring other physical variables (such as pressure, level) by transforming them into a tension signal[23].

CHAPTER 7

CONCLUSIONS

A study of currently available frequency domain transducers has been carried out. In general they consist of mechanical resonators which respond to the parameter being measured (temperature, density, pressure or tension).

A contribution made in the present work is the use of dynamically clamped units enabling the vibrating region to be isolated from the supports while retaining high mechanical strength. In the development of the density transducers the concept of magnifying the inertial loading by trapping a lamina of fluid between the two members making up the dynamic clamping has been used.

A variety of designs have been examined. For gases it was found that a high sensitivity can be achieved using a thin lamina while retaining a robust structure. Gas viscosity sets an upper limit to this sensitivity. For liquids the energy loss which reduces the sharpness of resonance is a major problem. A design has been achieved which gives an acceptabily sharp resonance while maintaining a high sensitivity. Simplicity and low cost are significant advantages of both the transducers.

For tension measurement a double beam unit has been

developed. Detailed analysis has shown that the sensitivity is controlled by the thickness to width ratio. Thus for a certain cross-sectional area (defining the maximum tension) a pair of thin wide beams gives best performance.

A variety of drive and pick-up techniques with their associated electronics have been examined. No completely perfect solution is apparent but a number of methods are satisfactory for particular applications.

Some further work in the case of the fluid density transducers should be

(1) to examine other suitable materials for the resonators (see Section 4.2).

(2) to develop the gas density transducer as the detector stage of a gas chromatographic system (see Section 4.11).

(3) to examine alternative driving techniques for the case of liquids (see Section 5.4).

(4) to look for rigorous theoretical solutions for the phenomenon of dynamic balancing (see Section 2.3) and for the conflicing effects of added mass and added stiffnesss (see Section 4.6).

Some further work in the case of the tension transducer should be

(1) to examine other suitable materials such as titanium, steel P18 and steel GK 40 (see Section 6.4).

(2) to examine the possibilities of using it for constructing devices for measuring other physical variables such as pressure and material level (see Section 6.5).

(3) to carry out a rigorous theoretical analysis for the dynamic balancing condition, possibly using a finite element computer analysis.

LIST OF PRINCIPAL SYMBOLS

A	amplitude of vibration
B	$L\beta$
C	velocity of sound in fluid, constant
C_o	rod velocity
E	Young's modules
e	exponential
F	drag force, excess fluid pressure
f_o	frequency in vacuum
f_f	frequency in a fluid of density ρ_f
f_g	frequency in a gas of density ρ_g
f_ℓ	frequency in a liquid of density ρ_ℓ
f_T	frequency under tension T
f_{1T}	fundamental frequency under tension T
f_{1O}	fundamental frequency under no tension
H	thickness
h_o	half the initial gap
h_t	gap at time t
j	$\sqrt{-1}$
K	wave number, stiffness
K_1, K_2	constants
K_C, K_R	constants
L	length
M	mass, molecular weight, $L\mu$
ΔM	added mass
m	mass per unit length

p	pressure
Q	quality factor
R	radius, gas constant
R_e	Reynolds number
R_L	resistive part of Z_L
r,θ,z	cylindrical polar co-ordinates
S	cross sectional area, stiffness
T	tension, ωt
t	time
U	velocity, $U_z/h_o\alpha\omega$
U_r	radial velocity
U_z	axial velocity
V_o	velocity amplitude
V_t	volume at time t
W	width
X_L	reactive part of Z_L
$\dot{x}$	$\frac{dx}{dt}$
$\ddot{x}$	$\frac{d^2x}{dt^2}$
Z_L	mechanical impedance of the fluid lead
α	A/h_o
β	$z/\lvert h_o(1+\alpha\sin\omega t)\rvert$, $(3T/2\pi^2ESH^2)^{\frac{1}{2}}$
μ	viscosity, given by equations (6.4) and (6.5)
π	3.14159
ρ	density
ρ_o	scale factor
ρ_f	fluid density

ρ_g gas density

ρ_ℓ liquid density

ω angular frequency

ω_o angular frequency in vacuum

ξ distance

γ_c ratio of specific heats.

APPENDIX 1

SOLUTION OF EQUATION (3.33)

Equation (3.33) is

$$\frac{\partial^4 U}{\partial \beta^4} = R_e \frac{\partial^3 U}{\partial \beta^3 \partial T} \qquad \text{(A.1.1)}$$

Let us look for a solution of the form

$$U = \phi(\beta) e^{jT} \qquad \text{(A.1.2)}$$

Equation (A.1.1) then reduces to

$$\frac{d^4\phi}{d\beta^4} - jR_e \frac{d^2\phi}{d\beta^2} = 0 \qquad \text{(A.1.3)}$$

The solution of equation (A.1.3) is

$$\phi = C_1 + C_2\beta + C_3 \frac{e^{K\beta}}{K^2} + C_4 \frac{e^{-K\beta}}{K^2} \qquad \text{(A.1.4)}$$

where $K = \sqrt{jR_e}$

and C_1, C_2, C_3, C_4 are constants whose values are determined by boundary conditions.

Under the assumption of equation (A.1.2), the boundary conditions of equation (3.34) become

$$\text{at } \beta = 0, \qquad \phi = 0 = \frac{d^2\phi}{d\beta^2} \qquad \text{(A.1.5)}$$

$$\text{at } \beta = 1, \qquad \phi = 1, \quad \frac{d\phi}{d\beta} = 0$$

With these boundary conditions, from equation (A.1.4), the values of C_1, C_2, C_3 and C_4 are found as

$$C_1 = 0, \qquad C_2 = \frac{2\text{Cosh } K}{KC}$$

$$C_3 = \frac{1}{C}, \qquad C_4 = -\frac{1}{C}$$

$$\text{where } C = \frac{2 \text{ Cosh } K}{K} - \frac{2 \text{ Sinh } K}{K^2}$$

With these values of C_1, C_2, C_3, C_4, from equations (A.1.2) and (A.1.4)

$$CU = \left| \frac{2\beta \text{ Cosh } K}{K} - \frac{2 \text{ Sinh } K\beta}{K^2} \right| e^{JT}$$

APPENDIX 2

NUMERICAL SOLUTIONS FOR THE RESONANT FREQUENCY OF A BAR UNDER TENSION

By putting,

$$L\mu = M$$

$$L\beta = B \qquad \text{(A.2.1)}$$

in equations (6.5) and (6.6),

$$M \tan(\pi M) = -\sqrt{M^2 + 2B^2}\, \tanh\pi\sqrt{M^2 + 2B^2} \qquad \text{(A.2.2)}$$

$$\sqrt{M^2 + 2B^2}\, \tan(\pi M) = M \tanh \pi\sqrt{M^2 + 2B^2} \qquad \text{(A.2.3)}$$

Under the transformation of (A.2.1), equation (6.4) can be written as

$$f_{nT}\ \frac{L^2}{C_o H} = \frac{\pi}{\sqrt{3}}\, M\sqrt{M^2 + 2B^2}$$

or $$K_n = \frac{\pi}{\sqrt{3}}\, M\sqrt{M^2 + 2B^2} \qquad \text{(A.2.4)}$$

where $K_n \equiv f_{nT}\ \frac{L^2}{C_o H}$ = frequency function

Solving equations (A.2.2) and (A.2.3) numerically using a computer program, values of K_n have been calculated from equation (A.2.4). These values, for B from 0 to 1 at step of .05, are given in Table A.2.1.

B	K_1	K_2	K_3
0	1.028	2.834	5.557
.05	1.031	2.837	5.560
.1	1.038	2.847	5.571
.15	1.051	2.864	5.590
.2	1.068	2.887	5.615
.25	1.089	2.917	5.648
.3	1.114	2.953	5.688
.35	1.144	2.995	5.735
.4	1.176	3.042	5.788
.45	1.212	3.095	5.849
.5	1.251	3.153	5.915
.55	1.292	3.216	5.988
.6	1.336	3.283	6.066
.65	1.382	3.354	6.150
.7	1.429	3.430	6.240
.75	1.478	3.510	6.334
.8	1.529	3.591	6.434
.85	1.581	3.676	6.538
.9	1.634	3.765	6.647
.95	1.688	3.856	6.760
1	1.742	3.949	6.877

TABLE A.2.1 : Values of frequency function K_n for values of tension function B.

LIST OF REFERENCES

1. Gardiner, D.J.
   "Comment"
   Transducer Technology, p.4, Volume 1, 1979.

2. Schuler, A.E.
   "Digital Transducer - Types and Trends",
   Instrumentation Technology, p.41-46, Dec. 1969.

3. Jones, B.E.
   "Instrumentation, Measurement and Feedback".
   Mc Graw-Hill Book Company (UK), 1977).

4. Dorrity, J.L. and Gilliland, B.E.
   "A Digital Force Transducer".
   IEEE Transactions on Instrumentation and
   Measurement, p.411-414, No.4, 1977.

5. Bell, J.F.W.
   "Variable Frequency Measuring Transducers".
   Transducer Conference - London, Sept. 1974.

6. Potter, P.N.
   "Frequency Domain Transducers and Their
   Applications".
   Instrument Practice, p.849-853, Dec. 1969.

7. Agar, J.
   "Frequency Modulating Transducers".
   The Radio and Electronic Engineer, p.89-95,
   Volume 38, 1969.

8. Wightman, E.J.
"Digital Process Control Transducers".
Instrument Practice, p.456-459, May 1967.

9. Derrick, G.
"Resonance Frequency : Measurement Tool of the Seventies".
Control and Instrumentation, p.40-43, February 1975.

10. Agar, J.
"The Vibrating Spool Fluid Density Meter".
Instrument Practice, p.437-439, June 1969.

11. Meyer, R.C.
"A New Digital Pressure Transducer".
Advances in Instrumentation, paper No. 601, 1972.

12. Paros, J.M.
"Precision Digital Pressure Transducer".
Advances in Instrumentation, paper No. 602, 1972.

13. Halford, R.J.
"Pressure Measurement Using Vibrating Cylinder Pressure Transducer".
Instrument Practice, p.823-829, August 1964.

14. Shenderovich, I.M.
"The Vibrotron - a New Precision Pressure Detecting Element".
Instrument Construction, p.13-16, No.7, 1962.

15. Belyaev, M.F.
"Vibration-frequency Pressure Transducer".
Instrument Construction, p.10-13, No.10, 1965.

16. The Application Engineering Group of Hewlett-Packard, Ltd.
"A Quartz Thermometer".
Instrument Practice, p.907-910, Oct. 1965.

17. Hammond, D.L., and Benjaminson, A.
"The Crystal Resonator - A Digital Transducer".
IEEE Spectrum, p.53-58, Vol.6, 1969.

18. Bell, J.F.W.
"Ultrasonic Thermometry Using Resonance Techniques".
Proc. 5th Symp. on Temperature, Washington, D.C.,1971.

19. Seth, T.N.
"Ultrasonic Pyrometer for Industrial Applications".
Ph.D. Thesis, University of Aston, 1974.

20. Fathimani, A.A.
"The Automation of Resonant Thermometer Probe Measurements".
Ph.D. Thesis, University of Aston, 1976.

21. Wyman, P.R.
"A New Force to Frequency Transducer".
IEE Conf. Publ. 106, p.117-123, 1973.

22. Voutsas, A.M.
"Twisted Beam Transducer".
A.I.A.A. Journal, p. 911-913, April 1963.

23. Sinyukhin, Y.A., and Skugorov, V.N.
"Vibrating-rod Transducer".
Instrument Construction, p. 4-6, No.2, 1966.

24. Skugorov, V.N.
"Vibrating Wire Transducers for Measuring Force and Pressure".
Instrument Construction, p. 1-3, No.1, 1966.

25. Tsodikov, Y.M.
"Differential Vibrating Wire Detecting Unit for Force and Deformation Measurements".
Instrument Construction, p.11-13, No.11, 1965.

26. Etkin, L.G.
"Vibration Dynamometers".
Instrument Construction, p.35-36, No.8, 1962.

27. Mason, W.P.
"Physical Acoustics and the Properties of Solids".
Van Nostrand, 1958.

28. Roth, W., and Rich, S.R.
"A New Method for Continuous Viscosity Measurement, General Theory of the Ultra-Viscoson".
Journal of Applied Physics, p.940-950, Vol. 24, 1953.

29. Berger, S.A. et al.
"A New Electromechanical Viscometer Designed for Biological Fluids".
IEEE Trans. on Biomedical Eng., p.64-70, Jan. 1978.

30. Mahil, K.S.
"The Development of a Fluid Consistency Transducer".
Ph.D. Thesis, University of Aston, 1975.

31. Glover, G.M., et al.
"A Magnetostrictive Instrument for Measuring the Viscoelastic Properties of Liquids in the Frequency Range 20 - 100 KHz".
Jour. of Scientific Instruments, p.383-388, Vol.1, 1968.

32. Krutin, V.N. and Smirnits, I.B.
"Measurement of the Viscosity of Newtonian Fluids by Means of Vibratory Probes".
Soviet Physics-Acoustics, p.42-45, Vol.12, 1966.

33. Kogan, I.N.
"Tubular Vibrator with Lumped Massess at the Ends as a Viscometer".
Soviet Physics-Acoustics, p.461-464, Vol.14, 1969.

34. Rosin, G.S.
"Absolute Viscosity Measurements by the Undamped Lengthwise Vibrations of a Plate in Fluid".
Soviety Physics-Acoustics, p.493-498, Vol.14, 1969.

35. Ledwidge, T.J. and Hughes, G.
"Gas Density Measurement by the Natural Damping of a Vibrating Reed".
Jour. of Scientific Instruments, p.385-387, Vol. 44, 1967.

36. Panin, I.A.
"Vibrational Gas Densimeters".
Measurement Tech. (USA), p.1090-1092, Vol.18, 1975.

37. James, G.S.
"Tuning Fork Frequency Standard".
Jour. Acoust. Soc. Am., p.1648, Vol. 33, 1961.

38. Max, H.
"Freqnecy-Adjustable Tuning Fork Type Vibrator for an Electrically Energized Timepiece".
Jour. Acoust. Soc. Am., p.950, Vol. 35, 1963.

39. Reefman, W.E.
"Tuning Forks Measure Frequency".
Electron. Prod. Mag., p.32-34, No.6, 1964.

40. Wulfsberg, K.N.
"A Tuning Fork Filter".
Jour. Acoust. Soc. Am., p.847-849, Vol. 22, 1950.

41. Holt, W.J.
"A Tuning Fork for High-Q Resonance".
Electronics, p.108, No.21, 1960.

42. Bruinsma, A.H.
"A Remote Control by Radio".
Philips Eindhoven N.V., 1952.

43. Kalmarczie, P.J.
"Energy Trapped Resonances in Solid Structures".
Ph.D. Thesis, University of Aston, 1976.

44. Lamb, H.
"On the Vibration of an Elastic Plate in Contact with Water".
Proc. Roy. Soc., p.205-216, Vol.98, 1921.

45. Junger, M.C., and Feit, D.
"Sound Structure and their Interaction".
MIT Press, Cambridge, 1972.

46. Junger, M.C.
"Vibration of Elastic Shells in a Fluid Medium and the Associated Radiation of Sound".
Jour. of Appl. Mechanics, p.439-445, Dec. 1952.

47. Lax, M.
"The Effect of Radiation on the Vibration of a Circular Diaphragm".
Jour. Acoust. Soc. Am., p.5-13, Vol.16, 1944.

48. Stephens, R.W.B., amd Bate, A.E.
"Acoustic and Vibrational Physics".
Arnold, 1966.

49. Lamb, H.
"Hydrodynamics".
Cambridge, 1956.

50. Landu, L.D., and Lifshitz, E.M.
"Fluid Mechanics".
Pergamon Press, 1963.

51. Cottrell, A.H.
"The Mechanical Properties of Matter".
Wiley, 1964.

52. Kerman, V.
"On the Foundation of High Speed Aerodynamics".
High Speed Aerodynamics and Jet Propulsion,
Princeton, N.J. University Press, 1954.

53. Robertson, J.M.
"Hydrodynamics in Theory and Application".
Prentice-Hall, 1965.

54. Olson, H.F.
"Acoustical Engineering".
D. Van Norstrand, Co., 1967.

55. Vennard, J.K., and Street, R.L.
"Elementary Fluid Mechanics".
Wiley, 1975.

56. Texas Instruments, Limited, Bedford.
"Standard Precision Fused Quartz Bourdon Capsules".
Bulletin 833B, 1973.

57. Vernitron Limited, Southampton.
"A Guide to the Use of PZT Piezoelectric Strain,
Vibration and Excitation Gauges".
Bulletin 66022/B, 1967.

58. Unilator Technical Ceramics, Clwyd.
"Piezoelectric Ceramics".

59. Morse, P.M.
"Vibration and Sound".
Mc Graw-Hill, 1948.

60. Gardner, F.M.
"Phaselock Techniques".
Wiley, 1968.

61. Signetics Corp.
Digital, Linear, MOS Applications, 1974.

62. Motorola Semiconductor Products, Inc.
Phase Locked Loop Systems Data Book, 1973.

63. National Semiconductor Corporation.
Linear Applications Handbook, 1972.

64. Simpson, H.M., and Pearson, J.
"Simple Apparatus for Measuring the Dynamic Shear Modulus of Cylindrical Specimens".
Rev. Sci. Instrum., p.418-420, Apr. 1979.

65. David, D.J.
"Gas Chronomatographic Detectors".
Wiley, 1974.

66. Chen, J.Y.F.
"Surface Wave Techniques for the Study of Engineering Structures and Materials".
Ph.D. Thesis, University of Aston, 1979.

67. Mc Loughlin, R.P.
"A Frequency Standard for Use at High and Low Frequencies".
Jour. Acoust. Soc. Am., p.46-70, Vol.17, 1945.